iSCAPE

Report on climate change and air quality interactions

D1.4

February 2017

This project has received funding from the European Union's Horizon 2020 research and innovation programme under grant agreement No 689954.

Project Acronym and Name	iSCAPE - Improving the Smart Control of Air Pollution in Europe	
Grant Agreement Number	689954	
Document Type	Report	
Document version & WP No.	V0.5	WP 1
Document Title	Report on climate change and air quality interactions	
Main authors	Silvana Di Sabatino (Lead UNIBO), Kirsti Jylhä (Lead FMI), Francesco Barbano, Alessio Francesco Brunetti, Achim Drebs, Carl Fortelius, Väinö Nurmi, Enrico Minguzzi, Beatrice Pulvirenti, Athanasios Votsis	
Partner in charge	UNIBO	
Contributing partners	UNIBO, FMI, ARPAE – (main contributors) UoS, UCD, UH, TUDO (provided reference data for their city)	
Release date	28/02/2017	

Document Control Page	
Short Description	*This report is the results of the work described in Task 1.4 of the ISCAPE project as an output Deliverable D1.4. The report aims to summarize current understanding of urban climate change, air quality studies and their interconnection. It provides a broad overview of challenges that are relevant for PCSs deployment to mitigate the impact of climate changes in future scenarios. It critically depicts the science basis for later numerical modelling and experimental studies within ISCAPE and provide suggestions for other WPs.*

Review status	Action	Person	Date
	Quality Check	*Coordination Team*	28/02/2017
	Internal Review	*John Gallagher, TCD* *Andreas Skouloudis, JRC*	15/02/2017 24/02/2017
Distribution	Public		

Revision history			
Version	**Date**	**Modified by**	**Comments**
V0.1	22/01/2017	Francesco Barbano; Alessio Francesco Brunetti	Silvana Di Sabatino; Beatrice Pulvirenti; Enrico Minguzzi
V0.2	27/01/2017	Kirsti Jylhä, Carl Fortelius, Väinö Nurmi, Achim Drebs, Athanasios Votsis	Silvana Di Sabatino; Beatrice Pulvirenti; Francesco Barbano
V0.3	08/02/2017	Francesco Barbano; Alessio Francesco Brunetti; Kirsti Jylhä, Carl Fortelius, Väinö Nurmi, Achim Drebs, Athanasios Votsis	Silvana Di Sabatino; Beatrice Pulvirenti; Enrico Minguzzi
V0.4	27/02/2017	Silvana Di Sabatino; Beatrice Pulvirenti; Enrico Minguzzi; Francesco Barbano; Alessio Francesco Brunetti; Kirsti Jylhä, Carl Fortelius, Väinö Nurmi	Reviewed by John Gallagher and Andreas Skouloudis
V0.5	28/02/2017	Aakash C. Rai	WP1 leader's edits.

Final	28/02/2017	Francesco Pilla	Quality check

Statement of originality:

This deliverable contains original unpublished work except where clearly indicated otherwise. Acknowledgement of previously published material and of the work of others has been made through appropriate citation, quotation or both.

Table of Contents

List of Tables

LIST OF FIGURES

List of abbreviations

AOT40: Accumulated Exposure Over a Threshold of 40 ppb
BAU: Business as Usual
CMIP: Coupled Model Intercomparison Project
CTM: Chemical Transport Model
DCC: Dublin City Council
ECA&D: European Climate Assessment and Data archive
EEA: European Environmental Agency
ENSO: El Niño Southern Oscillation
ERA: European Reanalysis
EV: Electric Vehicles
GCM: Global Climate Model
GDP: Gross Domestic Product
GHG: Green House Gas
HSY: Helsinki Region Environmental Services Authority
HWMI: Heat Wave Magnitude Index
IPCC: Intergovernmental Panel on Climate Change
KVR: Kommunalverbant Ruhrgebiet
LES: Large Eddy Simulation
LEZ: Low Emission Zone
LWP: Local Wind Pattern
MW: Main/far Wake
NAO: North Atlantic Oscillation
NCEP: National Centers for Environmental Prediction
NCAR: National Center for Atmospheric Research
ND: No Data
NW: Near Wake
OECD: Organization for Economic Co-operation and Development
PCS: Passive Control System
PDF: Probability Density Function
PIK: Potsdam Institute for Climate Impact Research
PPP: Purchasing Power Parity

QBC:	Quality Bus Corridor
RCM:	Regional Climate Model
RCP:	Representative Concentration Pathway
SCCP:	Surrey Climate Change Partnership
SLP:	Sea Level Pressure
SPP:	Surface Pressure Pattern
SRES:	Special Report on Emissions Scenarios
SSP:	Shared Socioeconomic Pathway
TCT:	Thermally Produced Turbulence
TEB:	Town Energy Balance
TMY:	Typical Meteorological Year
TPT:	Traffic Produced Turbulence
TRY:	Test Reference Year
UBL:	Urban Boundary Layer
UrBAN:	Urban Boundary-Layer Atmosphere Network
VOC:	Volatile Organic Compounds
WHO:	World Health Organization
WPT:	Wind Produced Turbulence

1 Executive Summary

The main objective of this report is to layout a broad overview of the latest understanding of climate and climate change and its connection with urban air quality. It critically reviews recent research studies that are not yet being used in practical applications and that are critical for later implementation of Passive Control Systems (PCSs) within the iSCAPE project. The Introduction is devoted to review the broad motivation for reducing air pollutant concentration in cities; it also deals with the potential benefits of using climate change information for city planning, a topic that is at the core of the iSCAPE project. The report is organized in two main parts, described as follows.

1. Climate and climate change in European cities

1.1. *Description of climate change modelling approach.* The study is performed starting from the regional to the urban scale. Issues to be kept in mind when monitoring the impacts of global climate change on urban and smaller scales are data quality and homogeneity; climate conditions in cities may not be captured by weather stations, as these are typically located in open vegetated land (rural or natural landscapes). Moreover, uncertainty is always involved in climates change projections. For simulations of future climate, climate model experiments are run under assumptions about the future evolution of atmospheric composition, land use change and other driving forces of the climate system. Global and regional climate models, typically having a grid size of tens of kilometres or larger, poorly resolve the urban land surface. The geographical pattern of the simulated climate response may be downscaled using various methods. Several physical-based surface models can simulate air-surface interactions at a horizontal scale of about 100 metres. However, many urban parameterizations still follow highly simplified approaches. The Town Energy Balance (TEB) model (Masson, 2000; Lemonsu et al., 2004), included in the surface interaction model SURFEX, is an example of a model capable of clearly separating buildings, air within urban canyons, roads, and, if present, trees, gardens etc.

1.2. *Setting of the role of physical variables in current climate and change.* The focus is to set the basis for subsequent studies within iSCAPE. The role of the physical variables that can be extracted from future climate change scenarios at urban scale is discussed. These variables are those that are relevant for establishing the link between climate change and air quality i.e. temperature, wind speed, pressure and solar radiation, and these variables have to be used to evaluate the efficacy of PCSs in future scenarios. This is also one of the main aims of iSCAPE. The main results from this sections are:

1.2.1. the observed annual-averaged pan-European temperature trend of 0.179°C per decade since 1960.

1.2.2. the average impact of urbanization on that trend is 0.0026°C per decade since 1960. The effect is strongest in spring and summer.

1.2.3. Among the iSCAPE cities, the projected summertime warming is largest for Bologna and smallest in Dublin. In winter, and also in spring and autumn, the most pronounced increases in temperature are likely to take place in Vantaa.

1.2.4. Precipitation is generally projected to increase in winter and decrease in summer. However, the sign of the change is uncertain in Bologna in winter and in Vantaa in summer.

1.2.5. Incident solar radiation and diurnal temperature range are projected increase in most of Europe in spring, summer and autumn.

1.2.6. The observed reduction in the mean annual solar radiation in southern Finland over the period from 1958 to 1992 was mainly attributed to a pronounced increase in cloudiness, with only a minor contribution from the direct effects of the relatively large aerosol load at that time.

1.2.7. Wintertime sea level air pressure is projected to decrease in Vantaa and increase elsewhere. In Dublin and Guildford, the projected trend is positive in all seasons and in Belgium and Germany in all seasons except for the summer simulations.

2. Air quality and climate change interaction in European cities

2.1. *Focus on the mean state of pollutants in the target cities.* This part magnifies the focus on the mean state of the main pollutants (NO_2, PM_{10} and $PM_{2.5}$) as well as O_3 that is relevant for climate change for the iSCAPE target cities. Given that, the scope is to identify the preferential conditions for PCSs deployment in each target city and provide state of art knowledge for subsequent work packages (WPs). Specifically, we find that pollutant concentrations have different impacts due to meteorological, geographical and structural features of the single city, but also as a result of local air quality policies. In general traffic-induced emissions (NO_2 and PM_{10}) have an influence on total concentration at street level, but not at urban scale. Residential heating systems also contribute again at street level, but its signal is weaker. Two pollutants, NO_2 and PM_{10} have a dependence on emissions at the street scale, while $PM_{2.5}$ is more homogeneous in the urban environment. Concerning the risks on human heath connected to exposure to high level of $PM_{2.5}$ has led to a decrease and an adjustment of concentrations at WHO suggested level for human health which is stricter than the European limit. Only Bologna, among the target cities requires to improve its efforts to mitigate the $PM_{2.5}$ concentrations. Ozone concentrations is quite homogeneous at the city scale. In rural areas ozone concentrations sensibly grow, supported by favourable conditions.

2.2. Assessments on pollutants linkages with climate change. Really few studies have been performed on the relationship between air quality and climate change, especially at small scales. It easier to find studies concerning air quality linked with the urbanization growth (with some problems of inhomogeneity between different nations due to different necessity and city types). At European scale, the climatological variables that mostly affect air quality are: surface temperature, precipitation and sea level pressure. Temperature scenarios, coupled with precipitation pattern projection, facilitate an increase in pollutants such as ozone due to increased biogenic emissions and photochemical rates and reduced wet removal. Changes in meteorological variables can modify global sea level pressure patterns, with consequences on local circulations and distribution of air masses. In the end, climate change induced by enhanced pollutant emissions will in turn increase pollutant concentration. So, a positive feedback is established, leading to an intensification of climate changes in those regions highly affected by pollution. It is important to underline that these connections between climate and pollutants concern the larger scales (global, or at least European). Specific studies at local scale have to be provide to achieve a better understanding on the future livability of our cities.

2 Introduction

At the core of the iSCAPE project there is an awareness of the consequences of increasing global urbanization and the inherent challenges due to climate change on air quality.

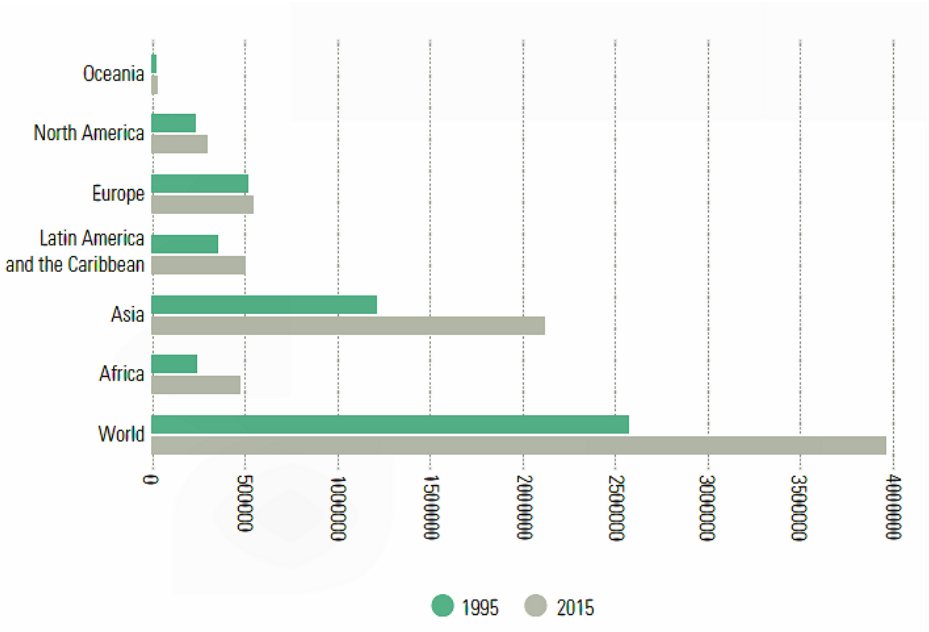

Figure 1: Urban population comparison between 1995 and 2015 (adapted from UN-Habitat, 2016).

Since the beginning of the industrial revolution, the percentage of the world's population settling in urban areas has been increasing, and this trend is expected to continue. In 1990, 43 % (2.3 billion) of the world's population lived in urban areas; by 2015, this has grown to 54 % (4.0 billion). Following the growth rate, 60 % (4.9 billion) of the world's population is expected to live in cities by 2030. This increase in urban population has not been evenly spread throughout the world. Asia has the highest number of people living in urban areas, followed by Europe, Africa and Latin America. Nevertheless, urban annual growth rates have been much faster in some regions than others (Figure 1). The highest growth rate between 1995 and 2015 was in the least developed regions with Africa being the most rapidly urbanizing; it shows a rate of 3.44 %, almost 11 times more rapid than that in Europe (0.31 %). As the urban population increases, the land area occupied by cities has increased at an even higher rate. The process of urbanization is particularly leading to an increase of large cities (5 to 10 million inhabitants) and megacities (more than 10 million inhabitants). Most megacities are in developing countries and this trend is set to continue as several large cities in Asia, Latin America and Africa are projected to become megacities by 2030 (UN-Habitat, 2016).

Despite economic growth and improvement of basic facilities, cities suffer from negative consequences of urbanization, such as environmental and air quality degradation, as well as respiratory problems. People living in large urban areas are routinely exposed to concentrations of airborne pollutants that epidemiological statistics claim they might cause negative health

effects in both the short and long term (Ericson et al., 2008). As urbanization, global population, and economic development increase, not only short-range but also long-range transport of pollution becomes an increasingly important factor for cities since air flow transports pollutants from upwind areas contributing to local air quality together with locally-emitted pollutants (Parrish and Stockwell, 2015). Transportation, industry and power generation are the main sources contributing to outdoor air pollution (Hilbert and Palmer, 2014). Most of the cities worldwide are facing levels of air pollutants exceeding regulatory limits (see Appendix A), with repercussions on inhabitants' health (Kumar et al., 2015). Traffic-induced emissions, such as respirable particulate matter, nitrogen dioxide, carbon monoxide and hydrocarbons, largely affect urban inhabitants, especially the population residing in close vicinity of roadways and streets as well as the pedestrians (Ahmad et al., 2005).

Air is composed of a variety of gaseous pollutants and particulate matter, those can be classified into primary and secondary. Primary pollutants are those directly emitted into the atmosphere by human activities (vehicle engines, industrial production etc.) and by natural processes (windblown dust, volcanic activity, etc.). Secondary pollutants are formed within the atmosphere when primary pollutants react with sunlight, oxygen, water and other chemical compounds present in the air. As for public health, major pollutants are particulate matter (PM), tropospheric ozone (O_3) and nitrogen dioxide (NO_2). NO_2 is produced by the combustion of fossil fuels and contribute to photochemical smog, as well as to acid rain. O_3 is a major component of photochemical smog, an air pollution phenomenon that forms when primary pollutants like NO_2 and carbon monoxide (CO) react with sunlight to form a variety of secondary pollutants. PM is mainly attributed to the combustion of fossil fuels, especially coal and diesel fuel, and is composed of tiny particles of solids and liquids including ash, carbon soot, mineral salts and oxides, heavy metals such as lead, and other organic compounds. PM includes particles from a few nanometres (10^{-9} metres) to several tenths of a micron (10^{-6} metres) in size. In general, the smaller the size of the particles, the greater the expected effect on human health (Heal et al., 2012).

Figure 2 shows pollutants which are transported to the city or which are locally emitted and dispersed at different horizontal local scales: street (of order 10-100 m), neighbourhood (0.1-1.0 km) and city (10-20 km) (Britter and Hanna, 2003). Their final spatial distribution is determined by several factors, such as the meteorology and the morphological characteristics of the city, as well as the population density and the type, nature and spatial location of sources. In general, the processes controlling the pollution phenomenon act at a range of spatial and temporal scales spanning the depth of the whole Urban Boundary Layer (UBL). Important parameters for dispersion around buildings are: building geometry and morphology (in terms of building arrangements and packing density), wind speed, wind direction, turbulence, atmospheric stability, temperature, humidity and solar radiation (Blocken et al., 2013), together with the presence of obstacles such as trees, low barriers and parked cars (Gallagher et al., 2015). Therefore, locally-induced wind fields consist of complex flow features such as recirculation zones and stagnation points which in turn strongly govern the dispersion of pollutants (Lateb, 2016).

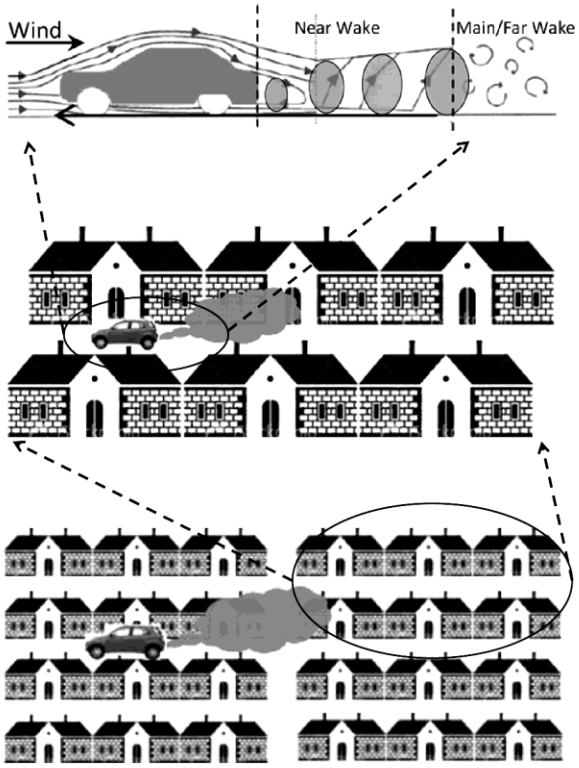

Vehicle wake (0 - 20m)

- Flow is more turbulent in NW region compared with MW region
- TPT is intense in NW and dominate the mixing
- Atmospheric turbulence (WPT and TCT) lead the further mixing in MW region

Street scale (10m - 100m)

- Flow features and mixing determined by surface roughness below building height
- Internal mixing layers below or above the buildings are of order of building or street dimensions
- TPT dominate the mixing over the WPT during calm wind conditions
- TCT may play role in mixing during hot sunny weather and light winds

Neighbourhood scale (100m - 1km)

- Flow and mixing above and between buildings is determined by the turbulence generated by interaction of flows from adjacent canyons, surface and wall roughness, WPT, TPT and TCT
- A growing internal layer of flow can be seen above buildings
- Average geometrical features dominate mean flow and mixing

City scale (10km - 20km)

- Flow and mixing over buildings is relatively less complex than within the city due to orographic (i.e. surface roughness elements) effects
- Mixing below the building heights in the ABL is dominated by surface roughness and the TPT; the atmospheric turbulence (i.e. WPT and TCT) plays a key role in flows over urban canopy

Figure 2: Description of the key flow and mixing features at urban scales. NW: near wake; MW: main/far wake; WPT: wind produced turbulence; TPT: traffic produced turbulence; TCT: thermally produced turbulence (by difference between air and urban surface). (Kumar et al., 2011).

Studies around the world are investigating the two ways of correlating air quality and climate change. The mass, size and chemical composition of anthropogenic aerosols affects cloud microphysics, and can have a global impact on the radiation budget of the atmosphere; this is indeed one of the major sources of uncertainties in global climate models (IPCC, 2013). On the other hand, climate change can affect air quality in many ways: warmer temperatures for instance enhance biogenic emissions; changes in atmospheric wind and turbulence can alter the way in which pollutant are dispersed, transported, and removed from the atmosphere.

Although both air quality and climate change arise from anthropogenic emissions, policies to reduce emissions are not guaranteed to be beneficial for both. One of the most debated fields of intervention is the use of biomass in energy production: while the use of biomass can be considered carbon-neutral (although the subject is somehow controversial, as referred in Berndes et al., 2016), it surely has a negative impact on air quality, due to the large quantity of PM, volatile organic compounds (VOCs) and Polycyclic Aromatic Hydrocarbons (PAHs) produced in the process. Diesel engines are more efficient, and therefore produce less CO_2 per km than gasoline engines, but they also produce a larger quantity of pollutants such as nitrogen oxides (NO_x). Under certain conditions that frequently occur in urban areas, a reduction of NO_2 concentrations increase ozone levels. The photodissociation of the NO_2 is the main mechanism to produce the molecular oxygen in troposphere:

$$NO_2 + h\nu\ (\lambda < 420nm) \rightarrow NO + O$$

The molecular oxygen reacts with the oxygen (O_2), throughout a catalyst M (an element of a compound that favour the reaction but it is not modify by the reaction itself):

$$O + O_2 + M \rightarrow O_3 + M$$

However, the ozone reacts quite immediately with the nitric oxide, product of the first reaction:

$$O_3 + NO \rightarrow NO_2 + O_2$$

These three reactions form a cycle of production-destruction for the tropospheric ozone, which is really fast and continuous during the day. In condition of small ventilation and small mixing, the concentrations of ozone are controlled by this cycle. During night, these reactions can't happen since solar energy is involved and the presence of the NO_3 triggers a new cycle for the destruction of the tropospheric ozone.

In recent years, a whole field of research has been started, to select which policies have the best chance to reduce both climate change and air pollution. Tools that can perform an "integrated assessment" of the two problems have been developed, with the aim to select the most cost-effective policies to tackle both air quality and climate change in a win-win approach.

In this report, we first give an overview of current understanding on current climate based on observations and its expected change in EU cities based on most updated numerical models; then we will focus on giving a snapshot of what is the level of AQ at EU level and specifically in the iSCAPE target cities.

3 Climate change in EU cities

Among city planners, inhabitants, and local politicians, there is still a lack of detailed understanding of how to use climate change projections in city planning. This might be partly due by the fact that climate change impacts occur at various urban surroundings and are strongly influenced by the individual urban properties (namely land-use and land-cover) (KLIMAKS TechReport, 2012). Additionally, urban development does not occur everywhere in a city simultaneously. Furthermore, the urban growth and development differ from region to region and from country to country (Mills et al. 2010).

Assessments of ongoing climate change – its strength, speed and signal-to-noise ratio – in European cities are based on both observations and model simulations. According to Chrysanthou et al. (2014), the average impact of urbanization on the observed annual-averaged pan-European temperature trend of 0.1790 °C per decade is 0.0026 °C per decade since 1960. The effect is strongest in spring and summer. In a pan-European sense, urban areas tend to warm faster than the rural areas in spring and cool down more rapidly in autumn.

In subsection 3.1, we first briefly address the challenge of gaining reliable time-series of past climate. We then move on to reviewing state-of-the-art assessments of future climate change at regional scale (Sec. 3.1.1) and urban scale (Sec. 3.1.2). Development of synthetic weather data for a future urban climate is considered in Sec. 3.1.3.

While one dimension in the uncertainties of future climate and its impacts is associated with divergent trajectories of atmospheric composition, land use change and radiative forcing of the climate system, the other dimension is related to social and economic development.

Subsection 3.2 provides five different storylines of global social and economic development and discusses the work towards local interpretations of these storylines.

An overview of the observed past and projections for future climate change in the iSCAPE study regions is given in subsection 3.3, In addition to temperature and precipitation, solar radiation, wind speed and air pressure are considered. Differences in projected climate changes between the regions of the iSCAPE cities are highlighted.

Finally, as a typical example of a green infrastructure (the one that is easier to address within climate change models) i.e. the roles of green roofs in mitigation of and adaptation to climate change are briefly discussed. Several design options for green infrastructure are contemplated within iSCAPE – and these options being assessed is one of the key outputs of iSCAPE. Therefore, the green roof example is reported here as a typical current study.

3.1 Assessment of climate change from regional to urban scales

Many studies are being conducted to homogenize and analyse long-term time series of weather observations from meteorological stations (e.g., Tuomenvirta, 2001; Maugeri et al. 2004; Brunetti et al 2004, 2006; Domonkos and Coll, 2016; Manara et al. 2016; Noone et al. 2016). Furthermore, a multitude of gridded data sets has been constructed using these observations together with geostatistical methods (e.g., Haylock et al. 2008; Tietäväinen et al. 2010; Antolini et al. 2016; Aalto et al. 2016). As an example, Beniston (2015) has used homogenous weather station data available from the European Climate Assessment and Data archive (ECA&D; Klein Tank et al. 2002) to study temperatures at 30 sites across Europe (including Dublin, Berlin and Rome, among others) since the early 1950s. He selected only homogeneous data to ensure

greater robustness in the extreme tails of the temperature PDFs, that are sensitive to the quality of observational data. He found a clear trend of warming of about 1°C over the last three decades (Figure 3), and a sharp increase in the ratio of record high and record low temperatures during the most recent year.

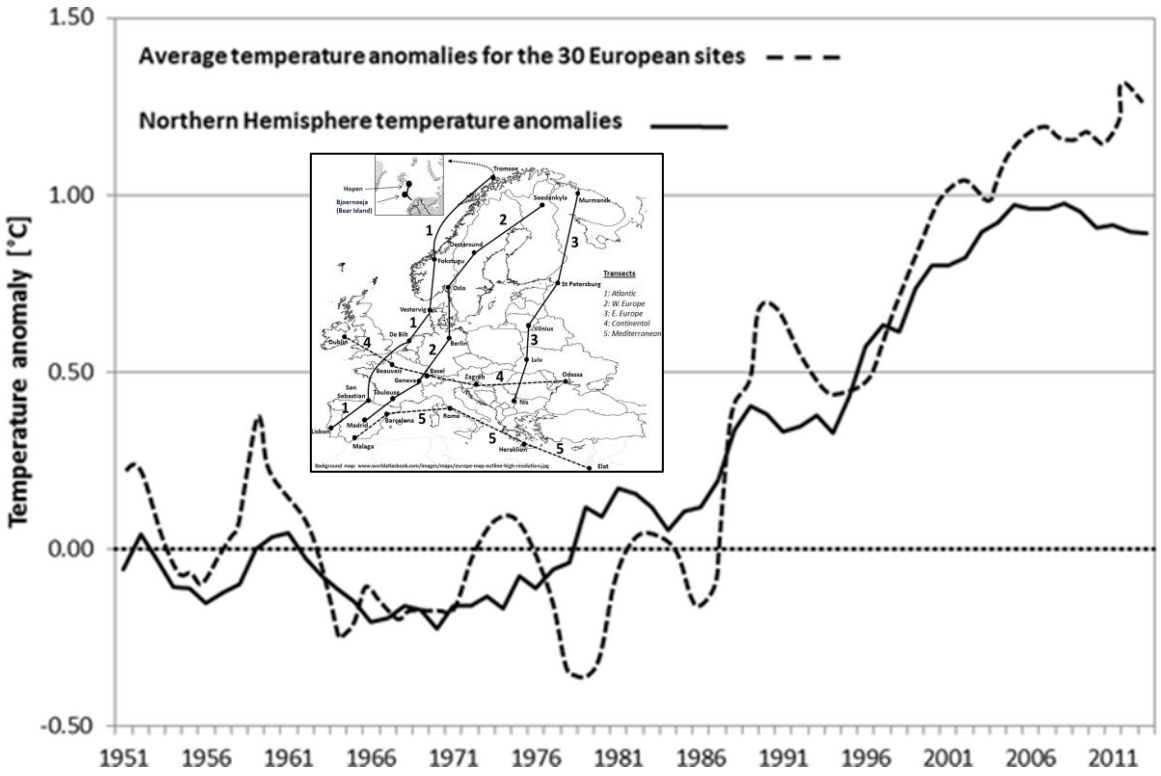

Figure 3: Mean temperature anomalies of 30 European sites (dashed line) and of the Northern Hemisphere (solid line), given as 5-year running means and computed based on the 1961-1990 baseline. For the locations of the measurement sites, see the inner map. From Beniston (2015).

In monitoring the impacts of global climate change on urban and smaller scales, data quality and homogeneity is not the only concern. A challenge is also presented by the fact that observed long-term weather data often do not represent climate conditions in cities. Weather stations are typically located in open vegetated land (rural or natural landscapes), whereas the actual climate conditions in cities are affected by urban morphology and design as well as by the materials in built structures. These are typically different in each region and country reflecting respective history, culture and typical climatic conditions. In addition to the complication of climate change detection based on these observations, this is also an issue from the viewpoint of validation and verification of physically-based numerical simulations of urban-scale climate.

The atmosphere continually interacts with the Earth's surface, including urban, rural and natural landscapes. These interactions take place via sensible and latent heat fluxes, and fluxes of momentum, but also, fluxes of carbon dioxide (CO_2), water vapour and other chemical species, continental aerosols, sea salt and snow particles, among others. Since these fluxes depend on the underlying surface, atmospheric numerical models need to treat different surface types, such as ocean, inland water bodies, vegetated land, and the built environment.

In the following subsections, we will give a concise introduction to climate modelling and development of climate projections at various scales. State-of-art methods to address the

heterogeneity of the surface in calculations of the surface fluxes will be discussed. Moreover, to give background information for subsection 3.3, essential recent and on-going climate modelling projects as well as up-to-date scenarios for CO_2, other greenhouse gases (GHGs) and aerosols are also briefly considered.

3.1.1 Climate simulations at regional scale

The basis for constructing climate change projections for Europe and its cities is given by the international development, since the 1970s, of global climate models (GCMs), also referred to as general circulation models, or more recently Earth System Models. The climate projections currently used in various applications are typically based on processing of output from GCMs that participated in the two latest phases of the Coupled Model Intercomparison Project, CMIP3 (Meehl et al. 2007) and CMIP5 (Taylor et al. 2012). The next phase, CMIP6, is in a preparation stage (Eyring et al. 2016).

For simulations of future climate, climate model experiments need assumptions about the future evolution of atmospheric composition, land use change and other driving forces of the climate system. The CMIP3 global climate models were run under the SRES (Special Report on Emissions Scenarios) and the CMIP5 models under the RCPs (Representative Concentration Pathways) scenarios for greenhouse gases (GHGs) and aerosols. The latter include RCP2.6, RCP4.5, RCP6.0 and RCP8.5, while the most widely used SRES scenarios turned out to be A2, A1B and B1. Future emissions and atmospheric abundances of CO_2 under the previously-used SRES and the current RCP scenarios are shown in Figure 4. For the near future decades, the different concentration scenarios for CO_2 almost coincide but start diverging after about the 2050s. The CO_2 concentrations under RCP8.5 distinctly surpass those under A2, A1B and RCP6.0, whereas RCP4.5 and B1 describe very similar trajectories.

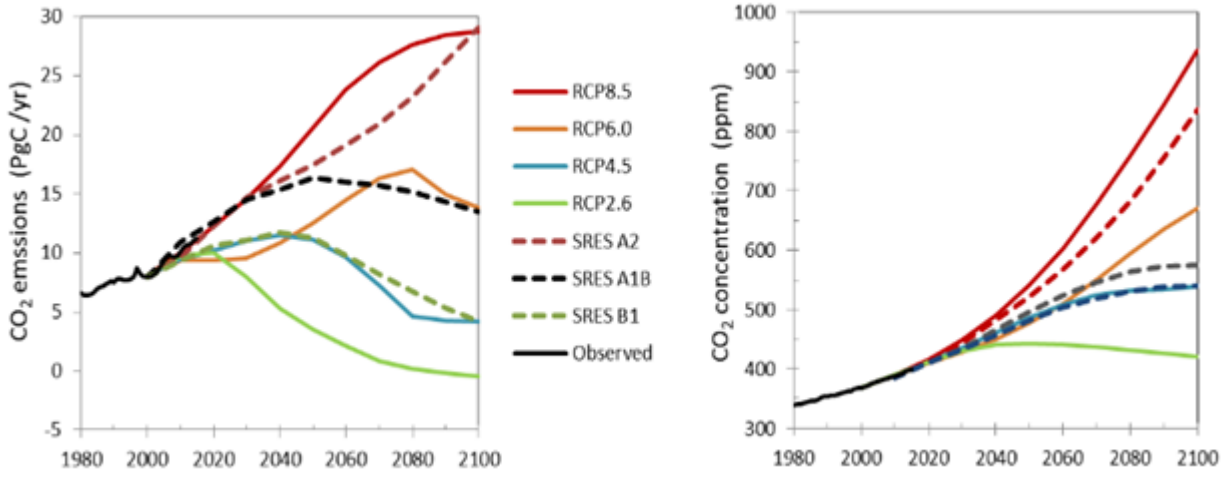

Figure 4: Temporal evolution of the global emissions (left: PgC/yr.) and atmospheric abundance (right: parts per million in volume) of carbon dioxide in 2000–2100 according to four RCP scenarios (solid curves) and three SRES scenarios (dotted curves); see the legend. Observed concentrations for years 1980–2015 are depicted as well. The curves for the RCP and SRES scenarios are based on IPCC (2013) and IPCC (2001), respectively. Past total emissions from fossil fuel combustion, cement production and land-use change are available from Global Carbon Budget (Le Quéré et al., 2016) and the observed abundance data are available for download from NOAA/ESRL. For abundances of other well-mixed GHGs and aerosols, see Annex II of IPCC (2013).

The spatial resolution of output from GCM simulations nowadays is typically as a 150 km grid or coarser. The geographical pattern of the simulated climate response may be downscaled spatially by using regional climate models (RCMs), various statistical/empirical methods or combinations of both. These approaches aim to bridge the gap between climate models and the resolution required by end users.

In dynamical downscaling by means of RCMs, time-dependent information about meteorological conditions in the boundaries of the domain of a RCM is taken from the GCM being downscaled (for more details, see Rummukainen, 2016; Giorgi and Gutowski, 2016). European activities to coordinate RCM experiments include the PRUDENCE project in 2001-2004 (Christensen et al. 2002, 2007), the ENSEMBLES project in 2005-2009 (van der Linden and Mitchell 2009) and the EURO-CORDEX initiative since 2011 (Jacob et al. 2013; Kotlarski et al. 2014). The horizontal grid size of the RCMs involved was about 50 km in PRUDENCE, 25 km in ENSEMBLES and 12 km in EURO-CORDEX (or coarser).

In statistical downscaling of GCM or RCM output, observations of local-scale weather are utilized (Maraun et al., 2010). Classical approaches involve establishing statistical relationships between observed large-scale and small-scale climate variables. It is assumed that the relation holds also in the future climate and that the large-scale variables (e.g., air pressure, geopotential height, temperature, humidity) in the future can be plausibly simulated by climate models (Tomozeiu et al., 2007, 2014; Gharbia et al., 2016). In another category of downscaling methods, gridded climate model output is statistically corrected and downscaled to point scales (e.g., Räisänen and Räty, 2013; Gharbia et al., 2016). Thirdly, weather generators may also be used to statistically downscale climate model output (Tham et al., 2011; Eames et al., 2011; Jones and Thornton, 2013). Systematic comparisons between various downscaling approaches have been conducted in the COST Action VALUE (Maraun et al., 2015).

Uncertainties in climates change projections arise from the future evolution of emissions, internal climate variability and a variety of aspects in modelling the climate system and its interactions at different spatial and temporal scales (e.g., Knutti, 2008). Being forced by the SRES or the RCP scenarios, the climate model simulations do not include economic crisis, so they doesn't account for their uncertainties. Some uncertainty is also involved in downscaling of climate model output. Because the performance in representing the observed climate is typically better for a multi-model mean than for any individual model, it is advisable to consider simulations performed with many models. The level of agreement between the models suggests which changes are more certain than others.

It may be mentioned that a difficulty from the viewpoint of assessing climate change impacts on air quality is the fact that Chemistry Transport Models (CTM) require meteorological data in three dimensions and at high temporal frequency. However, open archives of GCM and RCM simulations typically provide data at a few vertical levels only. A solution to this problem is suggested by Lemaire et al. (2016). They developed statistical air pollutant models that could be used together with output from several EURO-CORDEX RCMs.

3.1.2 Urban micro-climate simulations

Cities occupy less than 1 % of the global land surface, and their direct effect on the atmospheric general circulation and on global climate is probably not very large. Moreover, global and regional climate models, typically having a grid size of tens of kilometres or larger, poorly resolve the urban land surface. Consequently, cities have been largely ignored in projections of future climate change. However, the presence of the built environment strongly modifies the climate and therefore air quality (as noted in the Introduction section) at local to regional scales. As

approximately 50 % of the world's population lives in the urban environment, as well as a large fraction of economic activity residing in cities, climate and climate change in these built-up areas is an urgent subject of study. Climate projections of relatively coarse resolution can be dynamically down-scaled for individual cities or metropolitan areas, by using a nested climate model of higher resolution, provided that this latter is capable of a realistic simulation of air-surface interactions of built-up areas.

Several physical-based surface models can simulate these air-surface interactions at a horizontal scale of about 100 metres (i.e. at neighbourhood or city scales; see Figure 2). Examples of these models include CLASS (Verseghy et al., 1991), CLM (Lawrence et al., 2011), JULES (Best et al., 2011; Clark et al., 2011), LIS (Kumar et al., 2006), Noah (Ek et al., 2003), ORCHIDEE (Krinner et al., 2005), TESSEL (Balsamo et al., 2009), SUEWS (Järvi et al., 2011) and SURFEX (Masson et al. 2013). Such models may be used in standalone mode or coupled to an atmospheric model.

In climate models and numerical weather prediction models, the heterogeneity of the surface is frequently addressed by using a tiling approach, where several surface types may be present in a given grid box. In a tiling scheme, all the surface types present in a given grid cell experience the same atmospheric forcing, but react individually, according to their respective physical properties. Finally, fluxes representing all the different tiles are aggregated, so that the atmosphere reacts to one representative value for the entire grid-cell.

Atmospheric flow at horizontal scales of approximately 100 metres or less (i.e. at street and vehicle wake scales; see Figure 2) can be simulated using computational fluid dynamics (CFD) including large-eddy simulation (LES) models have a grid spacing of metres. These models can resolve the atmospheric flow within the urban canopy (that is the atmospheric layer between the surface and the top of the buildings) (e.g. Letzel, 2007). CFD models remain to be too computationally demanding to permit studies approaching even a regional scale or covering periods of more than a few days. Therefore, climate simulation models and numerical weather prediction models by necessity must parameterize the built environment in the framework of their respective surface interaction models.

Many urban parameterizations still follow highly simplified approaches (Masson, 2006). The most common way is to use a vegetation–atmosphere transfer model whose parameters have been modified. Cities are then modelled as bare soil or a concrete plate. The roughness length is often large (one to a few metres; Wieringa, 1993; Petersen, 1997).

More advanced schemes have addressed the complexity of the urban surface following a canyon approach, where the urban surface is treated as an array of different facets, and the energy budget equation is solved individually for each facet. For example, the models of Masson (2000), Martilli (2002) and Kondo et al. (2005) consider three separate facets of roofs, walls, and road surfaces, while e.g. Best et al. (2006), Dupont and Mestayer (2006) and Porson et al. (2009) chose to merge the walls and road surfaces into one single effective canyon, thus retaining only two energy budgets.

These urban canyon type models simulate more accurate fluxes to the atmosphere than the modified-vegetation models. A review and inter-comparison of all these models is available in Grimmond et al. (2010, 2011). However, when the focus shifts to impacts on the population in cities (in buildings or on the road) or economics (e.g. energy consumption in buildings), it becomes necessary to clearly separate buildings, air within urban canyons, roads, and, if present, trees, gardens etc. The Town Energy Balance (TEB) model (Masson, 2000; Lemonsu et al., 2004), included in the surface interaction model SURFEX, is an example of a model capable of making this distinction.

A multitude of physical processes are taken into account in the Town Energy Balance model TEB: 1) short-wave and long-wave trapping effect of canyon geometry; 2) anthropogenic sensible heat flux from heated or cooled buildings or from traffic and industry; 3) water and snow interception by roofs and roads; 4) heat conduction and heat storage in buildings and roads; and 5) interactions between canyon air and the built surfaces and the canyon micro-climate (temperature, humidity, wind, turbulence).

Waste heat emissions of buildings tend to increase surrounding air temperatures. The energy effects of buildings and building systems on the urban climate on neighbourhood or city scales may be simulated by surface interaction models (e.g. Sailor, 2011; de Munck et al., 2012; Bueno et al., 2012). This contrasts with dynamic building energy simulation algorithms that simulate heat transfer and air flows inside complex buildings dynamically (e.g., Crawley et al. 2008) but are run in an offline mode, i.e. using prescribed meteorological data as input (e.g., Jylhä et al., 2015a, 2015b).

The need to prepare cities for climate change adaptation requests the urban modeller community to implement sustainable adaptation strategies within their models to be tested against specific city morphologies and scenarios. Greening city roofs is part of the overall strategy. The GREENROOF module (De Munck et al., 2013) for the TEB model has been developed to simulate the interactions between buildings and vegetated roof systems at a city scale. This module describes an extensive green roof that is composed of four functional layers: vegetation (grasses or sedums); substrate; retention/drainage layers; and artificial roof layers. The following interactions are calculated: i) vegetation-atmosphere fluxes of heat, water and momentum; ii) hydrological fluxes throughout the substrate and the drainage layers; and iii) thermal fluxes throughout the natural and artificial layers of the green roof.

3.1.3 Development of synthetic weather data for a future urban climate

Synthetic temporally-high resolution meteorological data in an anticipated future climate are needed in simulations of climate change impacts on various sectors, such as air quality, agriculture, hydrology and building energy. According to Belcher et al. (2005) there are two general categories of methods for designing such future weather data sets. One category is based on analogies: use is made of recorded historical weather data from another location with a climate similar to the projected climate of the study location, however this ignores factors such as the solar angle and hours of daylight (Eames et al. 2011). The other category consists of various downscaling methods of climate model output, discussed in Section 3.1.1. One of these methods, i.e. morphing, or time series adjustment, has been applied in several studies to produce future design weather data sets (e.g. Belcher et al. 2005, Wang et al. 2010, Chan 2011). Morphing produces a new weather time series (p_i) that combines observed time series (o_i) with climate change projections. The method aims to minimize the influence of climate model biases and to preserve the realistic weather sequence of present-day data. Shifts in the mean, changes in standard deviation (a stretch or shrinkage) and even changes in skewness may be considered (Räisänen and Räty, 2013; Jylhä et al. 2015a, b).

The observed time series (o_i) used as a baseline for the synthetic future weather time series (p_i) may present a meteorological station or a grid point in a gridded present-day weather data set. Gridded data sets are typically constructed from station observations using kriging interpolation, but they can also be reanalyses products. An option is to construct a spatially-high resolution gridded set of the baseline time series (o_i) in an urban area by using reanalysis data as boundary conditions for a regional climate model or weather prediction model including a

surface interaction modelling system, such as HARMONIE/SURFEX (Section 3.1.2). However, this alternative is computationally expensive and time consuming, meaning that multi-year-runs are in practice out of the question in the scope of the iSCAPE project.

Month	Original year	Temperature (°C)	Relative humidity (%)	Solar radiation (MJ/m²)	Wind speed (m/s)
January	1990	-4.0	89	22.3	4.3
February	1998	-4.5	83	80.6	4.6
March	1994	-2.6	82	231.5	4.1
April	2009	4.5	67	431.6	4.3
May	2006	10.8	63	595.8	4.1
June	2005	14.2	72	607.0	4.0
July	2008	17.3	69	651.2	3.9
August	2003	16.1	76	456.1	4.2
Septemper	1997	10.5	79	295.2	3.9
October	1981	6.2	91	94.3	4.1
November	1989	0.5	89	29.2	4.0
December	1998	-2.2	87	15.8	4.4
Annual		5.6	79	3511.0	4.2

Table 1: Test reference year (TRY) for Vantaa. TRY consists of weather data for twelve months that originate from different calendar years (column 2), each month having weather conditions close to the long-term climatological average. The months for TRY were selected using Finkelstein-Schafer parameters for four climatic variables (air temperature, humidity, solar radiation and wind speed). Columns 3-6 give the TRY monthly means of these variables (Jylhä et al., 2011).

An issue is how long time series of observations (o_i) should be used as a baseline when constructing the synthetic future weather time series (p_i). While a 30-year period of real weather data is often preferred by climatologists, a practical choice is to use typical meteorological years (TMYs) or test reference years (TRYs). TRY is a synthetic year consisting of the most typical months from different years (e.g. Belcher et al. 2005, Jentsch et al., 2008, Ouedraogo et al. 2012; Kalamees et al. 2012). Following the EN ISO 15927-4 standard, typical months can be identified from daily weather data of a long (30-year) period using a statistical method which measures the similarity of two frequency distributions. Those months from these years that have the smallest differences from the long-term climatological distributions, as quantified by the so-called Finkelstein-Schafer parameters, are selected.

As an example, Table 1 shows the selected months in the Vantaa test reference year data set. The months were selected based on daily mean values of temperature, global solar radiation, humidity and wind speed. Monthly mean values of the test reference months and the corresponding climatological values are also given. Note that the weather observations were not made in the centre of Vantaa (Tikkurila) but at the Helsinki-Vantaa airport.

A similar method based on TRYs will be also adopted for the simulation of air quality in future scenarios and assess efficacy PCSs at target cities. This part of the research will be elaborated in WP6.

3.2 Shared Socioeconomic Pathways

The state-of-the-art global scenarios framework for climate change analysis and assessment not only addresses regional dimensions of climate change and uncertainties involved, but also socio-economic variables in terms of possible scenarios that take into account change in society and implementation of specific policies. After the Fourth Assessment Report by the IPCC, a new set of scenarios for the use of climate change research and policy design was put under development (IPCC, 2010). The development process for the new scenarios is essentially parallel - the different pathways for emissions (Representative Concentration Pathways RCPs, see Figure 4) and for socio-economic development (SSPs) were developed in parallel (Moss et al., 2010). Shared Socioeconomic Pathways (SSPs) describe the state and trajectories of societal and economic conditions globally and in different parts of the world. They are reference pathways and do not describe climate policies; the climatic impacts of these pathways depend on indirect consequences of the development. Five separate SSPs have been constructed (O'Neill et al., 2014). Original idea for the form of SSPs was based on three components: 1) a common conceptual framework 2) simple socio-economic narratives and 3) a lean set of quantified variables (Van Vuuren et al., 2012a). The five scenarios can be presented in a simple xy-plane, where on the y-axis the mitigation challenges are increasing, and on the x-axis, the adaptation challenges are increasing. This is depicted in Figure 5.

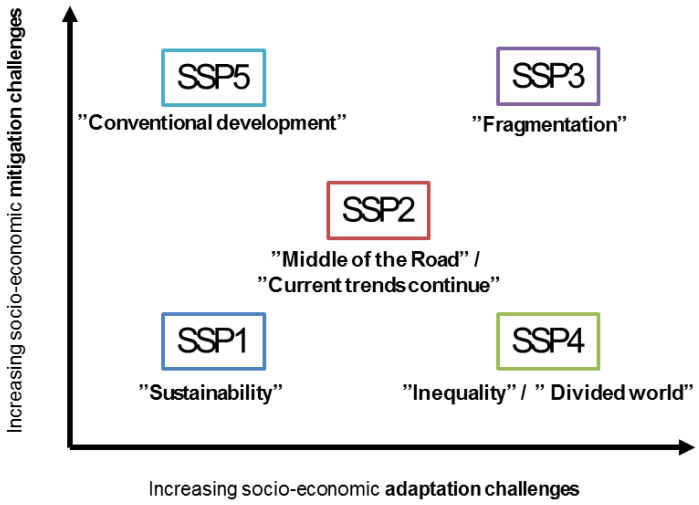

Figure 5: The shared socio-economic pathways. (O'Neill et al., 2014).

The storylines and the variables are available at the SSP database (IIASA, 2012a) and the provided supplementary material (IIASA, 2012b) is maintained by IIASA. Currently available scenario data is limited to the short narrative storylines and sets of key socioeconomic variables (GDP, population and some demographic parameters described further below). The storylines for the pathways are the following (IIASA, 2012b):

- SSP1 – Sustainability: This pathway presents a world making relatively good progress towards sustainability. Lot of effort is made to achieve global development goals as well as reducing energy and resource intensity and dependency on fossil fuels and the Millennium Development Goals are achieved within the next decade or two. Inequality both between countries and within economies is decreased as low-income areas develop rapidly.

Technologic development is also rapid. Economies are globalized and open but strict environmental protection policies are implemented.

- SSP2 – Middle of the Road / Current Trends Continue: In this world, current socioeconomic trajectories are assumed to continue. Some progress towards global development is achieved. Some low-income countries manage to make relatively good progress but many are also stuck with low level of development. The power of global institutions remains very limited and global economy is only partially open. Still most of the economies are politically stable, and the gap between high and low income countries slowly closes.
- SSP3 – Fragmentation / Fragmented World: This pathway represents the greatest challenges to both adaptation and mitigation. The world is fragmented into a few pockets of moderate wealth, areas of extreme wealth and many countries struggling to maintain standards of living for their strongly growing populations. World trade and international co-operation are severely restricted. Policies are oriented towards security instead of sustainable development, and the world is failing to achieve global development goals.
- SSP4 – Inequality / Unequal World / Divided World: In this pathway wealth is distributed very unequally both across and within countries. Small global elite produces most of the GHG emissions while the poorer population remains vulnerable to the climate change impacts. Global institutions work well for the rich elite but provide little support for the development of the poor masses. Mitigation challenges are however low, due to limited overall economic activity and the capabilities of the wealthy players to invest in low-carbon development.
- SSP5 – Conventional Development / Conventional Development First: In this pathway, the world has chosen conventional fossil-fuel dominated development as the solution to social and economic problems. This enables rapid economic growth across the world and helps in adapting to the impacts of climate change, but is hard to fit in with any ambitious mitigation targets.

Currently the available data at SSP database is limited to the following:

- Population by age, gender and education
- Urbanization
- Economic development (gross domestic product GDP, purchasing power parity PPP)

These variables are available at annual level at five-year intervals between 2010 and 2100. Depending on the variable, the global pathways can be separated into 5 or 32 regions; also, country level figures are available. The database contains data series developed by IIASA, National Center for Atmospheric Research (NCAR), OECD and Potsdam Institute for Climate Impact Research (PIK) as well as some historic data by World Bank. The projections between different groups hold a lot of variance. Figure 6 shows the variance between the projections of economic growth in the results of the different modelling groups. Thus, now, there is no unique set of quantitative values chosen for each SSP. However, IIASA has nominated certain data series as “illustrative”, which are consistent with each other and can be used comparably. (IIASA, 2012b).

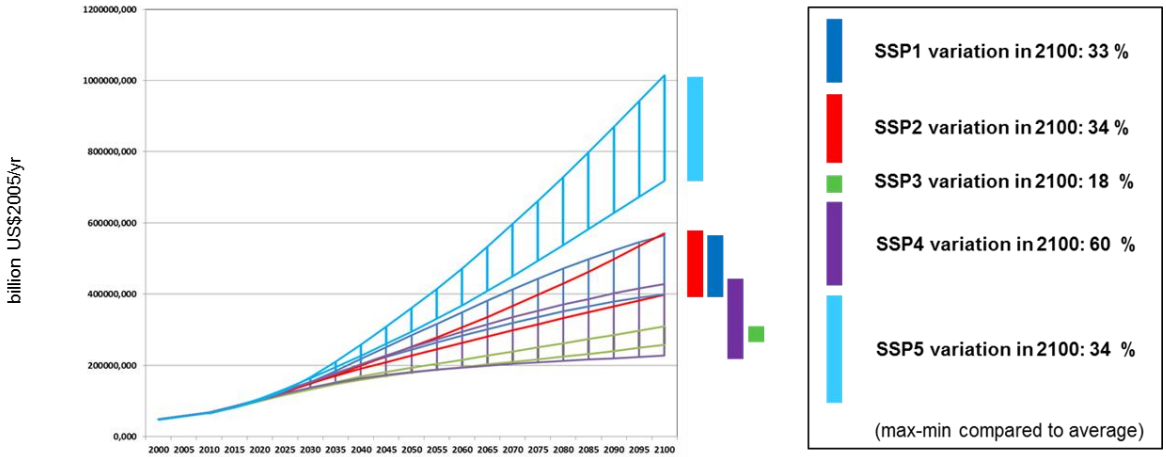

Figure 6: SSP GDP projections of different modelling groups. Global GDP in USD (2005) are presented in the vertical axis, the horizontal axis shows the year. (Data from (IIASA, 2012a)).

As previously stated, the economic and demographic forecasts per SSP scenario and per nation are available from IIASA for the whole world. In the EU FP7 project ToPDAd, these forecasts were related to EUROSTAT's regional economic accounts (at the NUTS-3 administrative level) and EUROSTAT/GEOSTAT's high resolution population database, which were used as baselines. Baselines and forecasts were then downscaled (GDP) or upscaled (population) to a 25x25 km grid for the European continent. These SSP forecasts were finally associated to plausible RCP scenarios of precipitation and temperature (downscaled from 0.5 degrees' grid to a 25x25 km grid), resulting in a regional dataset of paired SSP-RCP economic-population-climate forecasts.

3.3 Changing climate in the iSCAPE study regions

Following from the general overview given in previous sections, this section focuses on the latest understanding about climate change projections for the iSCAPE study regions. Starting from projected future changes, the emphasis is on various climatic variables that are relevant for air quality, together with considerations of past trends. The variables include daily mean temperature, difference between daily maximum and minimum temperature, precipitation sum, incident solar radiation, sea-level air pressure, and wind speed. We recall that daily maximum and minimum temperature is an important information also for low-cost sensors (see D1.5) usage in future years given that their durability is also depending on working temperature range.

The projections are based on a large ensemble of state-of-the art climate model simulations, CMIP5 GCMs (Sec. 3.1.1). The outcomes for the iSCAPE target regions are discussed in comparison with findings of previous research.

The number of CMIP5 GCMs used to construct the multi-model projections, as well as to study consistency in the direction of the change in the individual model projections, was 28 for daily mean temperature, precipitation, solar radiation and air pressure (Figure 7-11), 25 for the diurnal temperature range (Figure 10), and 24 for wind speed. Details about the GCMs and methods used to post-process the model data are given by Ruosteenoja et al. (2016), who also provided the data used to generate the maps.

To be discussed below are climate change projections for the year 2050 under the high-emission RCP8.5 scenario (Figure 4). The changes in the climate variables were calculated

between the baseline period 1981–2010 and the future period 1935-2064, having its midpoint in 2050, and translated to linear trends. The baseline period is analogous to the 20-year reference period 1986–2005 employed by IPCC (2013). Regardless of the time spans explored, however, the geographical distributions of the projected changes are qualitatively similar, but the magnitude of the responses is smaller for earlier periods (Ruosteenoja et al., 2016).

The changes are illustrated as maps across Europe, showing both multi-model mean projections and areas where more than 75 % of the models agree on the sign of the trend. The inter-model agreement can be regarded as good in those areas; elsewhere the climate response is uncertain.

The considerations of detected past trends are based on a literature review that mainly focuses on the most southern, western and northern study regions of iSCAPE: Italy, Ireland and Finland. These regions are at the edge of each climatic region with UK and Germany somehow in the middle.

3.3.1 Temperature

Expectedly, all models agree about a warming trend across all seasons over the whole Europe (Figure 7). Compared to the other iSCAPE study regions, the projected summertime warming is largest in northern Italy and smallest in Ireland. In winter, and also in spring and autumn, the most pronounced increases in temperature are likely to take place in Finland. These projections for the future warming are generally consistent with observed past trends, as discussed below.

In the iSCAPE target region in Italy, the annual mean temperature had a general trend of 0.31 °C per decade over the period 1961-2010, the largest warming in urban areas exceeding 0.50 °C per decade (Antolini et al. 2016). Long-term (1865-2003) seasonal trends in the Po valley ranged from 0.08±0.02 °C per decade in autumn to 0.11±0.02 °C per decade in summer (Brunetti et al. 2006).

On the island of Ireland, based on the average of five long-running observational temperature series, summer mean temperature has increased by 0.93 °C during the period 1900–2014, i.e. about 0.08 °C per decade (Matthews et al. 2016). Moreover, the likelihood of a summer as warm as the warmest recorded summer (1995) has increased by a factor of more than 50 over the observational period.

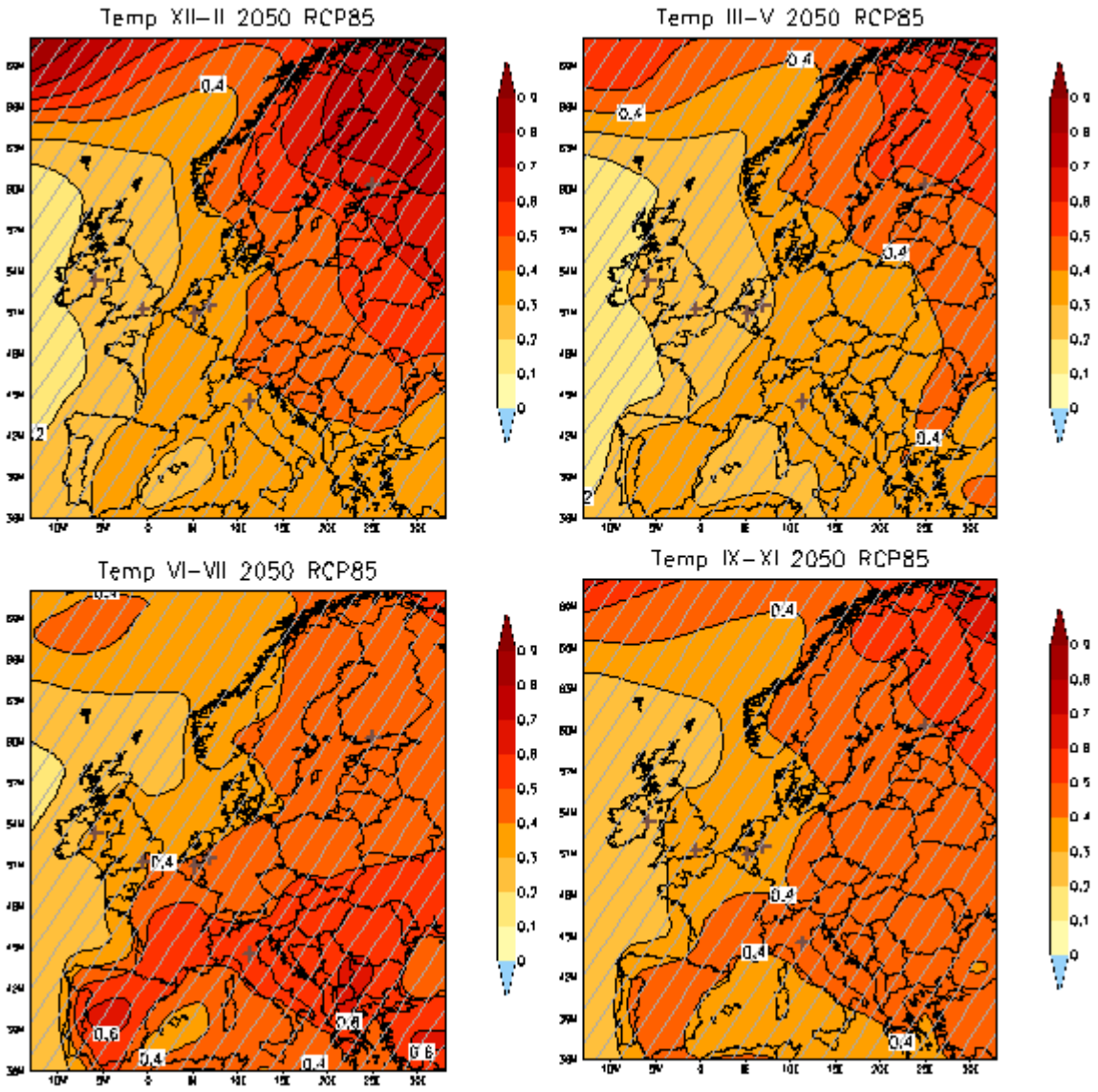

Figure 7: Projected seasonal mean warming (in °C per decade) by 2050 over Europe under the RCP8.5 greenhouse gas scenario. Shading depicts averages of the responses simulated by 28 global climate models (CMIP5 GCMs). The baseline period is 1981–2010 Areas where more than 75 % of the models agree on the sign of change are hatched (for temperature, this condition is fulfilled over the entire domain). The upper left panel depicts December–February, the upper right panel March-April, the lower left June-August, and the lower right panel September–November. The iSCAPE cities are shown by crosses. Based on model data described by Ruosteenoja et al. (2016).

In the iSCAPE target city of Vantaa, Finland, the annual mean temperature had a trend of 0.35±0.07 °C per decade over the period 1980-2009 (Jylhä et al., 2015a). The national temperature average in Finland increased by 0.69±0.56 °C per decade in winter and by 0.29±0.24 °C per decade in spring from 1959 to 2008, without statistically significant warming in summer and autumn (Tietäväinen et al., 2010) despite the record warm summer 2010 (Tietäväinen et al., 2012). The temperature change, between the last and the first 10 years of the period 1847-2013 was largest in December, 4.8 (3.8-5.9) °C (Mikkonen et al., 2014), corresponding to a linear trend of 0.31 (0.24-0.38) °C per decade.

3.3.2 Precipitation

Based on the model projections shown in Figure 8 and numerous previous studies, the general trend is towards wetter in northern Europe and drier in southern Europe. The contour of zero change, as well as the zone where the models notably disagree about the sign of the precipitation change, are located northernmost in summer.

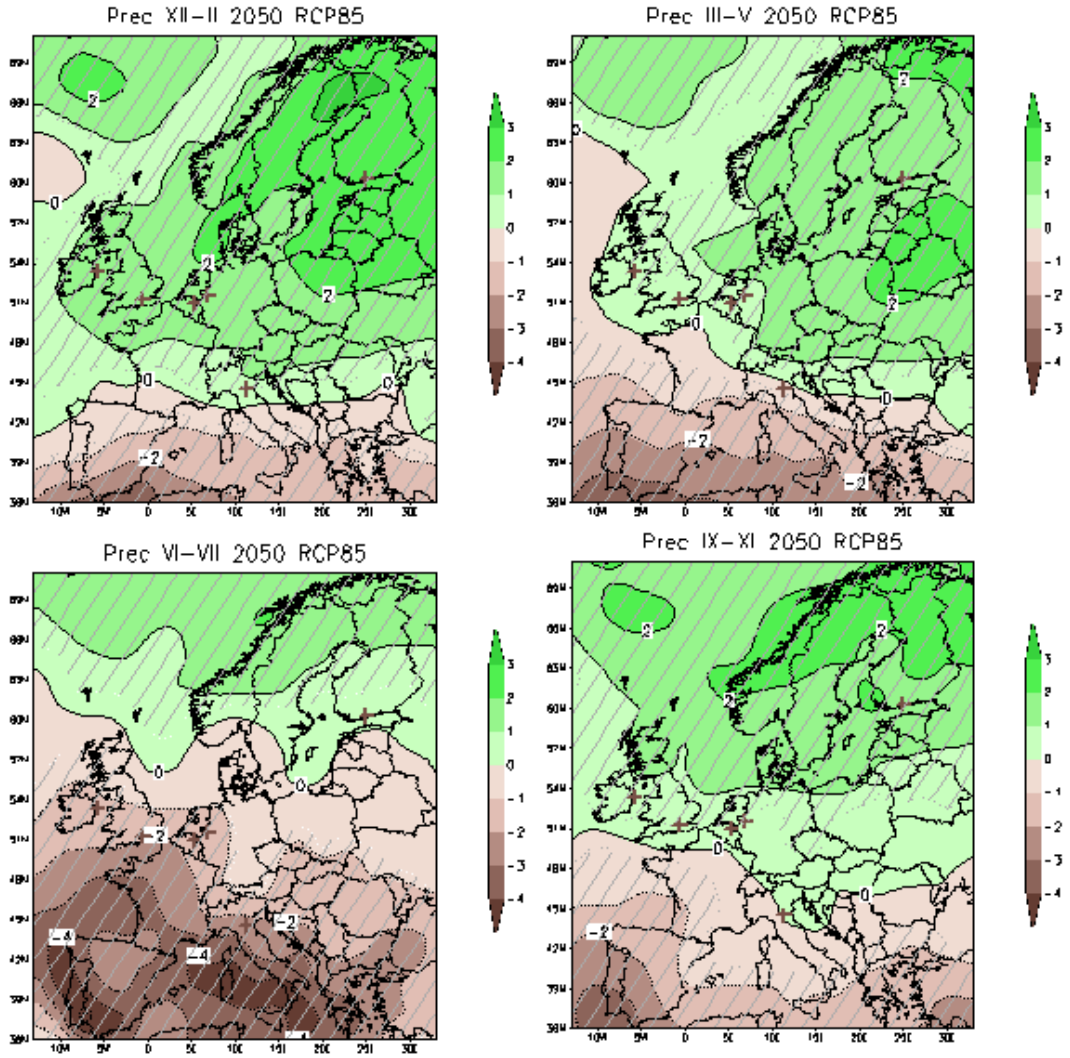

Figure 8: Projected seasonal mean precipitation change (in % per decade) by 2050 under the RCP8.5 scenario. For further information, see caption for Figure 7.

In the iSCAPE study regions, precipitation is generally projected to increase in winter and decrease in summer, except that the sign of the change is uncertain in northern Italy in winter and in southern Finland in summer. In spring and autumn, the agreement in the modelled changes is generally rather low for most of the iSCAPE target regions.

In the Italian iSCAPE region, past recordings of annual and seasonal total precipitation do not reveal any statistically significant century-scale trends (Brunetti et al., 2004, 2006), but during a

period 1961-2008 a general reduction has been observed in winter, spring and summer, and an increase in autumn (Tomei et al., 2010). Besides, the number of wet days has decreased over the period 1880-2002 on an annual basis, as well as in spring and autumn, accompanied with increases in precipitation intensity in summer, autumn and also winter (Brunetti et al., 2004).

In the Island of Ireland, studies by Noone et al. (2016) and Matthews et al. (2016) suggest some increases in winter and decreases in summer precipitation, in accordance with future projections in Figure 8, but the trends were not statistically significant. However, the likelihood of the wettest winter (1994/95) and driest summer (1995) has respectively doubled since 1850 (Matthews et al., 2016).

In Finland, no statistically significant trend has been detected for the country-wide spatial average of the annual precipitation total during the period 1961-2010 (Aalto et al. 2016). However, areas suggesting tendencies towards wetter climate are far more widespread than those suggesting vice versa.

3.3.3 Solar radiation

Incident solar radiation is projected increase in most of Europe in spring, summer and particularly in autumn (Figure 9). In winter increases are likely in Italy, but reductions are to be expected in Finland and perhaps Ireland, while the model projections are controversial in the UK, Belgium and Germany.

In northern Italy during the period 1959-2013, all-sky surface radiation has increased in summer and decreased in autumn (Manara et al., 2016). During the period 1981-2013, all-sky surface radiation increased in all the seasons, particularly so in summer and spring. It was suggested that under all-sky conditions, the variations caused by the increase/decrease in the aerosol content have been was partially masked by cloud cover variations.

In southern Finland during the period 1980-2009, the annual total radiation increased by 1.4 % per decade, most of all owing to an intensification of direct radiation in spring and autumn. In contrast, diffuse radiation weakened by 4 % per decade (Jylhä et al., 2014). Previously, during the period from 1958 to 1992, the mean annual solar radiation had decreased by 1.7 % per decade (Heikinheimo et al., 1996). This earlier reduction was mainly attributed to a pronounced increase in cloudiness, with only a minor contribution from the direct effects of the relatively large aerosol load at that time.

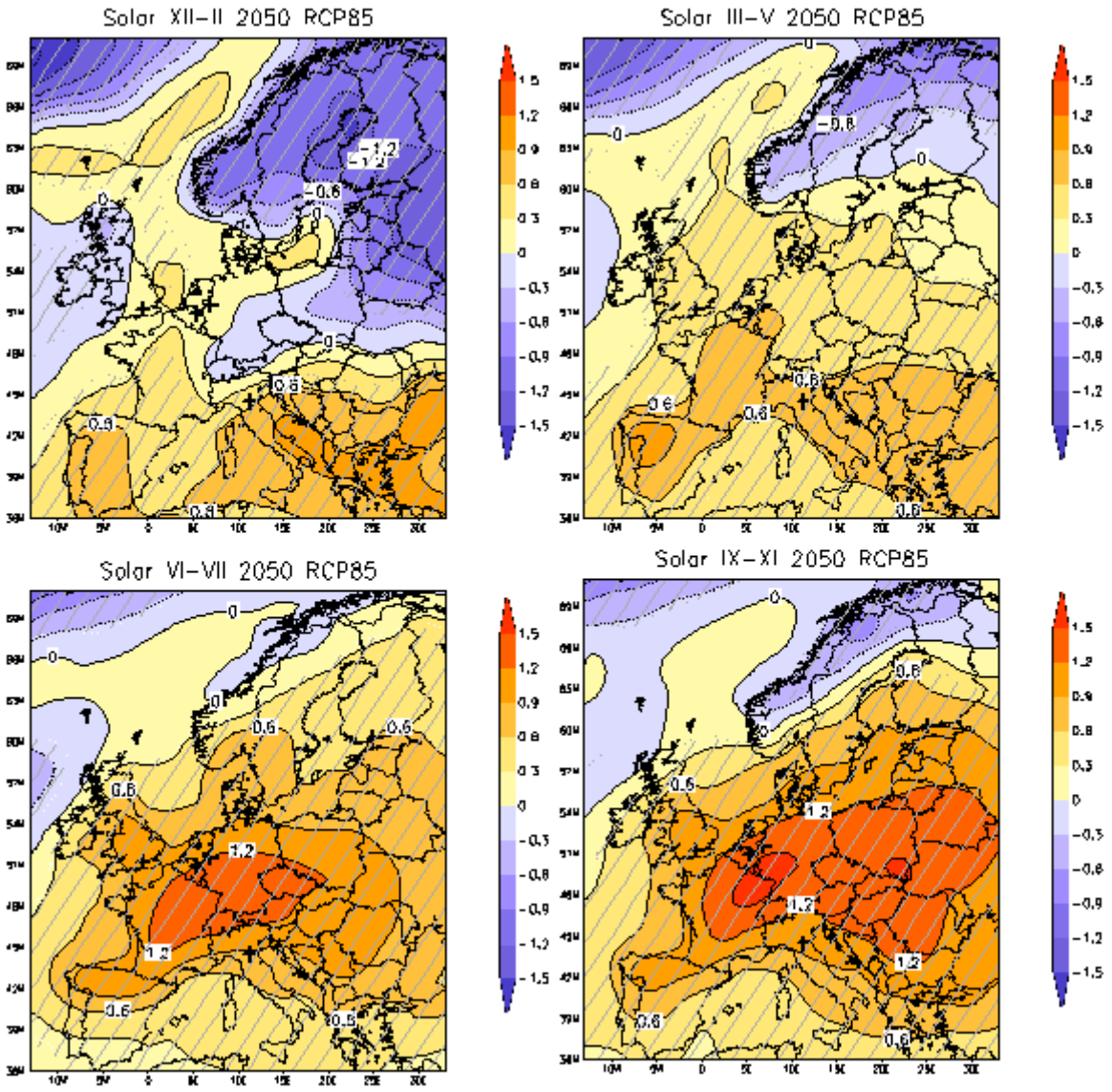

Figure 9: Projected changes in seasonal mean incident solar radiation (in % per decade) by 2050 under the RCP8.5 scenario. For further information, see caption for Figure 7.

3.3.4 Diurnal temperature range

Like incident solar radiation, also diurnal temperature range is affected by cloudiness. Therefore, geographical distributions of their past and projected changes have many similarities (Figure 9 and Figure 10).

The diurnal temperature range is projected to increase in most of central and southern Europe particularly in summer and also in autumn and spring (Figure 10), suggesting larger increases in daily maximum than in daily minimum temperatures. In contrast, reductions in the diurnal temperature range are projected to occur in the north especially in winter and autumn. This can be explained by projected larger increases in daily minimum, rather than in daily maximum temperatures.

In the Po Valley in Italy, the annual mean daily maximum temperature increase of 0.11±0.01 °C per decade over the period 1865-2003 exceeds the corresponding trend for daily minimum temperatures of 0.09±0.01 °C per decade (Brunetti et al., 2006). The observed changes in both variables are largest in winter or spring and smallest in autumn. The diurnal temperature range has increased in all the seasons. According to Simola et al. (2010), the changes in daily maxima and minima have materialized as simple, rigid shifts of the density functions alone, without invoking any change in shape.

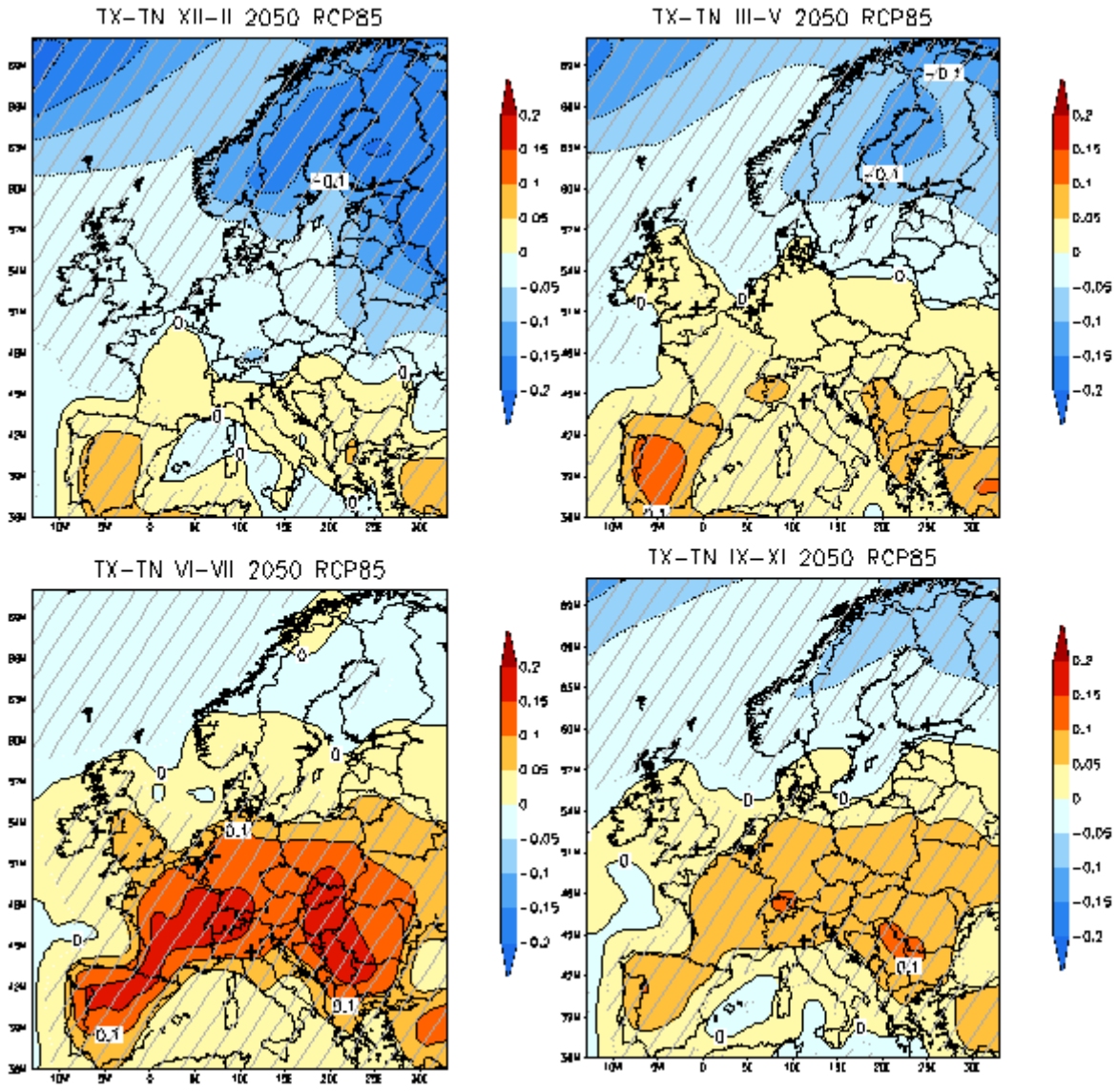

Figure 10: Projected changes in the diurnal temperature range (in °C per decade) by 2050 under the RCP8.5 scenario. For further information, see text and caption for Figure 7.

In Fennoscandia (covering, Norway, Denmark, Sweden and Finland), the daily minimum temperature during spring has increased by 0.40 °C per decade and the diurnal temperature range decreased by 0.18 °C per decade over 1950-1995 (Tuomenvirta et al., 2000). The diurnal

temperature range had a statistically significant annual trend also over the period 1910-1995. This result could be largely explained by changes in atmospheric circulation and increased cloud cover. As regards with country-wide spatial averages in Finland during the period 1961-2010, annual means of daily minimum and maximum temperatures increased by 0.4±0.2 °C per decade and 0.3±0.2 °C per decade, respectively (Aalto et al., 2016).

3.3.5 Air pressure and wind speed

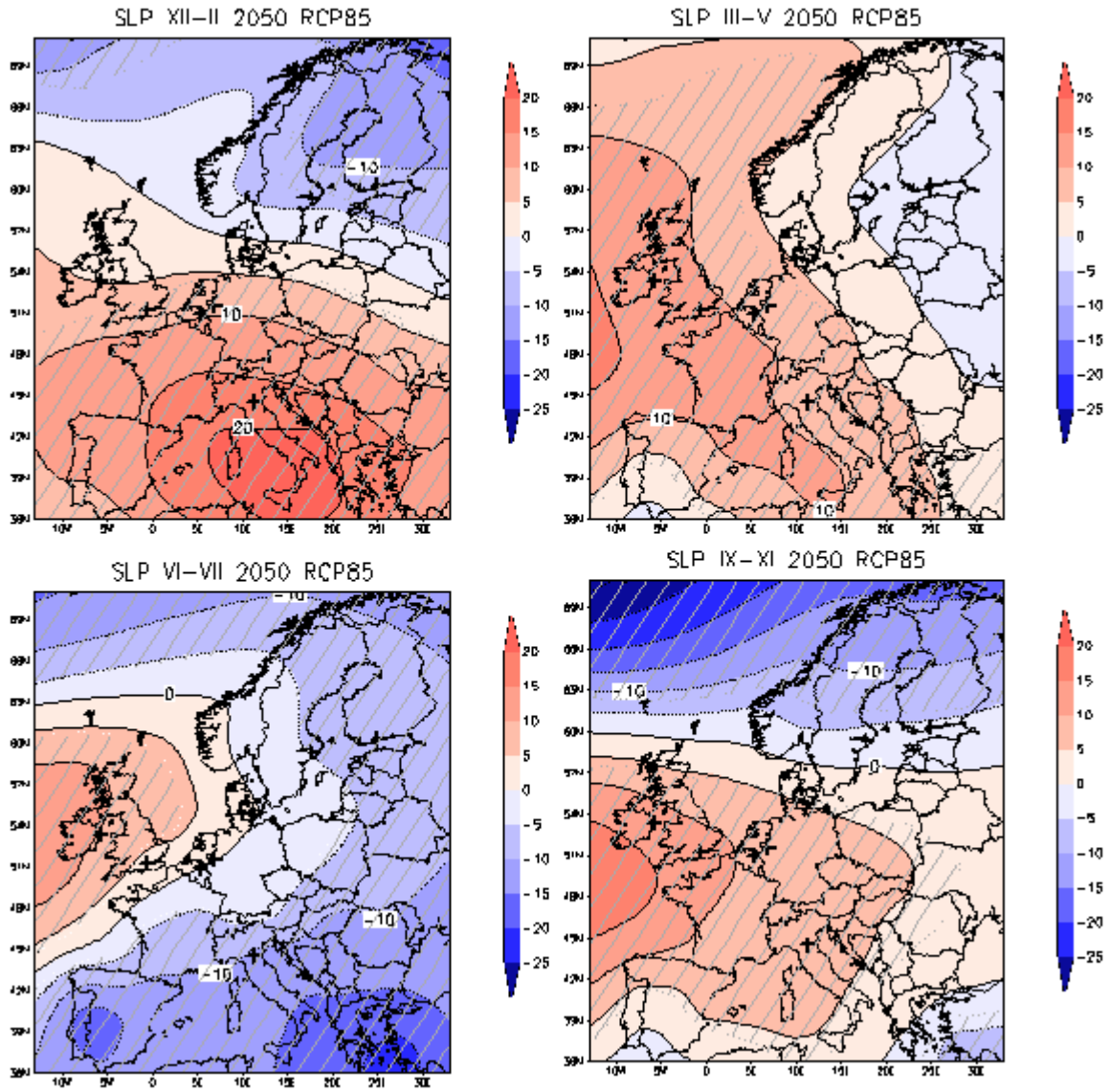

Figure 11: Projected changes in sea level air pressure (Pa per decade) by 2050 under the RCP8.5 scenario. For further information, see caption for Figure 7.

According to the climate projections in Figure 11, wintertime sea level air pressure will increase in southern and central Europe, but decrease in the north. In Ireland and England air pressure seems to increase in all seasons and in Belgium and Germany in all seasons except for the summer simulations.

The models agree on the negative sign of the change in southern Finland more clearly in winter and summer than in spring and autumn.

In the Po Plain, Italy, the annual (and spring) mean air pressures has shown an increasing tendency during the period 1881-2000 (Maugeri et al., 2004). A highly significant positive trend in winter and yearly air pressure all over Italy has been detected also during the period 1951-2000 (Maugeri et al. 2003). Instead, the national average of air pressure in Finland has varied from year to year without any trend across the period 1961-2010 (Aalto et al., 2016).

Future changes in surface wind speed appeared to be uncertain in most of Europe. Nonetheless, more than 75 % of the models agree on an increase in wind speeds in Ireland and England in summer and in Italy in autumn.

3.4 Summary and outlook for further urban climate change work in iSCAPE

There is a number of challenges when trying to assess recent and future impacts of the ongoing global climate change on urban and smaller scales. While the average impact of urbanization on the observed annual-averaged pan-European temperature trend is minor (Chrysanthou et al., (2014), the presence of built-up area strongly modifies the climate on local to regional scales. If a weather station is located in a centre of a growing city, the urban heat island phenomenon tends to reduce homogeneity of observational time series there, which needs to be taken into account. On the other hand, weather observations in an urban area are needed for purposes of validation and verification of physically-based simulations of urban-scale climate.

Future climate in a city depends both on its own growth, design and development, on natural climate variability at all scales, and on the evolution of global emissions of greenhouse gasses and aerosols (the RCPs). The primary tools to make scenarios for the future include a range of global climate models (GCMs) that may be dynamically (RCMs) or statistically downscaled. For the purpose of urban micro-climate simulations, physical-based surface models can be used in standalone mode or coupled to an atmospheric model. In parallel, it is possible to regionally downscale Shared Socioeconomic Pathways (SSPs) that describe the state and trajectories of societal and economic conditions globally and in different parts of the world.

Based on past climatic observations and a large ensemble of state-of-the art climate model simulations (CMIP5 GCMs), climate has and will get warmer in all the iSCAPE target regions. For precipitation, diurnal temperature range, incident solar radiation and air pressure, even the signs of the trend deviate from region to region.

It may be mentioned that while figures in Sec. 3.3 and subsections show climate change projections by the year 2050 under the high-emission RCP8.5 scenario, another target year and the three other RCPs (Figure 4) could have been considered as well. It is also important to keep in mind that besides multi-model means, it is useful to examine scatter across the models in the iSCAPE study sites.

In the next step in iSCAPE, we plan to construct multi-model climate projections on annual and monthly basis for all the iSCAPE cities based on output from the large ensemble of CMIP5 GCMs utilized for the previous figures in this section. The results will be put in the context of

previous and parallel work (e.g., EURO-CORDEX RCMs). Later phases of the work also include demonstrations of outcomes from simulations by the SURFEX model (Sec. 3.1.2).

4 Air quality and climate change interactions over Europe

4.1 Overview

Air quality in Europe has significantly improved in the last decades by the interventions of the agreed by the two AutoOil Programmes and later by the Clean Air approaches, mainly because of technological improvements and stricter legislation requirements for emissions; nevertheless, the problem of air pollution is far from being solved. Figure 12, taken from the 2016 edition of the EEA "report on air quality in Europe", shows that in almost every European country air quality standard are not fulfilled, at least for some pollutants.

NO_2 is mainly a primary pollutant, although it plays an important role in the chemistry of tropospheric ozone; high concentrations of this gas are measured in most large and medium size cities around Europe, usually at roadside monitoring stations.

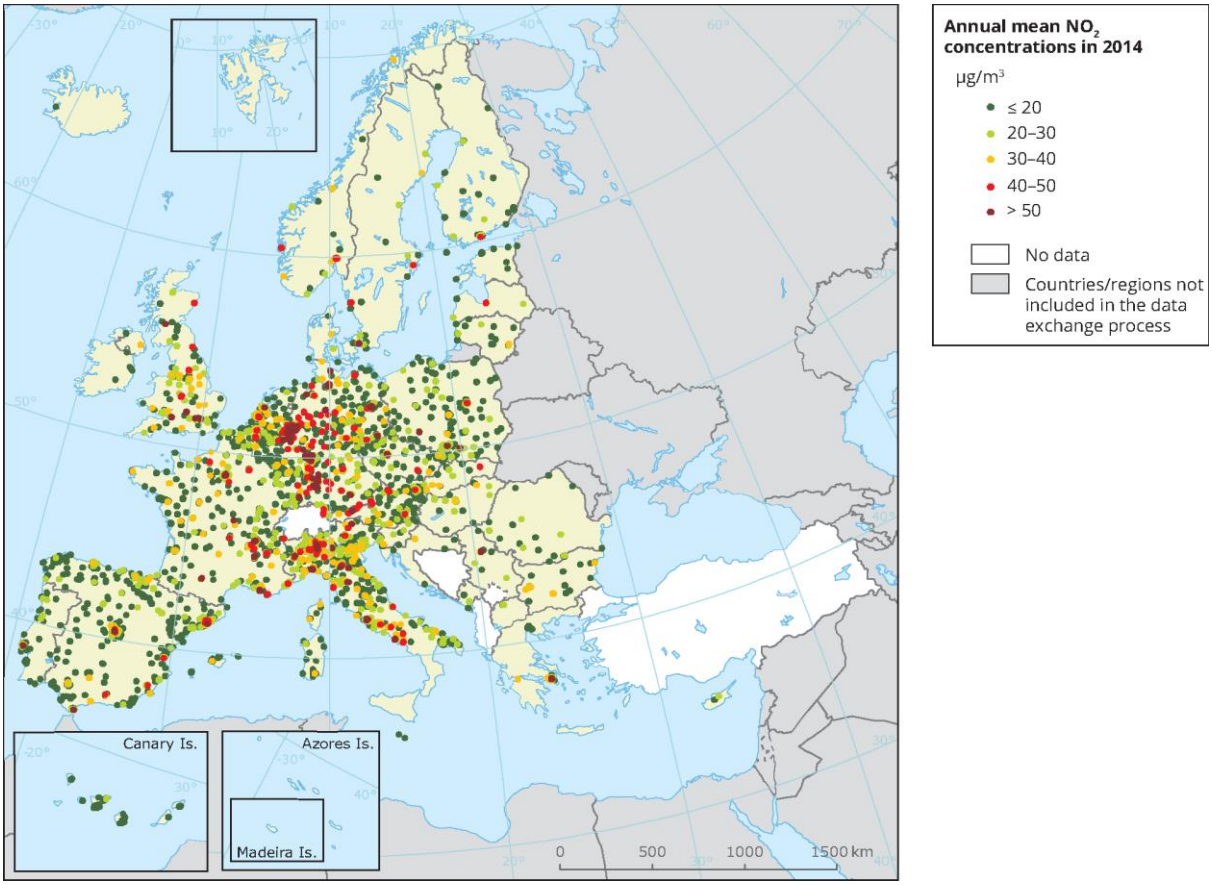

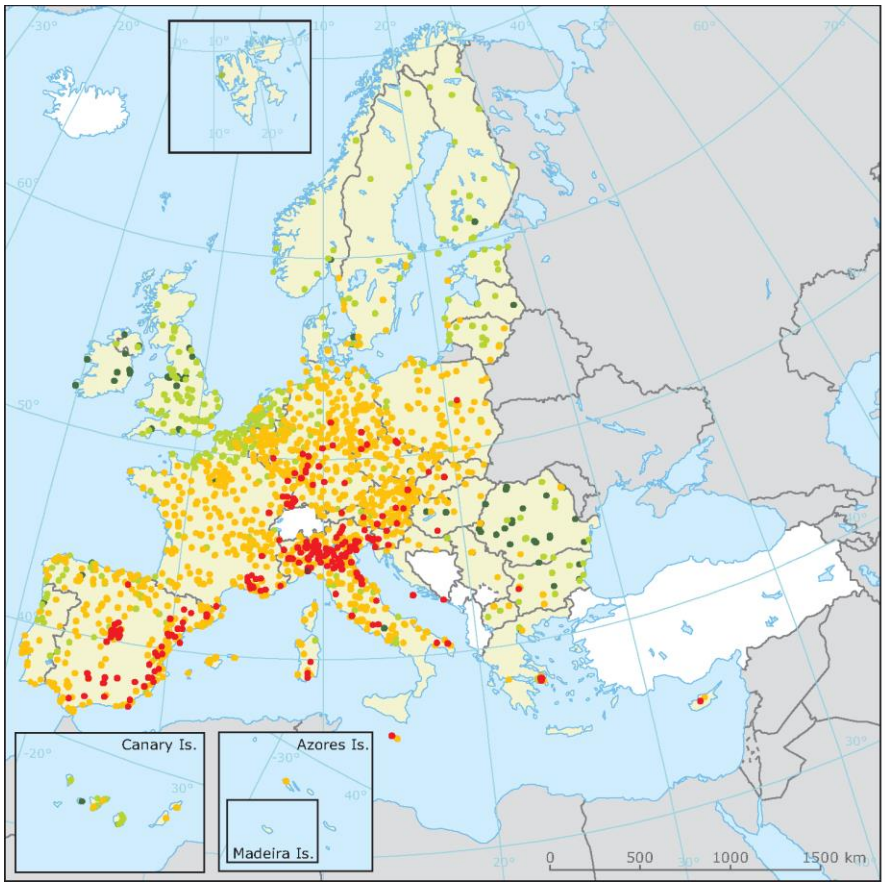

93.2 percentile of O_3 maximum daily 8-hours mean in 2014

µg/m³

- ≤ 80
- 80–100
- 100–120
- 120–140
- > 140

No data

Countries/regions not included in the data exchange process

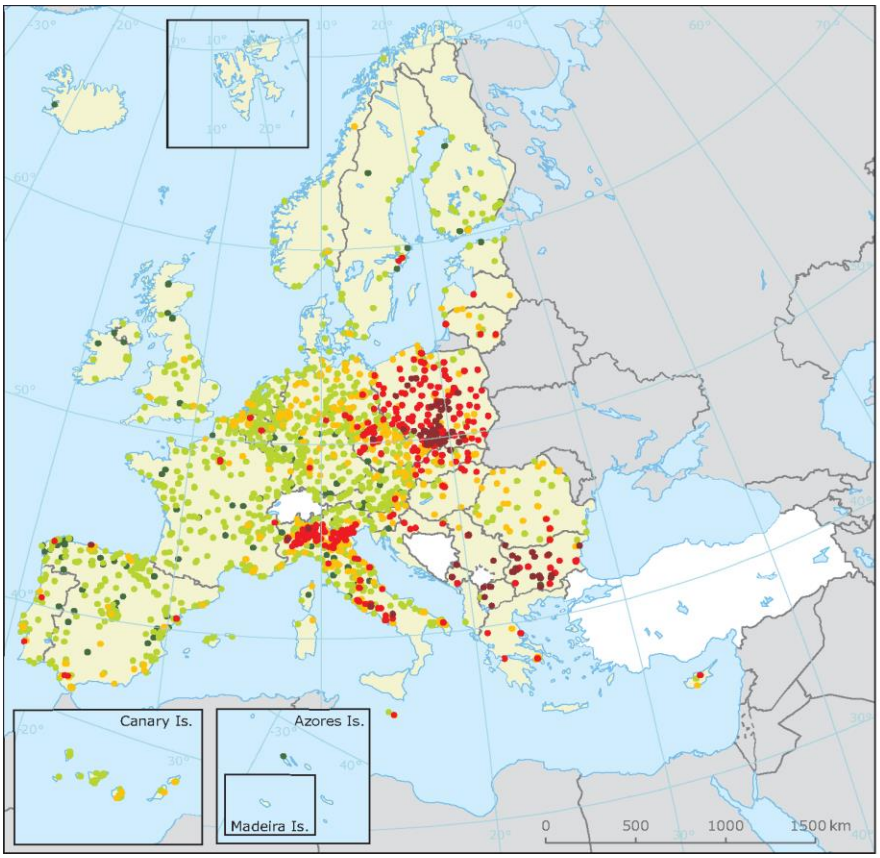

90.4 percentile of PM_{10} daily concentrations in 2014

µg/m³

- ≤ 20
- 20–40
- 40–50
- 50–75
- > 75

No data

Countries/regions not included in the data exchange process

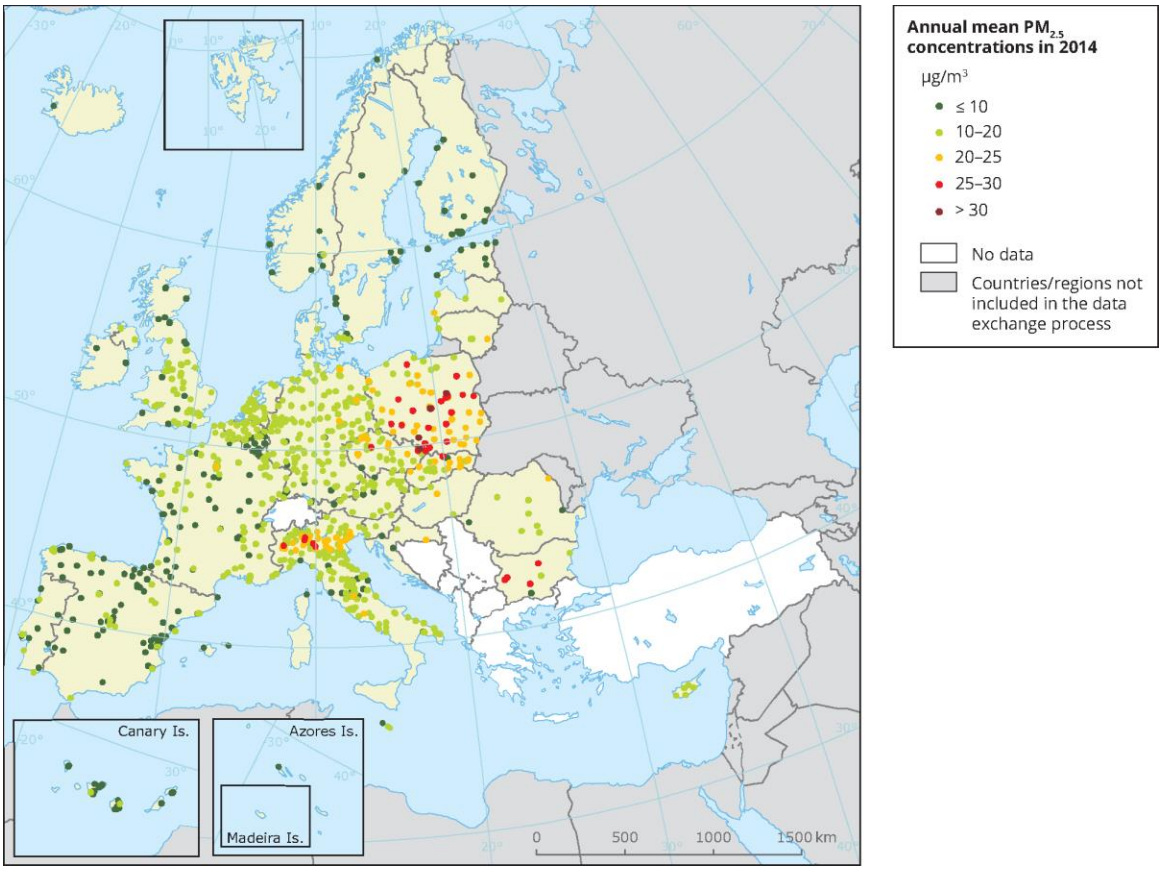

Figure 12: Fulfilment of EU legislation requirements for air quality in 2014: NO_2 (top left), O_3 (top right), PM_{10} (bottom left) and $PM_{2.5}$ (bottom right); every dot corresponds to a monitoring station; red and brown dots indicate that the pollution standards required for each pollutant are not respected. (European Environmental Agency, 2016).

Tropospheric ozone, on the other hand, is a secondary pollutant: it is produced by photochemical reactions that involve NO_2 and many different VOCs, and its concentrations are often rather uniform over large regions. It affects large parts of Mediterranean countries, and can reach high values also in rural areas; its reduction requires large-scale interventions on several classes of emitting sources.

Particulate matter (PM_{10} and $PM_{2.5}$) is both primary and secondary. The highest concentrations are observed at roadside monitoring stations in large cities (due to the local emissions from traffic), in eastern Europe (due to the use of older and more pollute technologies), and in areas where the meteorological conditions are particularly unfavourable to the dispersion of pollutants (Po Valley, some region of Central Europe).

The complete list of EU legislation requirements for air quality is in appendix A. It should be noted that some of the pollutants can harm human health also at low concentrations: for these pollutants, such as PM, the thresholds for concentrations are somehow arbitrary, and are being steadily reduced from year to year.

4.2 Air quality and local climate change interactions

Since Europe is strongly affected by climate variation (Giorgi, 2006), it is important to address all possible effect due to emissions including those at urban scale. Most studies, as largely highlighted in previous sections, address global and region scales; however, information at the local scale is key for understanding the link with urban air quality.

Early studies focused on climate change effects on tropospheric chemistry, particularly tropospheric ozone concentrations, such as Brasseur et al. (1998), Johnson et al. (1999 and 2001) and Derwent et al. (2001). First studies of the effects of climate changes on air pollution at European level are those of Langner et al. (2005), Szopa et al. (2006), Forkel and Knocke (2006). All these studies found marked increase of near surface summer ozone concentrations in response to climate change when assuming no emission control measures. These were attributed to much warmer and drier European summers (as discussed in sect. 3) under future climate conditions. Mixed results were found for the changes in sulfur and nitrogen concentrations.

As mentioned, European regions are one of the most sensitive to climate change. As largely discussed in sect 3, different generations of global and regional model simulations have indicated that the Europe is projected to undergo a warming much larger than the global average, as reported in Deque et al. (2005), Giorgi et al. (2001) and Giorgi and Bi (2005). Moreover, European summer temperature interannual variability might increase in future climate (Giorgi and Bi, 2005), leading to increased frequency of extremely hot summer, such as 2003 summer (Giorgi and Bi, 2005 and Schar et al., 2004). Temperature scenario has an influence on the precipitation pattern projection, which has strong seasonal and spatial trends. Winter precipitation is projected to increase in central to northern Europe and decrease over the southern Mediterranean, while summer precipitation is projected to decrease throughout central western Europe and the Mediterranean basin.

Pollutant concentration variations, within climate change studies are mainly linked to surface temperature, precipitation and sea level pressure (SLP) changes (Giorgi and Meleux, 2007). The increased temperature, especially over lands, implies higher biogenic emissions and faster chemical reactions, both factors being possibly conductive to higher pollutant concentrations. Regional patterns of precipitation change over land can have different impacts: a decrease (increase) of precipitations would inhibit (enhance) pollutant removal. In the end, increases in SLP are indicative of greater subsidence and stagnation, which inhibit pollutant dispersion (Mediterranean regions during winter). Conversely, decreased SLP are generally indicative of increased storm activity and thus increased pollutant dispersion and removal by precipitation (Mediterranean regions during summer). Land warming and drying will also modify SLP patterns; a possible consequence is an intensified anticyclonic ridge over western Europe and northeastern Atlantic that deflects the summer storms track to the north of western Europe and the Mediterranean (Pal et al, 2004), so further reducing wet removal of pollutants. This scenario leads to an increase of both NO_x and isoprene, which are critical ozone precursors. NO_x concentrations rise is restricted within the major metropolitan areas, while isoprene follows areas of strong warming and increased solar radiation.

5 Heat waves

5.1 Overview

In setting up the terminology that bridges climate change and air quality is essential to define heat waves this should not be confused with urban heat island (UHI) that is a local scale phenomenon. Different definitions of heat wave are available in literature, e.g. according to the time needed to have socio-economics or environmental impacts at a given spatial scale. A suitable definition, at least for Europe, of heat wave is given by Robinson (2001) which states that heat wave is a meteorological event of at least 6 consecutive days with maximum temperature exceeding the 1961-1990 calendar day 90th percentile, calculated for each day over a centred 5-day rolling average at each grid point. This choice can be considered well-posed because while heat waves of shorter duration can already lead to environmental and socio-economic impacts, this longer duration is settled in view of the expected increase in the number of long heat waves in a future, warmer, climate (Beniston et al., 2005).

Physical drivers for heat waves can be divided in three categories: synoptic systems, land surface and soil moisture interactions, and climate variability phenomena (Perkins, 2015). Heat waves all over the globe are associated with high-pressure synoptic conditions (anticyclones), which last for several days in the same region. These phenomena are typically called 'blocking high'. Soil moisture plays a key role in enhancing temperatures. When soil moisture is low, its interaction with temperature increases summer temperature variability, resulting in extreme temperatures (Seneviratne et al., 2006). This process is due to the major impact of sensible heat flux over latent one in conditions of dry soil, which induces a positive feedback between atmospheric heating and further drying of the soil (Alexander, 2010). Moreover, when it combines with the blocking high, the positive feedback amplifies. In this contest, land use can play a role, enhancing/mitigating the heat wave impact: irrigation for instance can reduce the intensity of the heat waves during the hottest hours of the day, increasing the soil moisture (Valmassoi, 2016). The role of climate variability in heat wave manifestation is has been investigated only through relationships with temperature extremes at global scale. Climate modal behaviours, e.g. ENSO, can influence global temperature distributions beyond a shift in the mean (Kenyon and Hegerl, 2008). Genesis of blocking high is largely associated with NAO (Della Marta, 2007a). Definitively, climate variability affects physical processes that contributes to heat waves development.

According to Stefanon et al. (2012), heat waves in Europe can be classified in: Russian (RS), West European (WE), East European (EE), Iberian (IB), Scandinavian (SC) patterns plus another centred over the North Sea (NS). Figure 13 shows the six typical patterns after the clustering made on the period between 1950 and 2009.

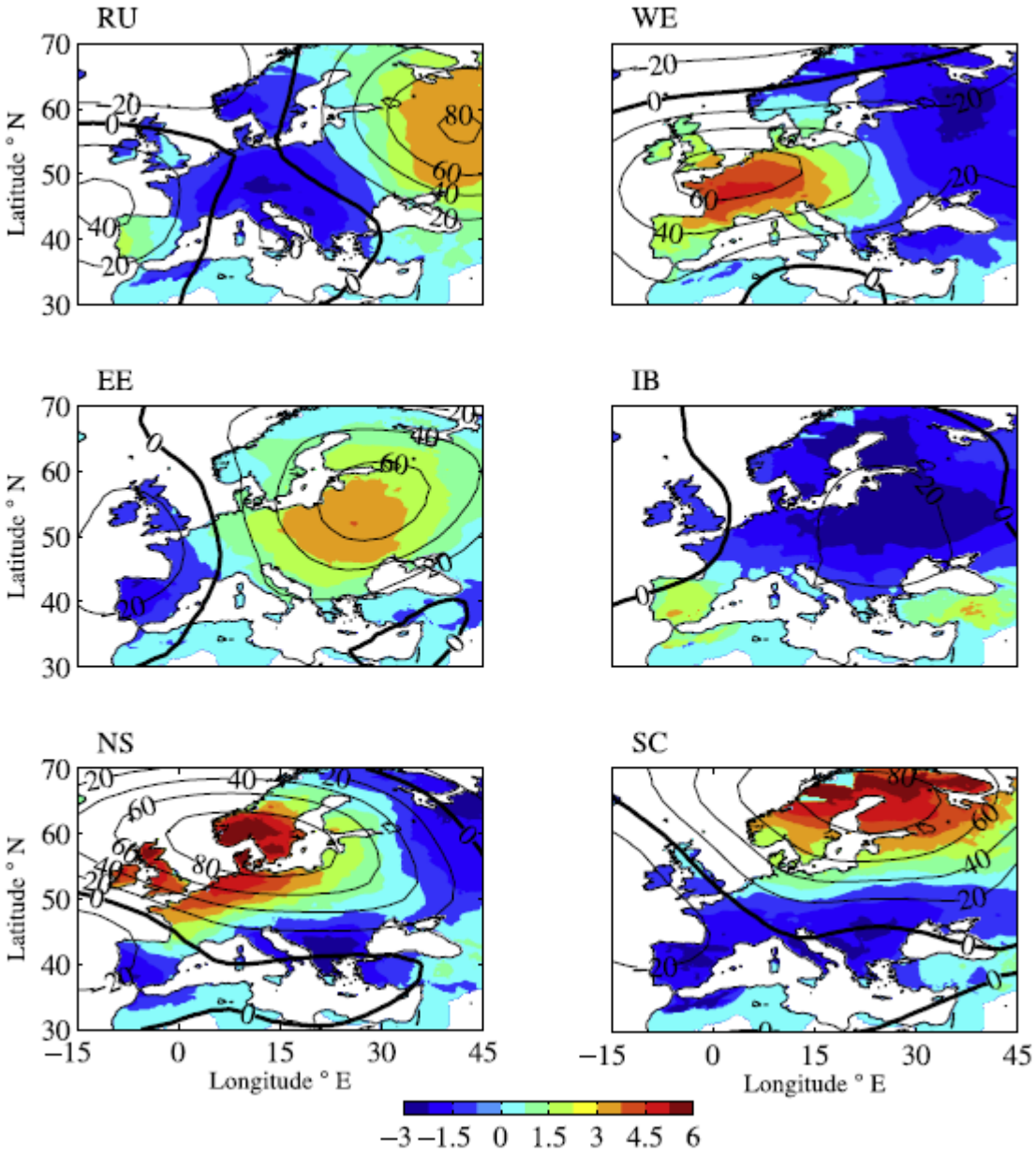

Figure 13: Six typical heat wave clusters over the Euro-Mediterranean region: (a) Russian, (b) Western Europe, (c) Eastern Europe, (d) Iberian, (e) North Sea and (f) Scandinavian. Daily maximum temperature anomalies are in colour and expressed in Kelvin degrees while isolines are the 500hPa geopotential height anomaly. (Stefanon et al., 2012).

Russian cluster groups 128 days of heat wave condition into 14 events over the period 1950-2009. This class expands in the very north-eastern part of the domain over Russia between 35° and 45° E with a temperature anomaly up to 4 °C. It has a shape that is very similar to the one observed during the catastrophic Russian heat wave of summer 2010, although data from 2010 were not included in the analysed period. The Western Europe cluster is centred mostly over France and has a magnitude of 5 °C. It includes 11 events for 82 days. The first half of August 2003 belongs to this cluster. The temperature anomaly pattern of the 2003 heat wave is very similar to the Western European pattern. The Eastern European cluster is approximately centred over Poland. Its magnitude is 4 °C with 23 events for a total of 182 days. It is relatively more spread out than the other clusters. A visual inspection of the different event maps shows events

localized around the Baltic Sea and the Black Sea. The Iberian cluster is located over the Iberian Peninsula, with a second centre over Turkey, along the same latitudinal band across the Mediterranean. It includes 75 hot days in nine heat wave events and displays the weakest temperature anomaly with maximum 3 °C. The North Sea cluster is the hottest, with a magnitude exceeding 6 °C above the mean. It includes 81 hot days in 11 events. The anomaly is centred over the North Sea and spans over Great Britain to the west, the Northern European coast and Eastern Scandinavia. Summer 1976 was very similar to the North Sea pattern. Finally, the SC (Scandinavian) cluster extends over most of the Scandinavian Peninsula with anomalies up to 6 °C. It includes 95 days in 10 events.

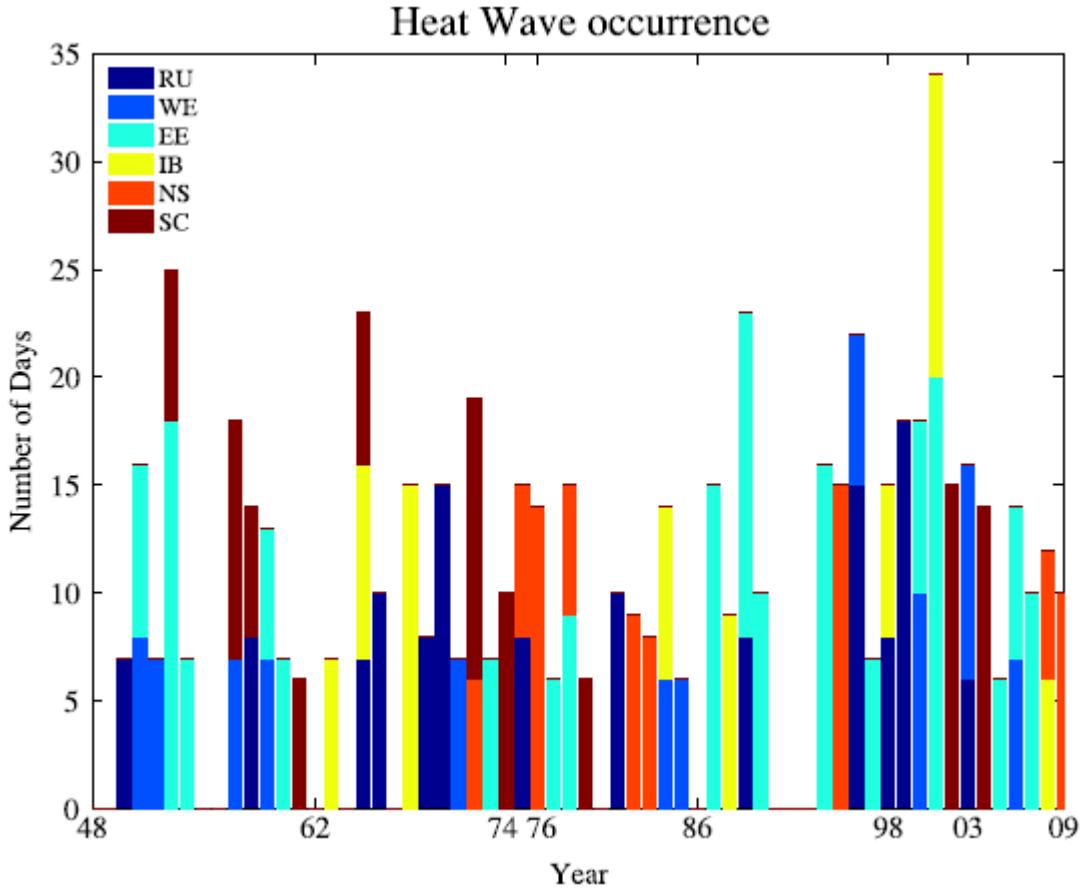

Figure 14: Heat wave climatology in the Euro-Mediterranean region between 1950 and 2009 with attribution to the six heat wave clusters. (Stefanon et al., 2012).

Figure 14 shows the distribution and duration of the heat waves during the investigated period, coloured following the classification. Recent events are present, such as 2003 and 2006 West European heat waves and 1976 North Sea. Mean duration of the heat waves is about 7 to 9 days, depending on which pattern is considered.

Since their dependence on extreme temperature, heat waves are also a topic for future climate studies. Scenarios with increasing GHG in climate projection show an enhanced inter-annual variability of the summer climate in Europe and potentially more frequent heat waves (Giorgi and Lionello, 2008). An increase in climate variability has a greater effect on the society than a change in the mean climate, since adaptation to changes in climate extremes is more difficult (Seneviratne et al., 2006).

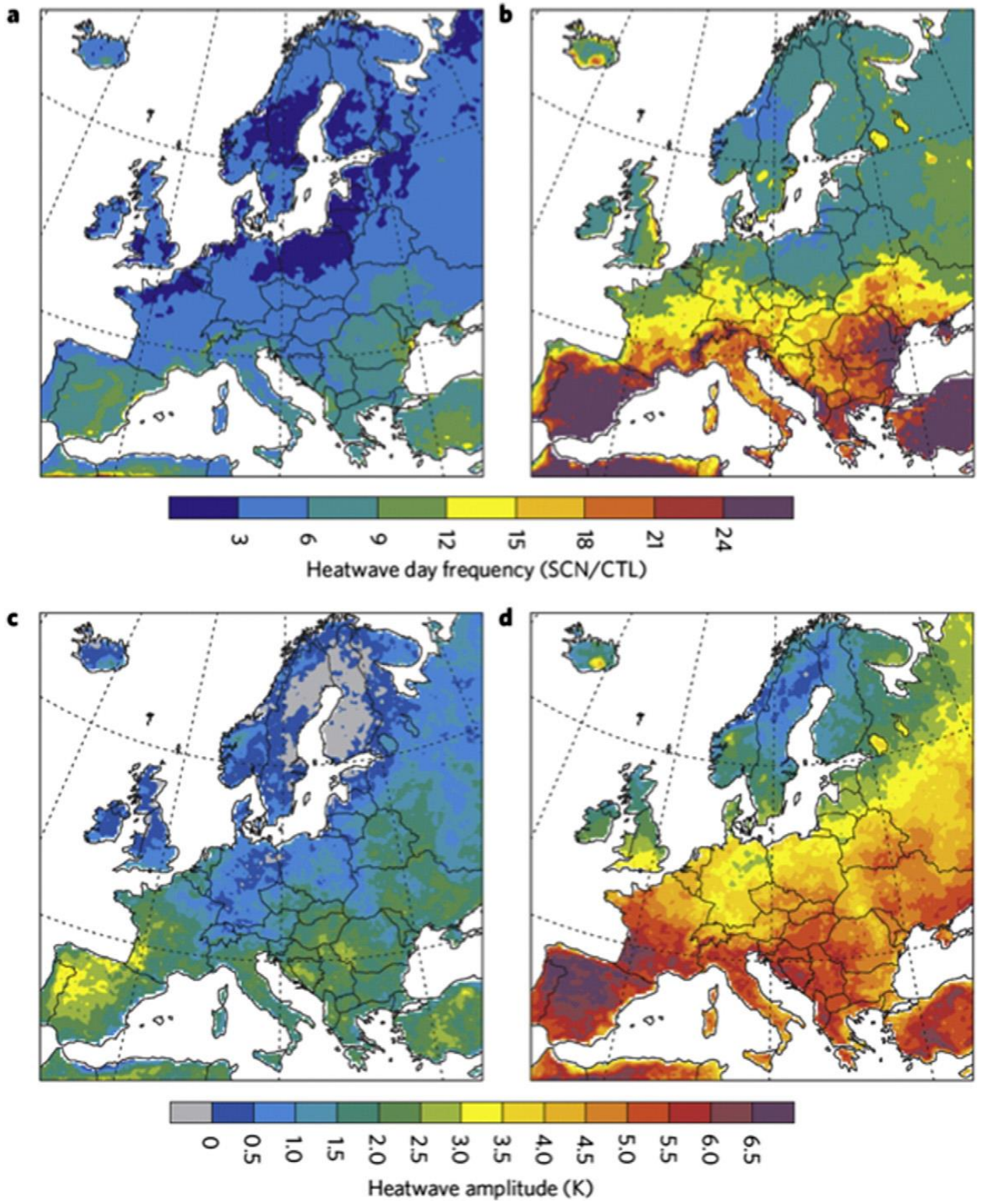

Figure 15: Projected changes via an ensemble of RCMs of average European heat wave frequency (a, b) ad amplitude (c, d) for 2021-2050 (a, c) and 2071-2100 (b, d), with respect to 1961-1990. (Fischer and Schär, 2010).

RCM projections over Europe (Figure 15) show spatial heterogeneity in increases of the intensity, frequency and duration of heat waves (Fischer and Schär, 2010). Larger increases in intensity and duration are projected for southern Europe, particularly over Spain and the Mediterranean, were heat wave days are projected to increase 20-fold by 2100. Other projections over the Mediterranean include dramatic increases in the frequency hot temperature extremes and heat stress by between 200–500 % by the end of the 21st century (Diffenbaugh et al., 2007). The frequency of a European mega-heat wave similar to 2003 is projected to increase by 5–10 fold over the next 40 years (Barriopedro et al., 2011). However, the 2010 Russian event was so extreme that the probability of a similar event occurring again does not increase for at least 50 years (Barriopedro et al., 2011) and is still considered a rare event by the end of the 21st century under a high emissions scenario (Russo et al., 2014).

5.2 Heat Wave Magnitude Index (HWMI)

A useful way to quantify heat waves is the recently introduced Heat Wave Magnitude Index (HWMI) (Russo et al., 2014), defined as the maximum magnitude of the heat waves in a year The HWMI computation for a specific year is a multiple stage process requiring several steps:

- Daily threshold. A daily threshold is calculated for the reference period in Russo et al. (2014), the reference period goes from 1981 to 2010).
- Heat wave selection. For each specific year, it is selected all the heat waves composed of at least a certain amount (to be defined) of consecutive days with daily maximum temperature above the threshold. This certain amount of days depends on the studied region (e.g. 6 days for Europe, 3 on global scale).
- Heat wave to subheat wave. Each heat wave is then decomposed into *n* sub-heat waves, where a sub-heat wave is a heat wave with minimum duration (6 days in Europe, 3 on global scale).
- Sub-heat wave unscaled magnitude. The sum of the maximum temperatures of a sub-heat wave.
- Sub-heat wave magnitude. The sub-heat wave unscaled magnitude is transformed into a probability value on a scale from 0 to 1, which is defined as the magnitude of the subheat wave.
- Heat wave magnitude. The magnitude of each heat wave is defined as the sum of the magnitudes of the n subheat waves.
- Heat wave magnitude index. The maximum of all wave magnitudes for a given year.

According to the index, Russo et al. (2014) found that, in the 11 years between 2002 and 2012, the percentage of global area affected by moderate (HWMI ≥ 2), severe (HWMI ≥ 3), and extreme (HWMI ≥ 4) heat waves was threefold greater than in the previous periods (1980–1990 and 1991–2001). This is evident from Figure 16 showing the geographical pattern of the maximum HWMI, from the ERA-I and NCEP-2 data, within three periods: 1980–1990, 1991–2001, and 2002–2012.

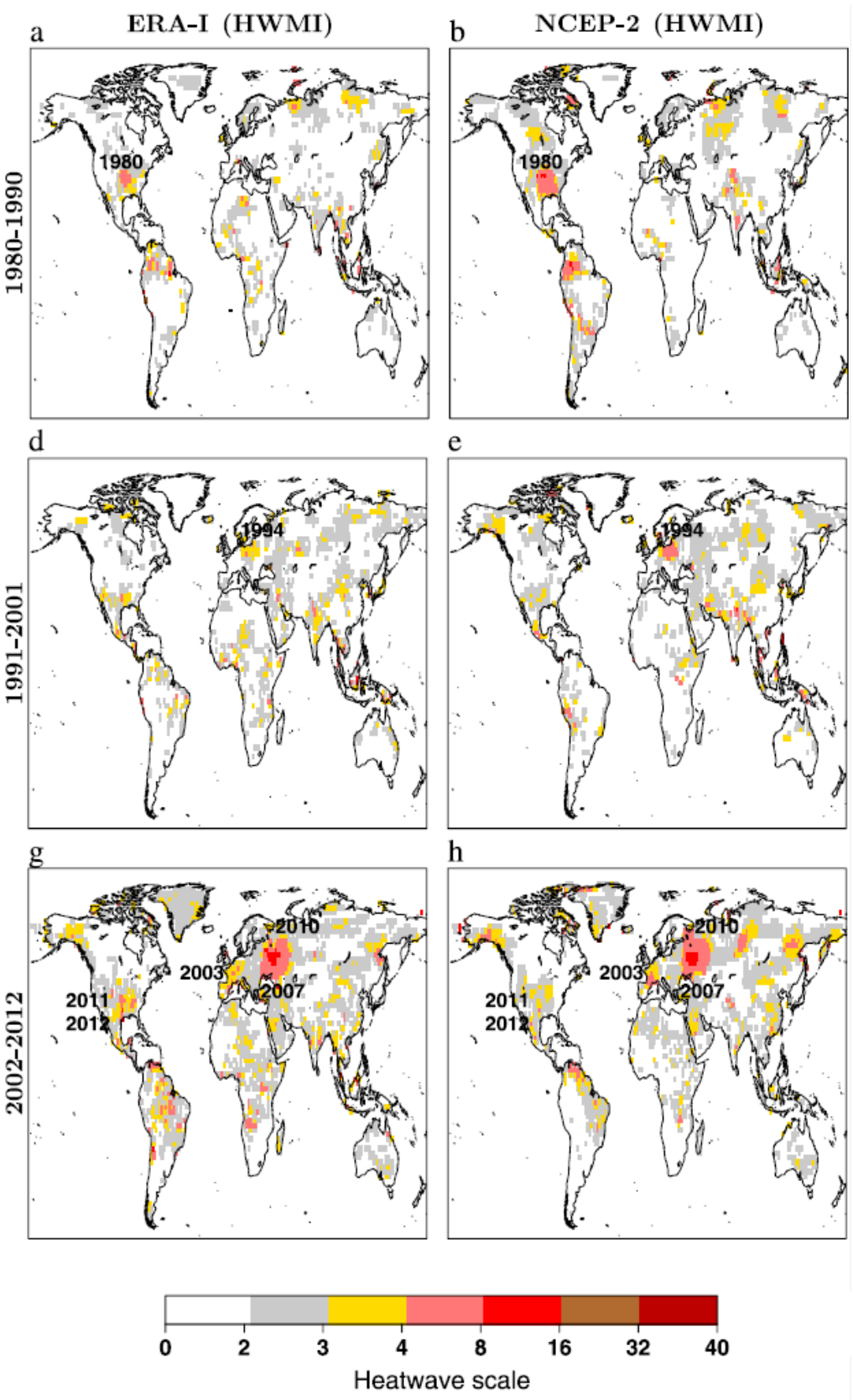

Figure 16: Heat Wave Magnitude Index in three periods of 11 years with reanalysis data: (a, b) 1980-1990, (d, e) 1991-2001, and (g, h) 2002-2012. (Russo et al., 2014).

The 2010 Russian heat wave shows the highest HWMI value and the largest extension with both the ERA-interim and NCEP-2 data sets. In particular, the 2010 Russian heat wave shows a spatial extension nearly 3 times larger and with a maximum HWMI approximately double that of the heat wave in Europe in 2003. Another extreme heat wave, albeit less frequently studied in the literature, occurred in the U.S. in 1980. According to the NCEP-2 reanalysis, the 1980 U.S. heat wave can be considered the second strongest in the period 1980–2012, whereas the ERA-I data show that this event was of comparable magnitude as the 2003 European heat wave.

Projections in a warming world has also been made, using reanalysis data and IPCC AR5 model outputs. According to the HWMI, the extreme Russian heat wave in 2010 can still be considered a rare event in the future climate under the less severe scenarios RCP4.5 and RCP2.6. In fact, it is difficult to link it to greenhouse gas-induced warming (IPCC, 2013). However, in a warmer future climate, the probability of extreme events, such as those in Russia 2010, Europe 2003, and the U.S. 1980, will increase and events considered rare today may be considered the norm under certain future scenarios.

6 iSCAPE cities

6.1 Overview

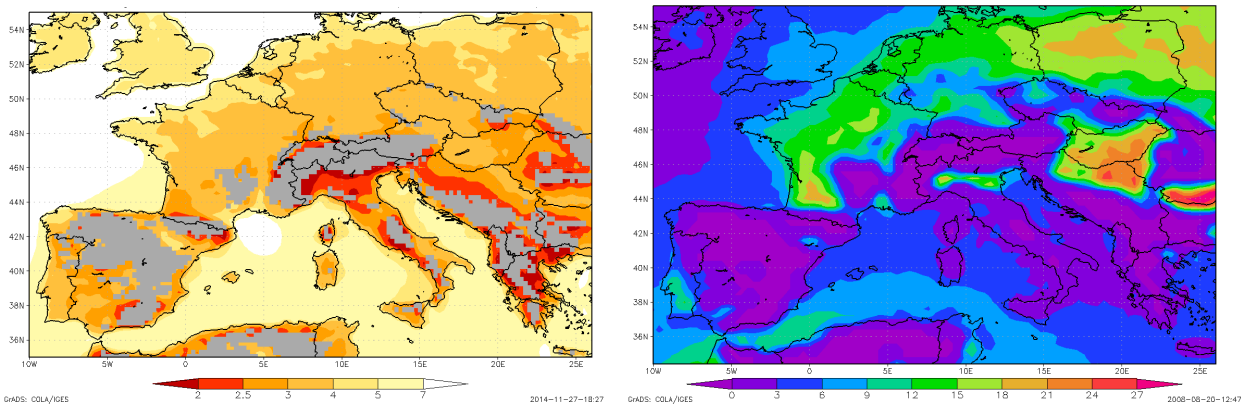

Figure 17: Meteorological conditions over Europe, according to ECMWF operational analysis in years 2006-2014: annual average of surface wind speed (m/s, left) and frequency of occurrence of large temperature inversions in winter months (%, right). (European Environmental Agency).

The problem of air pollution in urban areas is complex; cities in different parts of Europe experience different levels and types of pollution, and the best and most cost-effective policies to improve air quality can be different.

iSCAPE cities represent a wide variety of different geographic locations (Figure 18), type of pollution and meteorological conditions (Figure 17).

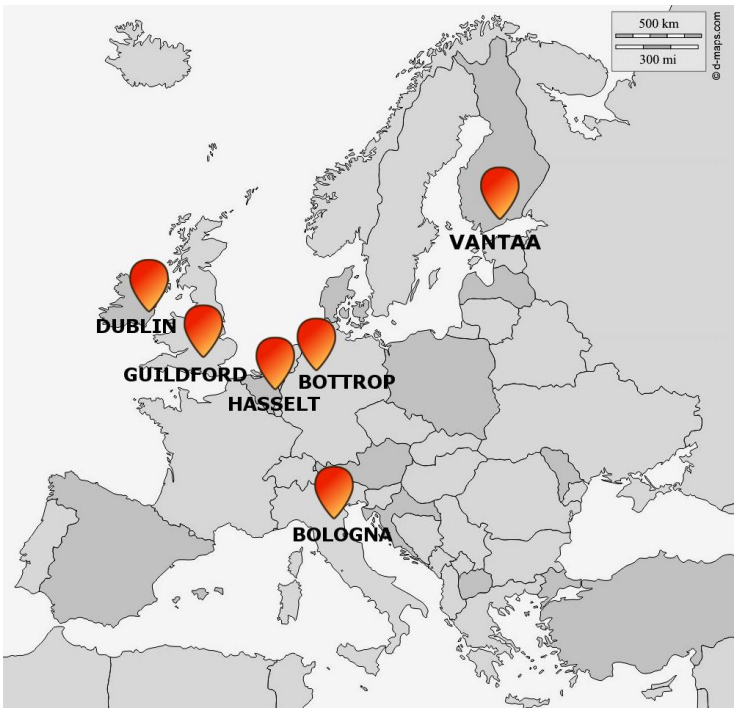

Figure 18: Locations of the different target cities in iSCAPE.

Bologna is located in Po Valley, a geographical area defined as the Po river basin and surrounded by mountain chains (it is only open to the Northern part of the Adriatic Sea). Po Plain includes the four biggest regions of Norther Italy (Piedmont, Lombardian, Veneto and Emilia-Romagna). Due to its geographical location, it is one of the places in the world where meteorological conditions are less favourable to the dispersion of pollutants: average wind speed has the lowest values in Europe, and temperature inversions are frequent, especially in winter months. Almost all types of pollutant are present; PM_{10} and ozone are above legislation limits in almost every city in the region, also in a significant fraction of rural areas.

Bottrop and Hasselt are in the middle of very populated and heavily industrialized areas. Emissions are strong, but meteorological conditions are more favourable than in Po Valley: average wind speed is higher, especially in winter, but episodes of stagnation and strong temperature inversions can nevertheless occur. PM_{10} and NO_2 values are above limits mostly at roadside stations, but also ozone concentrations can sometimes reach high values.

Air quality is generally better in Northern Europe: large cites and industrial areas are more spaced than in Po Valley, Ruhr, or Benelux; winds are stronger, and often carry clean air form the sea. The average PM concentrations in Dublin and Vantaa are almost half than in Po Valley, while Guilford experience intermediate values. NO_2 concentrations can nevertheless reach high values in the busiest streets and near the strongest emitting sources of all iSCAPE cities.

In the following subsections, a synthetic overview of air quality in each iSCAPE city is presented. Annual average concentrations of the main pollutants (NO_2, O_3, $PM_{2.5}$ and PM_{10}) are shown for years 2010-2015, to build a snapshot picture of air quality that is not affected by changes in emissions and interannual variability of meteorological conditions. Examples of air quality policies and assessment methodologies that has been applied to each city are also presented.

6.2 Bologna and Lazzaretto (IT)

6.2.1 Air Quality

Figure 19: Map of Bologna and surrounding. Yellow squares represent monitoring stations: Via Chiarini (26), Giardini Margherita (28), San Lazzaro (32) and Porta San Felice (33).

ARPAE provides four sites monitoring air quality in Bologna: Giardini Margherita, Via Chiarini, Porta San Felice and San Lazzaro (Figure 19). They collect data which represent respectively the urban background, the suburban background and the urban traffic (both last two sites) in the city centre. Not all the sites measure all the pollutants.

East and West Po Valley data are averaged values from different provinces of Emilia Romagna. East Po Valley includes the districts of Ferrara, Ravenna, Forlì-Cesena and Rimini; West Po Valley includes Piacenza, Parma, Reggio Emilia and Modena.

In the context of iSCAPE a detailed report of pollutants concentrations in different environments inside the city will provide an indication of different distribution patterns at street/neighbourhood scale. It also highlights the role of traffic-induced emissions in an urban environment, suggesting the requirement of new solutions which might lead to a reduction of impacts on human health.

Lazzaretto living lab is a controlled environment in real atmospheric conditions run by UNIBO's Engineering Campus, where students will be informed of iSCAPE project and if possible they will take part in the campaign of measures. It is located in one of the peripheral neighbourhoods of Bologna. Here measures of traffic-related concentrations are preparatory for assessing the role of photocatalytic coatings both on buildings and road surfaces in pollutant removal.

Table 2 shows the annual mean concentrations of NO_2. The mean concentrations obtained by the city centre monitoring station are 20 % higher than the European limit and higher than the mean concentrations obtained by the East Po Valley and West Po Valley urban traffic measuring stations. The mean concentrations obtained by the other monitoring stations in Bologna are 5-10 % lower than the European limit. The monitoring station called Giardini Margherita that is near to one of the biggest parks downtown shows mean values very close to the European limit. Trends over the 5 years' period is almost constant everywhere, except for Bologna San Lazzaro and the suburban mean in West Po Valley where concentrations are decreasing.

		Annual mean concentrations of NO_2 $(\mu g/m^3)$					
		2010	2011	2012	2013	2014	2015
Bologna	Giardini Margherita	34	36	31	ND	38	38
	Via Chiarini	ND	26	25	24	26	26
	Porta San Felice	52	62	55	54	54	61
	San Lazzaro	44	36	36	39	26	28
East Po Valley	Urban Traffic	40	37	37	35	33	38
	Rural Background	19	16	16	15	14	15
West Po Valley	Urban Traffic	48	51	46	42	41	46
	Suburban Background	31	27	26	23	19	22

Table 2: Annual mean concentrations of NO_2. Differences between urban traffic and background measurements are shown. The European limit for NO_2 annual mean concentrations is 40 µg/m^3. ND stands for no available data. (ARPAE, 2015).

Table 3 shows the annual concentrations of O_3 in Bologna, computed as the annual averaged value of 8-hours daily mean concentration. No information can be obtained from a comparison with the European limit because it concerns the number of days in which the 8-hour mean

concentration exceeds 120 µg/m^3. This number should not exceed 25 days, averaged over three years.

		Annual mean concentrations of O_3 $(\mu g/m^3)$					
		2010	2011	2012	2013	2014	2015
Bologna	Giardini Margherita	40	48	46	52	44	41
	Via Chiarini	ND	46	46	42	38	43

Table 3: Annual mean value of maximum daily 8-hour mean O_3 concentration. Differences between urban traffic and background measurements are shown. The European human health threshold for O_3 maximum daily 8-hour mean concentration is 120 µg/m^3 (not to be exceeded for more than 25 days averaged over three years). ND stands for no available data. (ARPAE, 2015).

Table 4 shows the number of annual concentrations exceeding the threshold for ozone concentration, i.e. when the daily averaged value, computed on 8 hours, is bigger than 120 µg/m^3. Data are obtained only for the urban background and the suburban background stations. Table 4 shows that values are higher than the European limit, because this number should not exceed 25 days, averaged over three years.

		Number of annual concentrations exceeding the threshold for O_3 $(\mu g/m^3)$					
		2010	2011	2012	2013	2014	2015
Bologna	Giardini Margherita	15	66	58	75	44	41
	Via Chiarini	ND	73	70	52	25	43
East Po Valley	Urban Background	18	31	29	25	24	37
	Rural Background	58	83	58	40	16	39
West Po Valley	Urban Background	48	80	64	61	31	62
	Rural Background	65	83	75	67	32	63

Table 4: Annual number of ozone concentrations excesses of the threshold for human health (daily average computed on 8 hours bigger than 120 µg/m^3). European limits state that the threshold must not be exceeded for more than 25 days averaged over three years. ND stands for no available data. (ARPAE, 2015).

Table 5 shows the annual mean concentrations of PM_{10}. The mean concentrations obtained by the city centre monitoring station are 10 % lower than the European limit, but higher than the mean concentrations obtained by the East Po Valley and West Po Valley urban traffic measuring stations. The mean concentrations obtained by the other monitoring stations in Bologna are 20 % lower than the European limit. The monitoring station called Giardini Margherita shows mean values very close to the suburban background station, called via Chiarini. In the last two years, Urban Traffic concentrations are decreasing, closing the gap with the other urban environments.

		Annual mean concentrations of PM_{10} $(\mu g/m^3)$					
		2010	2011	2012	2013	2014	2015
Bologna	Giardini Margherita	24	29	26	19	ND	26
	Via Chiarini	ND	31	29	24	22	26
	Porta San Felice	34	37	37	32	25	29
	San Lazzaro	27	31	30	25	24	28
East Po Valley	Urban Traffic	30	34	33	28	25	25
	Urban Background	25	30	29	20	24	26
West Po Valley	Urban Traffic	36	40	40	33	31	36
	Urban Background	26	30	28	23	28	30

Table 5: Annual mean concentrations of PM_{10}. Differences between urban traffic and background measurements are shown. The European limit for PM_{10} annual mean concentrations is 40 μg/m^3. ND stands for no available data. (ARPAE, 2015).

Table 6 shows the number of days with PM_{10} concentrations exceeds 50 μg/m^3. Table 6 shows that the values measured by the Urban Traffic monitoring stations are higher than the European limit, while the values measured by the other monitoring stations are near to the limit. As viewed for concentrations, also daily exceedances are decreasing in all the environments.

		No of days with PM_{10} concentrations exceeds 50 $(\mu g/m^3)$					
		2010	2011	2012	2013	2014	2015
Bologna	Giardini Margherita	29	42	33	10	ND	23
	Via Chiarini	ND	40	40	18	19	25
	Porta San Felice	63	69	73	57	23	38
	San Lazzaro	35	50	43	25	20	35
East Po Valley	Urban Traffic	48	60	63	41	29	48
	Urban Background	38	47	49	26	23	33
West Po Valley	Urban Traffic	72	88	92	56	43	59
	Urban Background	47	61	61	35	28	40

Table 6: Number of days with PM_{10} concentrations exceeds 50 μg/m^3 (value not to be exceeded more than 35 times per year). Differences between urban traffic, urban background and rural background measurements are shown. ND stands for no available data. (ARPAE, 2015).

Table 7 shows the annual mean concentrations of $PM_{2.5}$. The mean concentrations in all the monitoring stations are 5-10 % lower than the European limit, and almost equal one to another, with the exception of Giardini Margherita which is slightly less polluted.

		Annual mean concentrations of $PM_{2.5}$ $(\mu g/m^3)$					
		2010	2011	2012	2013	2014	2015
Bologna	Porta San Felice	21	23	22	20	18	20
	Giardini Margherita	17	20	18	15	15	18
East Po Valley	Urban Background	20	22	21	17	17	18
	Rural Background	19	22	20	35	17	19
West Po Valley	Urban Background	22	25	24	20	16	21
	Rural Background	21	22	22	19	18	21

Table 7: Annual mean concentrations of $PM_{2.5}$. Differences between urban traffic, urban background and rural background measurements are shown. The European limit for $PM_{2.5}$ annual mean concentrations is 25 µg/m^3 (updated to 2016). (ARPAE, 2015).

Traffic induced emissions play a key role in the distribution of pollutants in the city of Bologna and, in general, inside the Po Valley. These could explain the high NO_2 concentrations at Porta San Felice, and for the other urban traffic sites, with respect to the other environments. On the other hand, PM_{10} concentrations at trafficked sites are not so higher than in the other environments, suggesting a weak dependence of traffic flow and annual mean PM_{10} concentrations. However, at daily scale, road traffic can induce PM_{10} concentrations, while on a long-time-average this dependence is lost.

6.2.2 Effect of atmospheric warming on ozone concentrations

The fifth IPCC report (IPCC 2013) pointed out the mutual interconnection between air quality and climate change. Different pollutants may contribute to climate change, enhancing or reducing its intensity. On the other hand, a variation on climate features might improve or deteriorate air quality on different regions on the Earth. Interactions can be multiple, with a high degree of complexity. For the specific case of Po Valley, the most influent climate quantities are temperature, humidity, precipitation and solar irradiance.

A precipitation decrease will inhibit the wet precipitation of pollutants, enhancing their atmospheric concentrations. Long drought periods can increase the frequency of fires, and so of the pollutants emissions related to them. The particulate excess will modify cloud cover and composition. The soil water deficit will also support the heat transport and so convective turbulence in boundary layer.

Climate change can also modify synoptic wind patterns; so, large scale distribution and dispersion of pollutants may be influenced. For example, stagnation conditions in Mediterranean Europe are favorited by those changes (Holton et al., 2012).

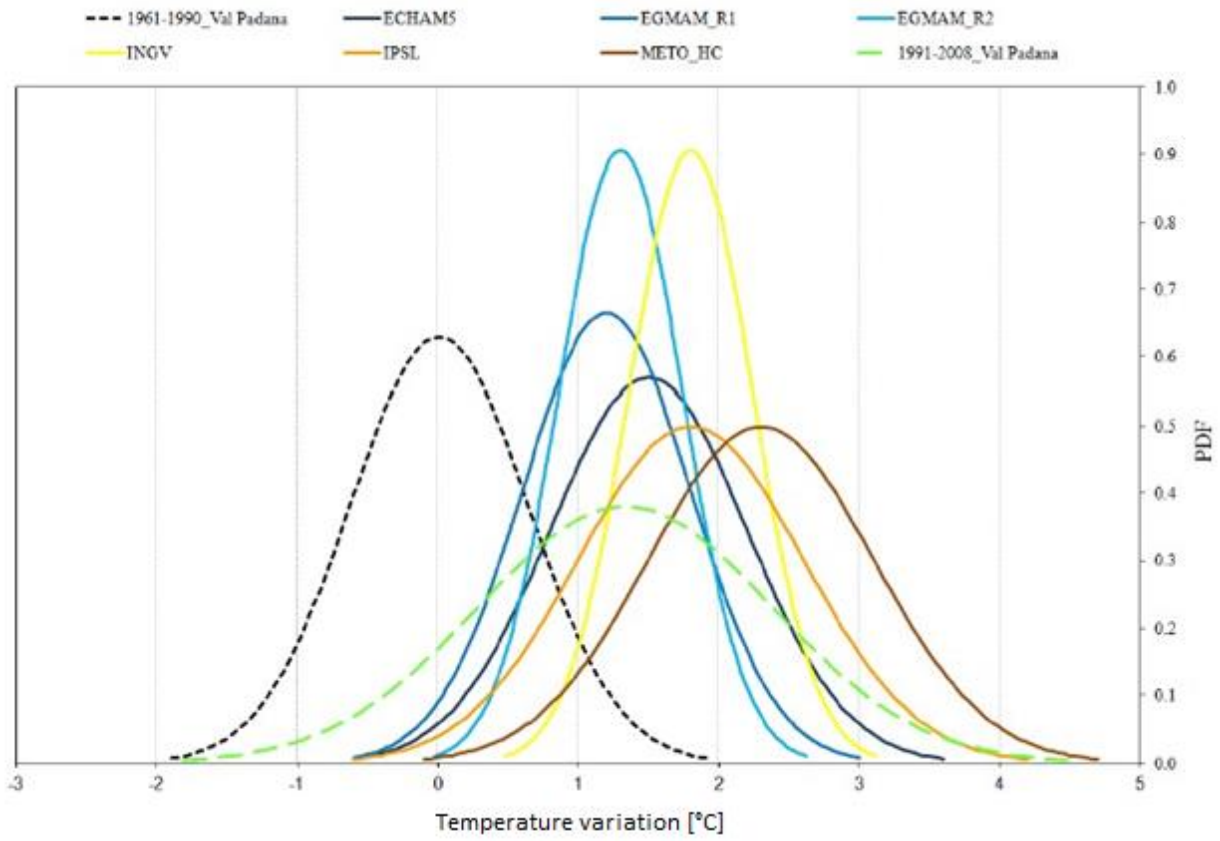

Figure 20: Probability density functions (PDFs) of maximum temperature in Parma during summer. Dashed black line represents the current climate, while colored lines are different models simulations of the same period (2021-2050). (Chiesa, 2013.).

Temperature, humidity and solar irradiance are involved in most of the photochemical processes, which contributes to ozone and particulates production (Chiesa, 2013). An increase in global temperatures will enhance those reactions and the efficiency by which vegetation will produce VOCs. On the other hand, vegetation may change with climate, as well as its VOC productions. Moreover, a modification on vegetation morphology in the Po Valley can variate surface wind patterns and so local boundary layer dynamics.

In the last decade, few different studies on maximum temperature projections have been published (Tomozeiu et al., 2007; Tomozeiu et al., 2010; Villani et al., 2011), made with different climatic models. Projections are specific for Po Valley, and represent summer maximum temperature for the period 2021-2050. All studies confirm a 1.5-2 °C increasing trend, with respect to the period 1961-1990, as shown in Figure 20. Temperature increase is mostly associated with an augmented heat waves frequency and an increase in tropospheric ozone concentration during summer.

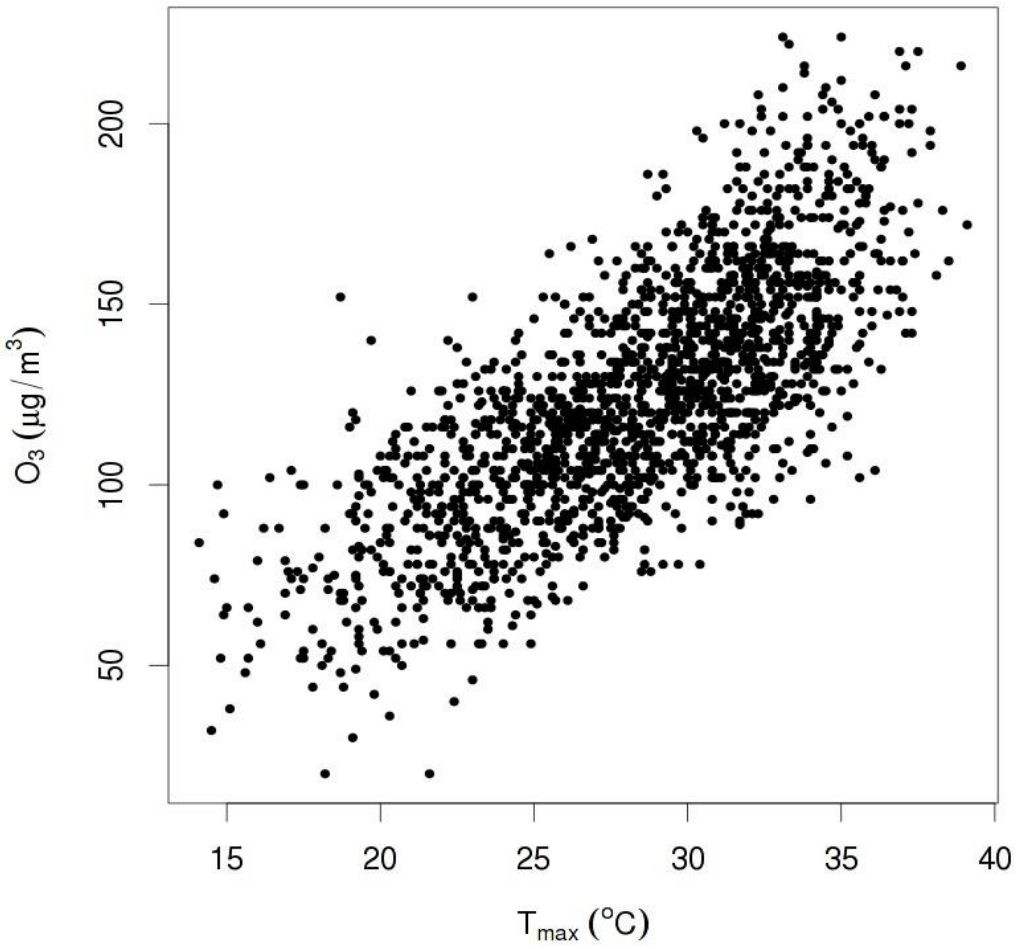

Figure 21: Scatter plot of observed daily maximum temperature and ozone 8-hours mean concentration for summertime during the period 2001-2012. (Chiesa, 2013).

The correlation found with the observed data is also conserved in future scenarios (Figure 23). Figure 21 shows a strong increase in ozone concentrations from 1961-1990 and 2001-2012 periods, following the maximum temperature enhancement (Figure 22). However, despite the different temperature possible scenarios described in Figure 23 ozone concentrations projections for the period 2021-2050 are close one to another and to the period 2001-2012.

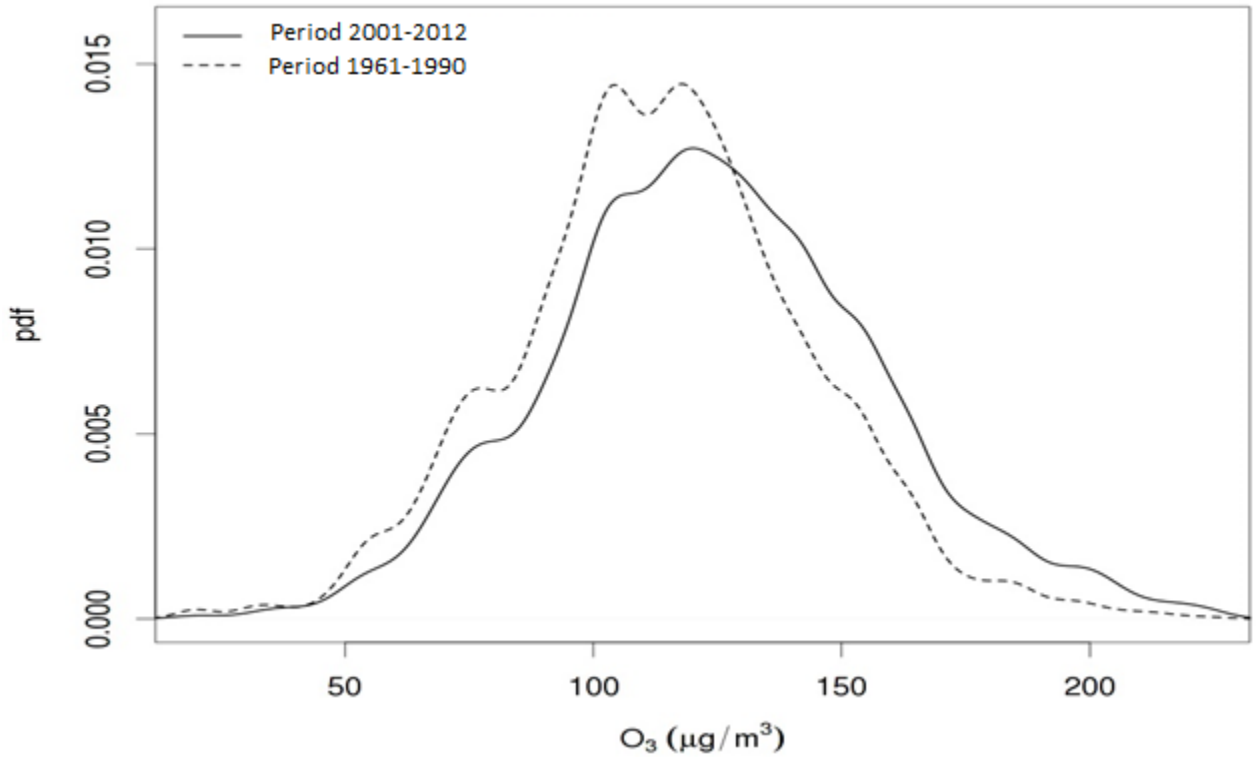

Figure 22: Ozone concentration distribution for both the periods 1961-1990 (dashed line) and 2001-2012 (solid line). (Chiesa, 2013).

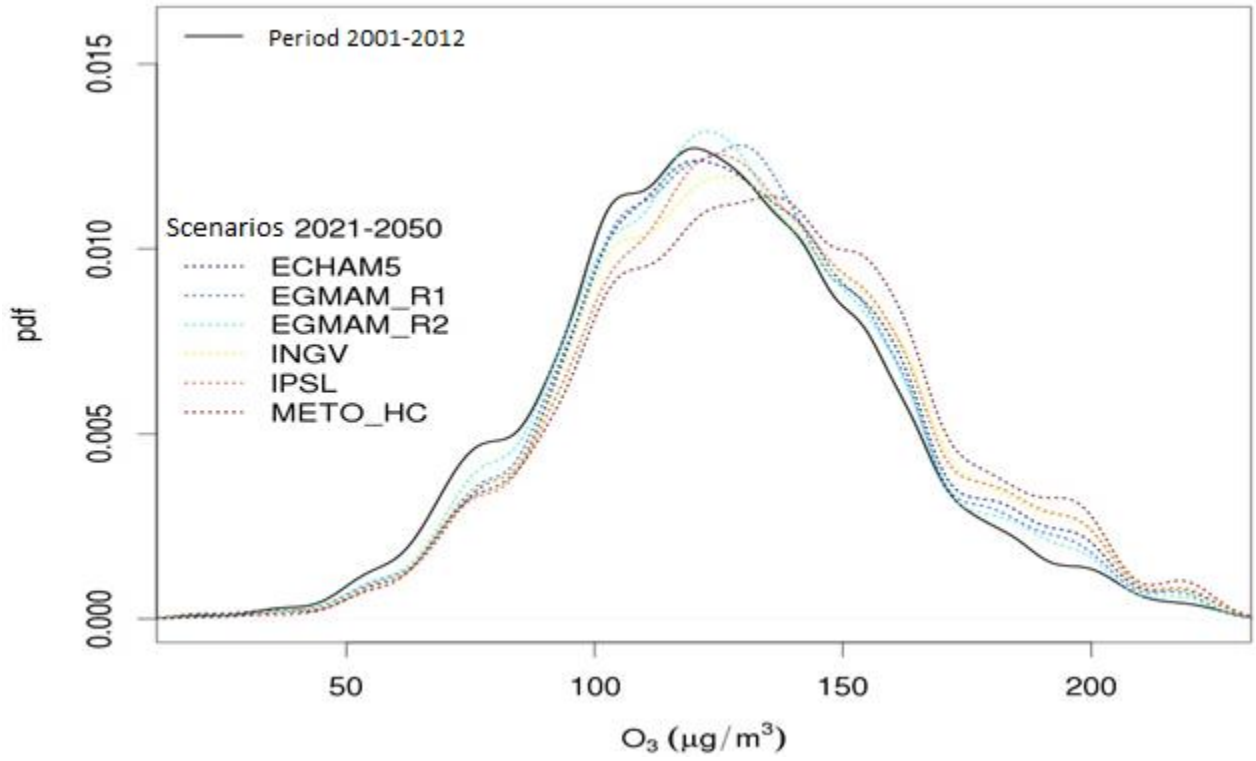

Figure 23: Frequency distribution of daily maximum concentration of ozone in Parma during summer. Solid black line represents the current climate. Colored lines represent climatic projections for the period 2021-2050. (Chiesa, 2013).

6.2.3 Local wind patterns versus air pollution

The Po valley is in Northern Italy, widespread in the regions Emilia-Romagna, Veneto, Lombardian and Piedmont, and is a semi-closed basin surrounded by Alps and Apennines mountain chains and the Adriatic Sea. Here, surface winds are very weak, and strong temperature inversion can be observed near the ground and in the boundary layer. Morgillo et al. (2016) used clustering analysis to classify surface pressure patterns (SPPs) and local wind patterns (LWPs) to investigate their relationship with local air pollution. The classification of SPPs was performed in a domain covering the Alps region and Mediterranean basin, using as input the time series of daily geopotential height at 500 hPa (Jan 1985–Dec 2014). LWPs was carried out over the Po Valley, starting from hourly time series (Jan 2005–Dec 2014) of wind speed and direction, observed at 10 m above the ground by 17 anemometers.

The resulting pressure classification consisted into nine SPPs covering the prevailing geostrophic flux in the domain: 1) North-West; 2) North-West strong; 3) West weak; 4) flat; 5) South-West strong; 6) North-North-East weak; 7) North-North-West strong; 8) South-South-West weak; 9) West.

As for local wind patterns, nine prevailing surface wind in the domain have been found: 1) West; 2) North to North-West; 3) North-East, extended; 4) North-East, limited; 5) East; 6) S; 7) SE; 8) incoherent; 9) SW.

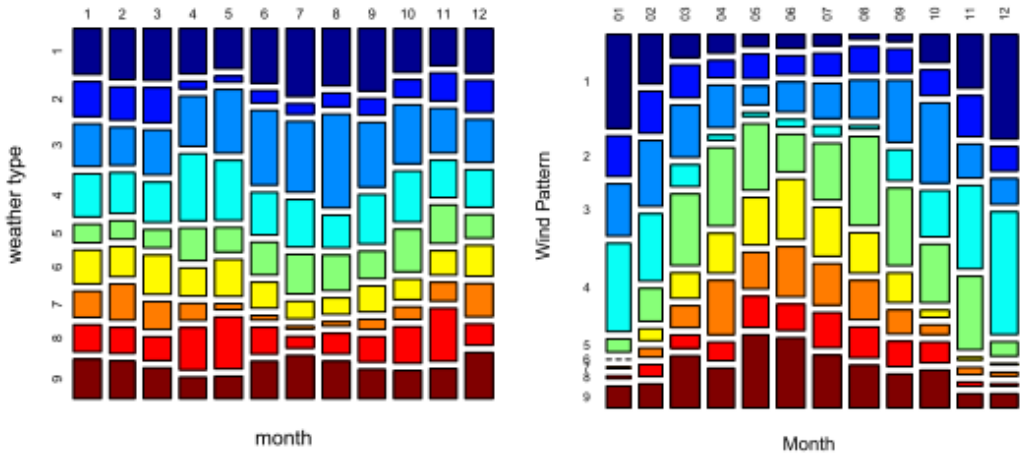

Figure 24: Monthly relative occurrences of daily synoptic pressure patterns (left) and local wind patterns (right) (Morgillo et al., 2016).

As can be seen in Figure 24, the SPP1 (NW), SPP3 (W weak) and SPP4 (flat) were the most frequent occurring direction during the year. Focusing on daily recurrences it is possible to notate that SPPs are more persistent than wind regimes. Moreover, it is seen that SPPs and LWPs seemed to have no strong connection, suggesting that local wind regimes in the Po Valley are to some extent decoupled from the synoptic situation.

The coupling of wind and pressure patterns with concentration of PM_{10}, O_3, and NO_2 were furthermore investigated. Measures of these pollutants were performed at 10 urban background sites in Emilia Romagna for a 10-years period. In winter time, concentration observed seems to follow the SPPs and LWPs change trend. On the other hand, during summer period, tendency appeared more independent. If concentration were averaged over the entire year, the seasonality of meteorological patterns dominates. PM_{10} and NO_2 have double concentration

during winter LWP and SPP classifications than in the summer ones. Moreover, during winter time they are generally associated with the same LWPs and SPPs O_3 increases concentration during LWPs from 5 to 9, which are typical of summer months.

Concentrating on $PM_{2.5}$ chemical composition, time series data in the period November 2011 – May 2014 was collected from an urban background site in Bologna (south-easterly Po valley). To filter out the seasonality, the relative anomaly with respect to the monthly average is considered. The results are summarized in Figure 25.

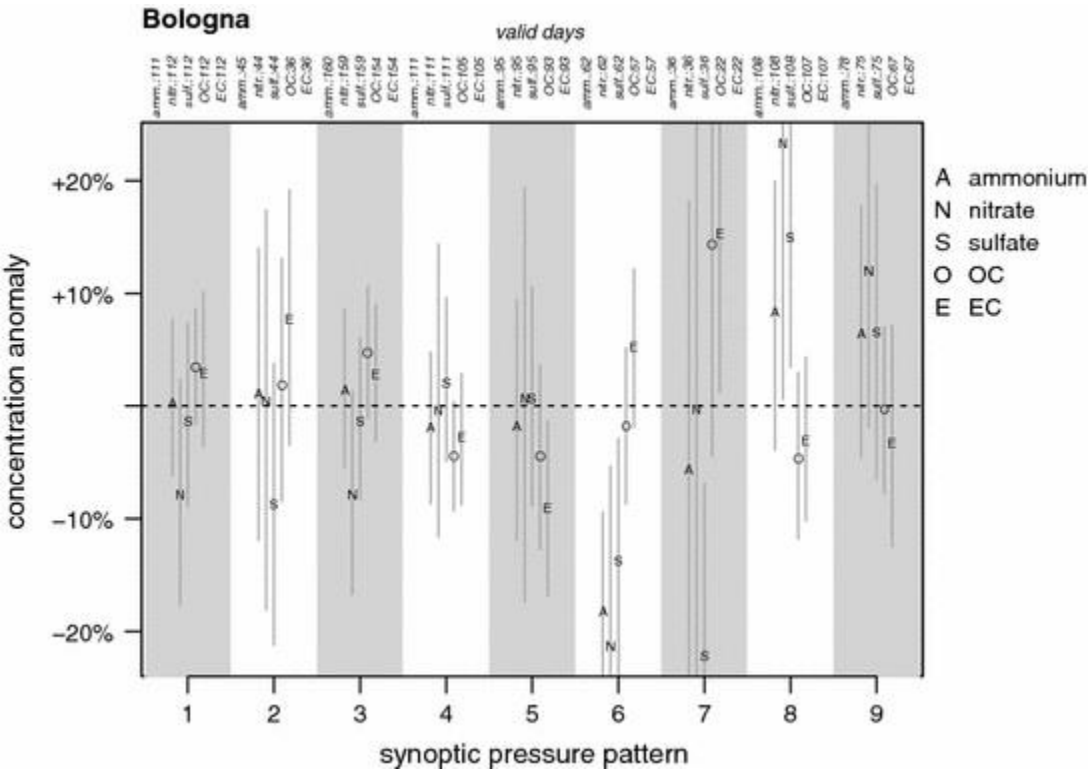

Figure 25: Concentration anomaly of nitrate, sulfate, ammonium, elemental and organic carbon measured in the $PM_{2.5}$ in a background site in Bologna, Italy (Nov2011–May2014). Letters relative anomalies, averaged for each Synoptic Pressure Pattern. Vertical lines intervals of confidence of the mean. (Morgillo et al., 2016).

It was concluded that LWP2 (N) is associated to relatively high nitrates, while LWP7 (SE) and LWP8 (incoherent) are linked with low nitrates and high elemental carbon. SPP6 (NNE weak) is associated with low ammonium, nitrate and sulfate. SPP 7 (NNW strong) is correlated with low sulfate and high elemental carbon; SPP8 (SSW weak) with high nitrate and sulfate concentrations.

6.3 Bottrop (DE)

6.3.1 Air Quality

Air quality data for Bottrop (Statistisches Jahrbuch, 2014 and LANUV-Fachbericht 73, 2015) are there compared to mean values for the Rhein-Ruhr region (Kurzfassung der Jahreskenngrößen,

2015). PM_{10} are only available for Bottrop so no comparison can be shown. There are no data of $PM_{2.5}$ for Bottrop.

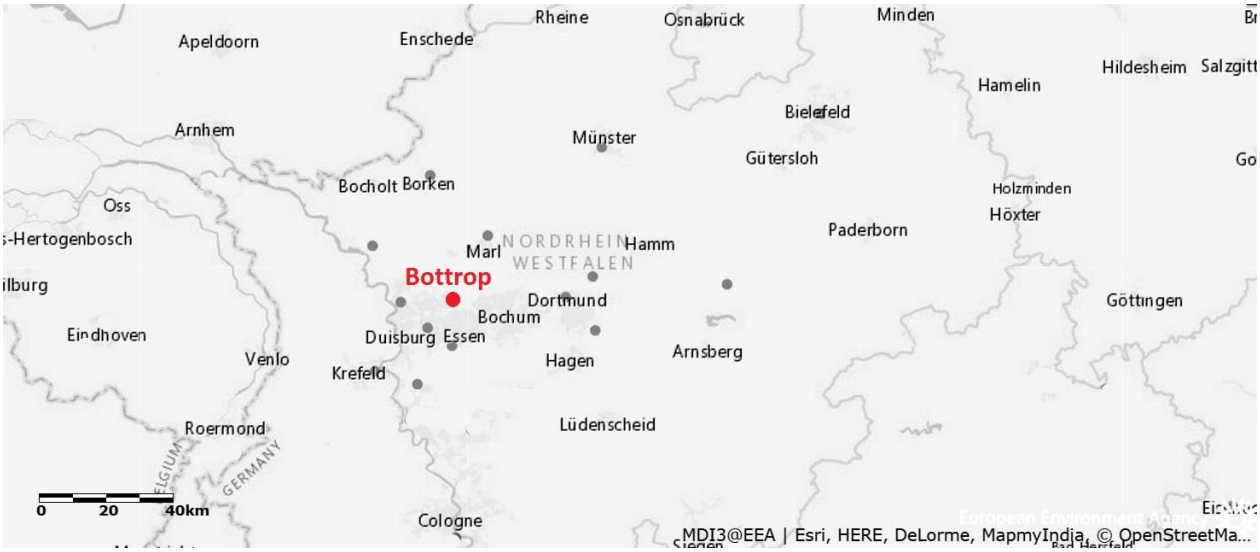

Figure 26: Map of the monitoring stations (dots) in Bottrop and in the Ruhr region. (European Environmental Agency, 2016).

Figure 26 shows the distribution of the monitoring sites in the Ruhr-Rhein region. Data are reported in the following tables.

In the context of iSCAPE, Bottrop will access innovative technologies and use proven method to develop a new concept of mobility and climate proof urban renewal. With this aim, the following tables present baseline states for those pollutants for whom traffic is the main source in an urban environment (NO_2 and PM_{10}), or it is relevant for climate change (O_3).

Table 8 shows the annual mean concentrations of NO_2. The mean concentrations for Bottrop and the remaining region are almost identical, and 20 % lower than the European limit. There is a slight decrease of concentrations with the years.

		Annual mean concentrations of NO_2 ($\mu g/m^3$)					
		2010	2011	2012	2013	2014	2015
Innovation-City Ruhr	Bottrop	29	29	28	27	27	26
	Rhein - Ruhr Stations	30	28	27	27	26	26

Table 8: Annual mean concentrations of NO_2. Differences between Bottrop and the Rhein-Ruhr region measurements are shown. The European limit for NO_2 annual mean concentrations is 40 $\mu g/m^3$.

Table 9 shows annual concentrations of O_3, computed as the annual averaged value of 8-hours daily mean concentration. No information can be obtained from a comparison with the European limit because it concerns the number of days in which the 8-hour mean concentration exceeds

120 µg/m^3. Although, concentrations are constant over the period, except for an increase in 2015.

		Annual mean concentrations of O_3 $(\mu g/m^3)$					
		2010	2011	2012	2013	2014	2015
Innovation-City Ruhr	Bottrop	36	34	35	37	35	40
	Rhein - Ruhr Stations	37	36	37	39	37	41

Table 9: Annual mean value of maximum daily 8-hour mean O_3 concentration. Differences between Bottrop and Rhein-Ruhr region measurements are shown. The European human health threshold for O_3 maximum daily 8-hour mean concentration is 120 µg/m^3.

Table 10 shows the annual mean concentrations of PM_{10} and the number of days with concentrations exceeding 50 µg/m^3. The mean concentrations obtained by the city centre monitoring station is 40 % lower than the European limit and the number of days with concentrations exceeding 50 µg/m^3 is lower than 35, on average. Both concentrations and exceedances are also in a small decreasing trend.

		PM_{10} in Bottrop					
		2010	2011	2012	2013	2014	2015
Innovation-City Ruhr	Annual mean concentrations $(\mu g/m^3)$	28	28	25	23	22	22
	No. of days with concentrations > 50 $(\mu g/m^3)$	24	44	26	12	14	19

Table 10: Annual mean concentrations of PM_{10} and number of days with concentrations exceeding 50 µg/m^3. The European limit for PM_{10} annual mean concentrations is 40 µg/m^3.

6.3.2 Urban growth and population exposure

The Ruhr area has been chosen to investigate the impact of uncontrolled urban growth (sprawl) on air pollution and associated population exposure (De Ridder et al., 2008, Part I), and to explore a different urbanization scenario (De Ridder et al., 2008, Part II). The investigation is performed throughout a coupled modelling system dealing with land use changes, traffic, meteorology, and atmospheric dispersion and chemistry. Simulations are extracted from a multistep process. In a first step, an overview is given of the establishment of satellite-based digital land use, population, and employment density maps, and its subsequent coupling to a traffic model.

Outputs of the latter has been used to estimate traffic flows and vehicle speeds on a road network of the study area. In a next step, this information is used to calculate traffic emissions, which are then combined with emissions from other sources (mainly industrial) to provide the

overall emissions. The latter are then used as input into a transport-chemistry model, together with simulated meteorological fields, and concentrations of relevant pollutants (ozone and particulate matter) are simulated.

As shown in Figure 27, ozone and particulate matter simulations reflect the pattern of land use, showing high PM_{10} values and relatively low ozone (owing to the titration effect) in the densely-populated areas, where the emissions are high.

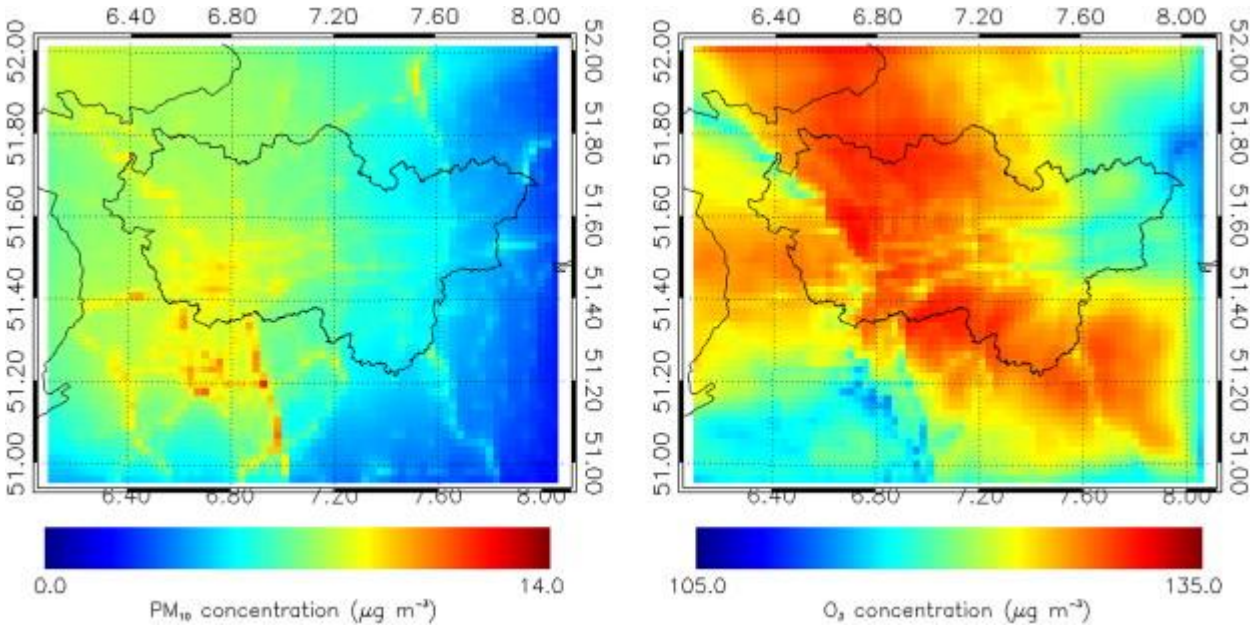

Figure 27: Simulated local PM_{10} (left) and O_3 (right) concentrations in µg/m^3, averaged over the simulation period (3 weeks). (De Ridder et al., 2008, Part II).

These simulated concentration fields represent a base case, used as reference scenario in De Ridder et al. (2008, Part II).

The land use enhancement generates an increase of population in the region, and it subsequently leads to an enhancement of energy consumption and traffic-induced emissions. The traffic induced emissions growth by 16.7 % with respect to the base scenario. The simulated changes in traffic intensities on all road segments were counted and expressed as per-day total distances travelled by all cars (passenger and heavy), yielding an increase of 16.7 % for total vehicle kilometres.

The calculation of emissions to the atmosphere is performed as done before in De Ridder et al. (2008, Part I), leading to an increase of PM_{10} increase of 12 % with respect to the base scenario. This is less than the 16.7 % simulated increase in total traffic kilometres, which is mainly because traffic-related emissions do not constitute the total emissions. Also, ozone concentrations show a growth, due to the temperature increase in urban sprawl condition. This temperature increase was attributed to the increased share of built-up areas in the domain, which convert incoming radiation to sensible heat rather than to latent heat (evaporation), owing to the limited water availability of surfaces characterized by impervious materials. Apart from being an indication of an enhanced urban heat island effect, this temperature increase also affects photochemistry, hence ozone concentrations.

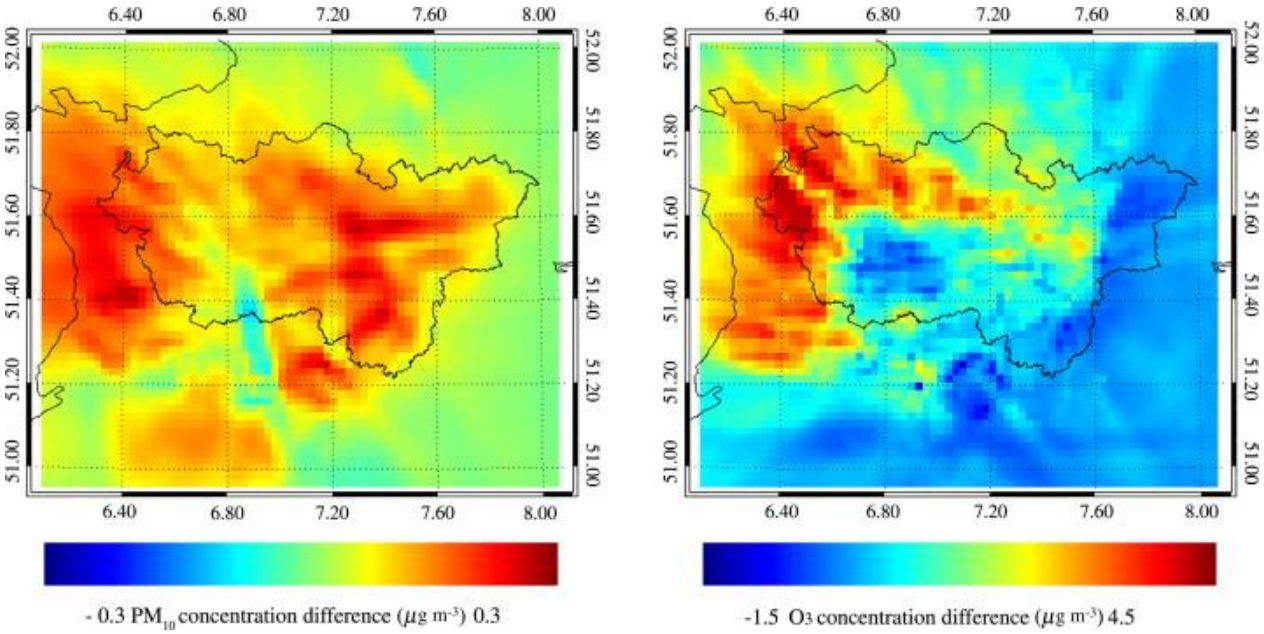

Figure 28: Percentage change of PM_{10} (left) and O_3 (right) concentrations between the urban sprawl scenario and the base state, averaged over the simulation period. (De Ridder et al., 2008, Part II).

The combination of increased temperatures and altered emissions yields the ozone concentration pattern changes displayed in Figure 28, showing increased values (compared to the base case) for a large portion of the domain. The simulated changes are highest in the north-west sector of the domain, which is consistent with the prevailing south-easterly wind direction during the simulation period. Concerning fine particulate matter (Figure 28), it is found that concentration changes are small: about a few tenths of a μg m^{-3}, despite a 16.7 % increase of traffic kilometres.

Despite the emissions enhancement, the subsequent overall pollutant concentration changes are relatively modest, and in good agreement with the urbanization development.

6.4 Dublin (IE)

6.4.1 Air Quality

Dublin city provides four sites monitoring air quality, as reported on the map (Figure 29).

Rathmines, Winetavern Street and Coleraine Street are situated adjacent to heavily trafficked roads; Ballyfermot, Marino and Finglas are situated in a predominantly residential area; St Anne's Park and Phoenix Park sites provide background sites; Blanchardstown and Dun Laoghaire are urban traffic and residential supporting sites respectively. Not all the pollutants are measured in all sites.

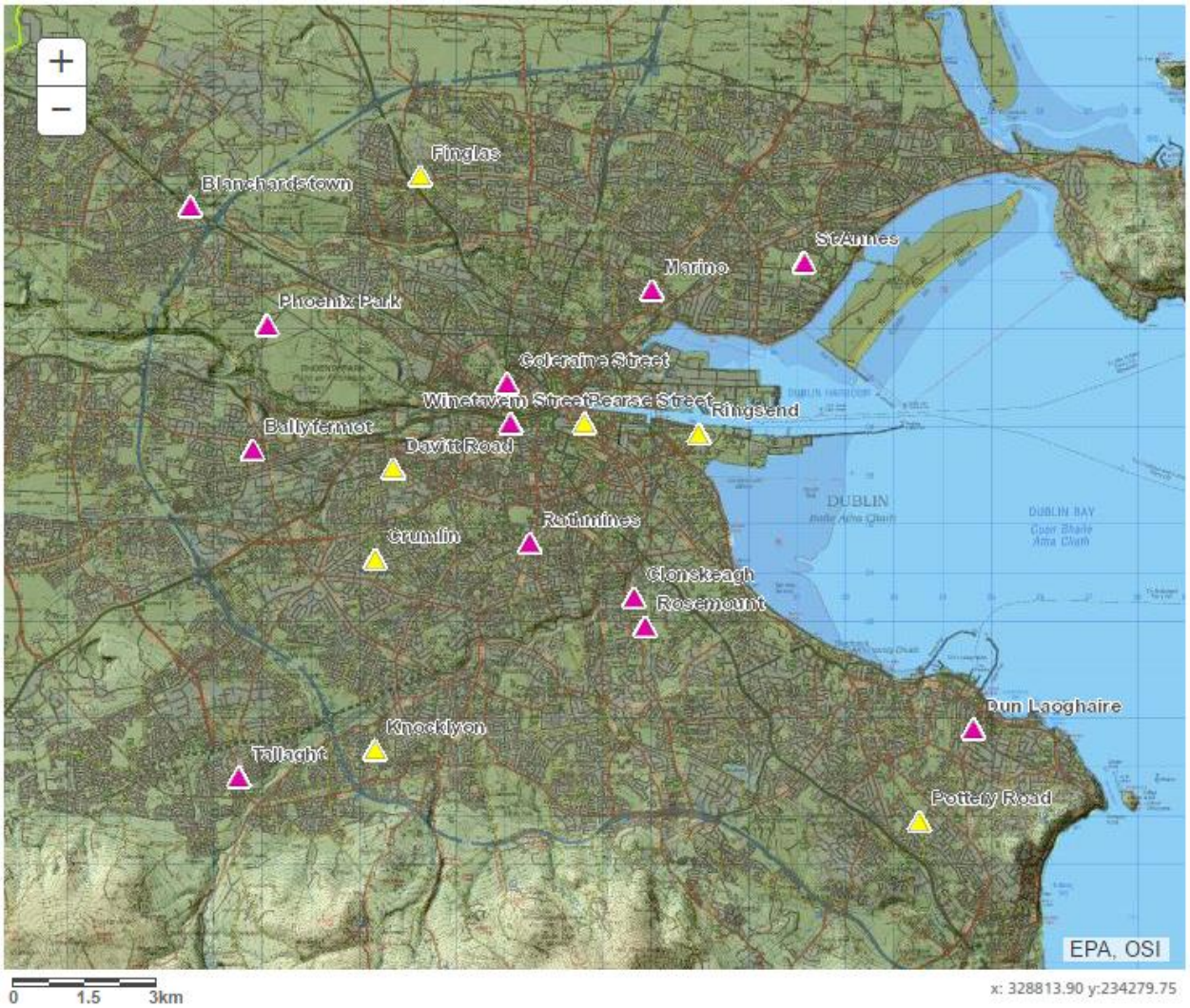

Figure 29: Map of Dublin city sites for air quality monitoring. Pink triangles indicate current monitoring sites; yellow triangles indicate past monitoring sites. (Environmental Protection Agency Maps).

Measurements in Dublin provide an overview of traffic-related pollutants to have a framework for setting up the experiment on vegetative boundaries. This is addressed to pollution exposure reduction for pedestrians by engineering flow patterns and ventilation conditions in a high-trafficked street canyon in Dublin.

Table 11 shows the annual mean concentrations of NO_2. The mean concentrations obtained by the city centre trafficked stations are 20 % lower than the European limit and higher than the mean concentrations measured by the background sites. City centre stations also show a small decreasing trend, while tendency at the background sites is hardly suggestable since the lack of available data until 2012. The reason for the decrease in NO_2 concentrations could partly be due to meteorological conditions (a predominance of wet and windy weather), as well as a decrease in traffic numbers for the period, reflective of the downturn in the economy (O'Dwyer, 2015).

		Annual mean concentrations of NO_2 ($\mu g/m^3$)					
		2010	2011	2012	2013	2014	2015
Dublin	Winetavern St	35	34	29	31	31	31
	Coleraine St	33	26	26	26	25	25
	Ballyfermot	23**	ND	ND	16*	16	16
	St Anne's Park	ND	ND	ND	12	12	13
	Dun Laoghaire	ND	ND	ND	16	16	16
	Blachardstown	ND	ND	ND	28	28	25

*Table 11: Annual mean concentrations of NO_2. Different sites inside Dublin city are shown. The European limit for NO_2 annual mean concentrations is 40 μg/m^3. ND stands for no available data. * data are collected from 15th March 2013; ** data are collected until 30th September 2010. (Air Quality Monitoring and Noise Control Unit Annual Report).*

Table 12 shows the annual mean concentrations of PM_{10}. The mean concentrations obtained by the city centre trafficked stations are less than half of the European limit, and by the same order of magnitude of mean concentrations measured at the background sites.

		Annual mean concentrations of PM_{10} ($\mu g/m^3$)					
		2010	2011	2012	2013	2014	2015
Dublin	Rathmines	16	16	14	17	14	15
	Winetavern St	19	14	13	14	14	14
	Ballyfermot	13*	ND	ND	12	11	12
	St Anne's Park	ND	ND	ND	19	17	15
	Dun Laoghaire	ND	ND	ND	17	14	13
	Blachardstown	ND	ND	ND	20	18	17
	Phoenix Park	11	12	11	14	12	12

*Table 12: Annual mean concentrations of PM_{10}. Different sites inside Dublin city are shown. The European limit for PM_{10} annual mean concentrations is 40 μg/m^3. ND stands for no available data. * data are collected until 10th October 2010. (Air Quality Monitoring and Noise Control Unit Annual Report).*

Trafficked sites, as Phoenix Park, have constant trend, while again the other stations have several missing data, so no trend is suggested. In city centre, traffic emissions are the main source of PM_{10}, while in residential and background areas, emissions from residential solid fuel combustion dominate. The equal concentrations measured in all sites is a benefit from the increasing use of gas in place of solid fuel, more ecologic vehicles and a ban on the use of bituminous coal, with the result that levels of PM_{10} are similar across all zones.

Table 13 shows the number of days with PM_{10} concentrations exceeds 50 μg/m^3. Table 13 shows that the values measured are very lower than the European limit, suggesting that the daily concentrations of PM_{10} have small fluctuations from the annual mean values for all the sites.

		No of days with PM_{10} concentrations exceeds 50 $\mu g/m^3$					
		2010	2011	2012	2013	2014	2015
Dublin	Rathmines	3	10	3	8	3	5
	Winetavern St	7	7	0	3	1	4
	Ballyfermot	1*	ND	ND	3	2	3
	St Anne's Park	ND	ND	ND	1	1	3
	Dun Laoghaire	ND	ND	ND	5	2	3
	Blachardstown	ND	ND	ND	11	5	9
	Phoenix Park	1	3	0	3	0	2

*Table 13: Number of days with PM_{10} concentrations exceeds 50 µg/m^3 (value not to be exceeded more than 35 times per year). Different sites inside Dublin city are shown. ND stands for no available data. * data are collected until 10th October 2010. (Air Quality Monitoring and Noise Control Unit Annual Report).*

Table 14 shows the annual mean concentrations of $PM_{2.5}$. The mean concentrations obtained by the monitoring stations are less than half of the European limit, and also slightly decreasing with time. Dublin level of $PM_{2.5}$ concentrations fluctuates around the WHO guideline value of 10 µg/m. Primary and secondary $PM_{2.5}$ concentrations can come from a lot of different sources (e.g. commercial, industrial and agriculture sector) and particulate-pollutant interactions, and usually is a good indicator of human activity. Since Dublin $PM_{2.5}$ measurement sites are in trafficked and residential areas, the probable main contributor to the collected data comes from the residential solid fuel combustion.

		Annual mean concentrations of $PM_{2.5}$ $(\mu g/m^3)$					
		2010	2011	2012	2013	2014	2015
Dublin	Marino	10	9	8	9	8	8
	Coleraine St	12	11	10	11	9	9
	Finglas	ND	ND	ND	ND	7*	8

*Table 14: Annual mean concentrations of $PM_{2.5}$. Different sites inside Dublin city are shown. The European limit for $PM_{2.5}$ annual mean concentrations is 25 µg/m^3. ND stands for no available data. * data are collected from 24th February 2014. (Air Quality Monitoring and Noise Control Unit Annual Report).*

6.4.2 Emission reduction policies

Dublin city studies about air quality in climate change inside the urban environmental are mainly focused on the practicability of city policies. There are policies which will improve both air quality and reduce greenhouse gas emissions, but there are also policies which will improve one but make the other worse (Monks et al., 2009). The win-win policies generally involve measures which reduce energy consumption and travel, or, at least in the latter case, encourage modal shifts to forms of travel which use less energy per passenger and per kilometre. Energy efficiency measures are the obvious place to start in implementing measures which improve

both air quality and climate change, not least because the economy case is generally very strong. Other win-wins involve increased use of non-combustion renewables like wind, tidal and solar power.

Dublin city mainly focuses on greenhouse gases reduction, acting in energy, planning, transport and waste management fields. Policies primarily focus on CO_2 and its emission reduction. Studies from the Dublin City Council (DCC) suggest that CO_2 emissions in the city can be divided between four major sectors: residential 32 %, services 23 %, manufacturing 20 % and transport 25 % (Climate Change Strategy, 2008-2012). DCC's strategy regarding Green House Gases (GHGs) will cover the period 2008-2012 in the short term, but it also looks forward to a medium-term view to 2020 and beyond. A brief description of the strategy is now presented for each field of action.

In the energy field, policies deal with the incentives of renewable energies (solar, water and biogas) and efficiency on public efforts. Public installation of solar panels has been completed for existing buildings in specific neighbourhoods. In biogas field, the city is recovering the methane that is naturally formed when sludge is treated and the methane gas is burned for electricity production. Other 100kw electricity producer water turbine has been installed. Public lights have been totally updated and modernized.

DCC started the Action Plan on Energy for Dublin to provide a framework for development in the three sectors that contributes most to climate change in Dublin: the residential, the commercial and the transport sectors. Over the past ten years, in the residential sector, an efficient gas fired central heating has replaced the old solid fuel fires, with major benefits to both the environment and quality of the living space. All new residential and commercial buildings require the energy standard to be rated at least B1 from 2008 and A3 from 2009.

The delivery of the brown bin service to householders across the city is a key part of the waste strategy. The service will divert organic away from landfill and thereby reduce the GHG emissions. The separately collected material will be diverted to higher waste treatment solutions, such as composting and anaerobic digestion, and provide for better resource efficiency.

Transport strategy focuses on the reduction of emission per person, working on the implementation of walking routes in the centre, as well as bicycle lanes (160 km have already been constructed). Another point is the facilitation for public transport: Quality Bus Corridors (QBCs) have been implemented throughout Dublin. In autumn 2007 there were 13 QBCs routes operating in the DCC area and more are planned. Measurements show that there is an 18 % decline in cars on these routes.

In matter of traffic emission reduction Brady and O'Mahony (2011) proposed a study on the possible impacts of electric cars in the city. They evaluate the potential reduction in road traffic related emissions in Dublin under three different electric vehicle (EV) market penetration scenarios by 2020. This studies support a 2008 announcement from the Irish Minister for Transport of a target for 10 % of the private car fleet to be powered by electricity by 2020 (Dempsey, 2008), as a part of initiative to address issues of climate change and air quality. This decision follows the publication of 2008 GHG emissions by source of the Environmental Protection Agency (2009): it states that in 2008 transport in Ireland accounted for 21.3 % of national GHG emissions.

As mentioned, Brady and O'Mahony use three different market penetration scenarios, named 'high', 'medium' and 'low'. They found that, of all 226300 vehicles estimated in Dublin by 2020, EVs will achieve 25 % market share in 'high' penetration scenario, 15 % in 'medium' and 10 % in 'low' (which is the most likely scenario). To make comparison, a Business as Usual (BAU) scenario was investigated (no EV car on market).

Table 15 presents both the estimated tailpipe emissions and the emissions due to electricity generation for each of the scenarios investigated. The results show a net reduction in both CO_2 emissions and tailpipe air pollutants. The results for the BAU scenario suggest that there will be a significant reduction in CO, VOC, PM, NO_2, and NO_x emissions in 2020, without the introduction of EVs to the fleet. These reductions can be attributed to the introduction of Euro 5 and 6 emissions standards and the retirement of older and higher pollutant emitting vehicles. The introduction of EVs cause a further reduction in all road traffic related emissions, which is smaller than BAU projection, for at least 'medium' and 'low' scenarios.

Pollutant	2010	BAU 2020	% Change from 2010	High Scenario	% Change from BAU 2020	Medium Scenario	% Change from BAU 2020	Low Scenario	% Change from BAU 2020
Tailpipe CO2	337,102	317,700	-6	248,678	-22	282,316	-11	296,296	-7
Grid CO2	-	-	-	37,999	-	19,475	-	11,776	-
Net CO2	337,102	317,700	-6	286,677	-10	301,791	-5	308,072	-3
CH4	28,54	13,02	-54	11,38	-13	12,18	-6	12,51	-4
N2O	5,24	7,03	34	4,42	37	5,69	-19	6,22	11
CO	3.384,65	828,60	-76	713,85	-14	769,75	-7	792,99	-4
VOC	376,71	113,37	-70	94,26	-17	103,57	-9	107,44	-5
NOX	283,79	200,50	-29	148,80	-26	172,38	-14	182,19	-9
NO2	41,46	13,30	-68	13,16	-1	13,23	-1	13,25	0
PM2.5	29,93	21,30	-29	15,90	-25	18,53	-13	19,62	-8
PM10	42,31	35,12	-17	25,76	-27	30,32	-14	32,22	-8

Table 15: Emission results. All values are in tonnes (Brady and O'Mahony, 2011).

In conclusion, the results indicate that electric vehicles will have limited impact on climate change and urban air quality for at least the next decade, because of the time required for electric vehicles to acquire a significant share of the fleet. Nevertheless, the study supports existing evidence that EVs can contribute to long term emissions reductions.

6.5 Guildford (UK)

6.5.1 Air Quality

Figure 30 shows the monitoring stations active in the Surrey county.

Framework measurements taken in Guilford are taken as starting point for studies on barrier on air pollutants concentration and associated exposure under different vegetation and meteorological conditions.

In Table 16 NO_2 concentration are shown for various measurement sites. In bracket is reported the typology of the site. The last three lines are obtained throughout a mean of the same typology sites. The mean concentrations obtained by the city centre monitoring station are close to the European limit and higher than the mean concentrations obtained by urban and rural background measuring stations. The difference between roadsides and backgrounds measurements suggest an important contribution by the traffic-induced emissions to the total amounts.

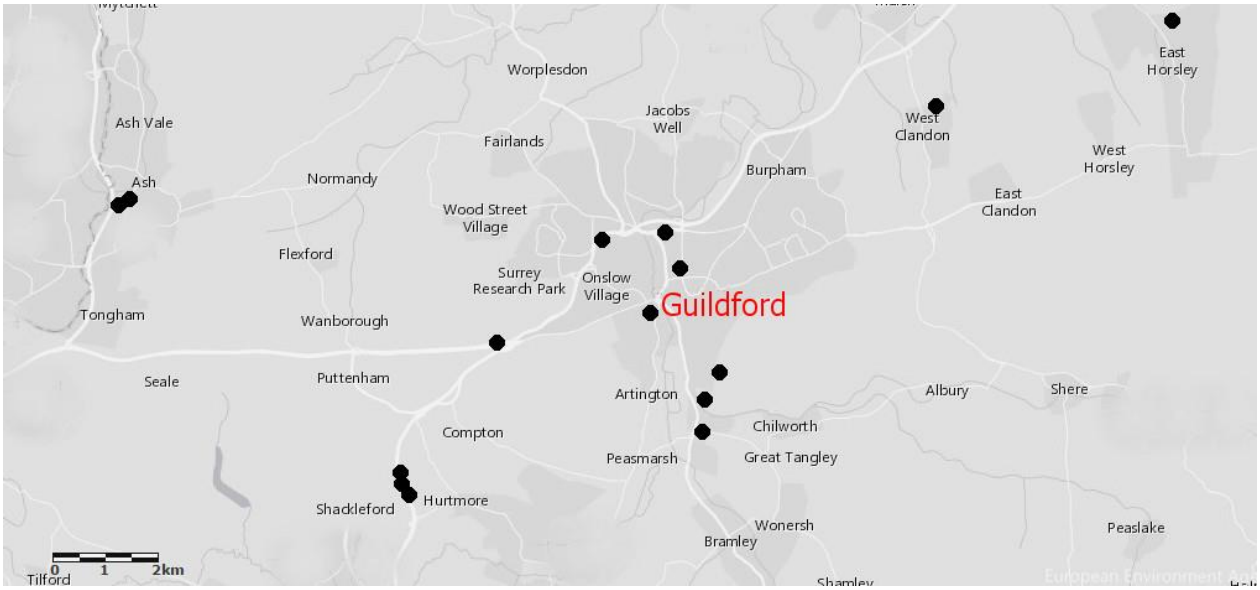

Figure 30: Map of the monitoring stations (black dots) in Guildford and Surrey county. (European Environmental Agency, 2016).

Since 2010 there are no more PM_{10}. As there have been no change to the road system in the Guildford area, the Borough considers the current emissions not to be changed from the past. Table 17 shows the annual mean concentrations of PM_{10} and the number of days with concentrations exceeding 50 μg/m^3. The mean concentrations obtained by the roadside monitoring station are half of the European limit and the number of days with concentrations exceeding 50 μg/m^3 is lower than 35.

		Annual NO_2 mean concentration in Guildford region ($\mu g/m^3$)					
		2010	2011	2012	2013	2014	2015
Surrey county	Guildford (Roadside)	39	42	39	38	31	38
	Guildford (Urban Backround)	22	21	22	22	16	20
	Compton (roadside)	ND	ND	ND	ND	40	29
	Urban Backround	19	16	19	18	16	17
	Roadside	28	26	26	26	26	28
	Rural Backround	17	13	13	14	14	13

Table 16: Annual mean concentrations of NO_2. Different sites inside Dublin city are shown. The European limit for NO_2 annual mean concentrations is 40 μg/m^3. ND stands for no available data. (Guildford Borough Council, 2016).

Past PM_{10} data in Guildford, Bridge Street (Roadside)				
	2006	2007	2008	2009
Annual mean concentrations $(\mu g/m^3)$	23	30	24	24
No of exceedences of hourly mean of 50 $\mu g/m^3$	7	27	21	5

Table 17: Annual mean concentrations of PM_{10} and number of days with concentrations exceeding 50 µg/m^3. The European limit for PM_{10} annual mean concentrations is 40 µg/m^3. (Guildford Borough Council, 2016).

No further data for air quality in Guildford are available. Following the indication of the Guildford Borough Council (2016), a monitoring network for $PM_{2.5}$ is not available, but there will be a plan to simulate the distribution of this pollutant in the city to highlight the areas of major exposition and potential damage for human health.

6.5.2 Surrey climate change strategy

There are significant economic, social and environment risks related to not acting to reduce emissions and adapt to climate changes. The Surrey Climate Change Partnership (SCCP) has commissioned a joint strategy to formulate a new and far reaching agreement for Surrey local authorities. This strategy aims to provide a framework to effectively address climate change across Surrey, and to take advantage of opportunities for Surrey from a low carbon economy.

The structure of the strategy is based on three core objectives:

- **Reducing emission** – The strategy is addressed to comprehend causes and ways by which climate change affect Surrey area. The main emission sources, in this context, are summarized in Figure 31.

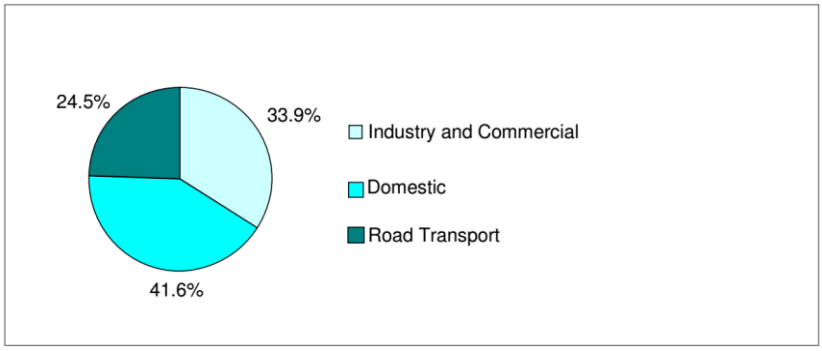

Figure 31: Allocation of total CO_2 emissions in Surrey by source. (City of Surrey, 2009).

As pie chart (Figure 31) underlines, housing is the highest contributor of carbon emissions in the Country, responsible for 42 %. This can be consequence of a significant proportion of the housing stock was built prior to the adoption of sustainability standards and recent Building Regulations requirements for energy performance. Industry and commercial sector are responsible for 34 % of total emission. Public and private

organizations are managing to reduce emission, both because of rising prices and tougher economic conditions. Transport, accounting for 24.5 % of CO_2 emissions, reflects the affluent, rural nature of the County where car ownership is higher than the national average. Recognizing the critical importance of an effective transport network, the plan aims to improve highways network management and maintenance, reducing congestion and helping containing emissions.

Sustainable new development is included too, since it represents an important opportunity to provide low carbon solutions. London Fridge covers most of Surrey and, according to South East Plan, it must undergo a requalification of previous developed land and buildings within urban areas. The purpose of the plan in this section is to ensure that new and refurbished development achieves sustainable levels of resource use and reduces greenhouse gas emissions.

Resources use is of crucial importance to reduce operational costs as the price of utilities and cost of waste disposal escalate. For instance, the County's reliance on landfill is identified as a major issue that must be focused on waste minimization and recycling policies. Renewable energetic resources are going to be financially affordable and technologically viable for widespread adoption and environmentally acceptable. On the other hand, Surrey has several examples of installed renewable technologies to offer a low carbon solution for the future.

- **Adaptation** – Defines our ability responding to climate change, which found vulnerable the County in several cases (e.g. 2000 floods and 2003 heat waves). The problem can be hindered through a series of risk management actions:
  1. **Prevent:** reduce the probability of an impact or change occurring;
  2. **Prepare:** understand the climate risk or opportunity;
  3. **Respond:** actions taken to limit the consequences of an event;
  4. **Recover:** rapid and cost effective action to return to a normal;

- **Raising Awareness** – Our understanding of the problem determines how we deal with the climate change and its issues. It is crucial, therefore, to inform, engage and involve all parts of the County. The strategy plans several actions, such as:
  1. **Public awareness:** raise awareness of climate change with public community and partnership organizations and businesses. Ad-hoc communications campaign are implemented targeting specific neighborhood, such as article in local press or magazines, saving weeks' initiatives and stalls at market;
  2. **Educational awareness:** promote awareness and embed principles throughout Surrey's educational system. Route chosen for this purpose are embedding climate change learning within local curricula and adopting low carbon and energy efficiency measures in the education facilities.

6.6 Hasselt (BE)

6.6.1 Air Quality

Air quality data for the city of Hasselt taken alone are not available. However, mean annual concentrations for the whole Flemish region is reported. Measurement sites distribution is shown in Figure 32.

Figure 32: Map of the monitoring stations (dots) in the Flemish region. (European Environmental Agency, 2016).

Air quality data in this section will account for a general overview of pollution level in the Flemish region. In the context of iSCAPE, it can be used as a baseline refence to test different responses such as changes in transport modes, frequency of trips, adaptations which are required to make the broader activity pattern consistent with the change (i.e. increase of out-of-home social activities or an increased use of cars).

Table 18 shows the annual mean concentrations of NO_2, O_3, $PM_{2.5}$ and PM_{10}. The mean concentrations obtained for NO_2, and PM_{10} are 25-30 % lower than the European limit, while the $PM_{2.5}$ annual mean concentrations are half of the European limit. No information can be obtained from a comparison with the European limit because it concerns the number of days in which the 8-hour mean concentration exceeds 120 $\mu g/m^3$. This number should not exceed 25 days, averaged over three years. Apart from $PM_{2.5}$, concentrations show decreasing trends.

	Annual mean concentration in Flemmish region $(\mu g/m^3)$					
	2010	2011	2012	2013	2014	2015
NO_2	29	29	28	27	26	ND
O_3	40	37	20	15	20	ND
PM_{10}	33	32	30	28	28	ND
$PM_{2.5}$	12	8	11	10	10	ND

Table 18: Annual mean concentrations of NO_2, O_3, $PM_{2.5}$ and PM_{10} in the Flemish region expressed in µg/m^3. The European limit for both PM_{10} and NO_2 annual mean concentrations is 40 µg/m^3, for $PM_{2.5}$ is 25 µg/m^3. O_3 data represent the annual mean value of the maximum daily 8-hour mean concentration, which limit for human health is 120 µg/m^3 (not to be exceeded for more than 25 days averaged over three years). Data for 2015 are not already available. (Flanders Environmental Agency, 2014).

6.6.2 Measure for air quality improvements

One way to lower pollution level in cities is to move traffic from a ring road into a tunnel, as proposed in the city of Antwerp, in Belgium (Van Breusselen et al., 2016). The proposal aims to put the entire urban ring road into a tunnel and to filter the outgoing air pollution. Comparing to the existing "open air ring road", the project predicts changes between -1.5 and +2 µg/m^3 in $PM_{2.5}$ within 1500 meters from the ring road. For NO_2 a loss between -10 and +0 .17 µg/m^3. The calculation emissions arise from daily traffic volumes, from which hourly output for pollutants are generated. Species simulated are NO_2, NO_x and $PM_{2.5}$, which includes exhaust and non-exhaust emission. On the other hand, even after filtering, a tunnel ring road displaces a lot of traffic emissions from the ring road close to the densely-populated city centre to the tunnel exits. Therefore, elevated annual concentration differences of $PM_{2.5}$ and NO_2 can be seen on the maps near the exits of the tunnel complex and partly also at the motorway exits (Figure 33).

Policies can be put into practice to reduce emission too. As instance, it is possible to organize city traffic, coordinating traffic lights stop with vehicles movement or regulating entries in the city (Guijt and Dijkema, 2015). A Low emission zone (LEZ) is an area where only vehicles with an emission class below a certain limit can enter. In 2009 a LEZ was implemented in city of Amsterdam, and in 2015 it was proposed again in the City of Antwerp. Prevision are made to foresee air quality effects in Antwerp, because it is still ongoing. In 2020, it is estimated that PM_{10} and $PM_{2.5}$ will be reduced with 69 % and 41 % respectively. NO_2 is expected to show a reduction of 12 %. This LEZ zone influenced traffic-related air pollutants with a decrease of 4.9 % for NO_2, 5.9 % for NO_x, 5.8 % for PM_{10} and 12.9 % for elemental carbon.

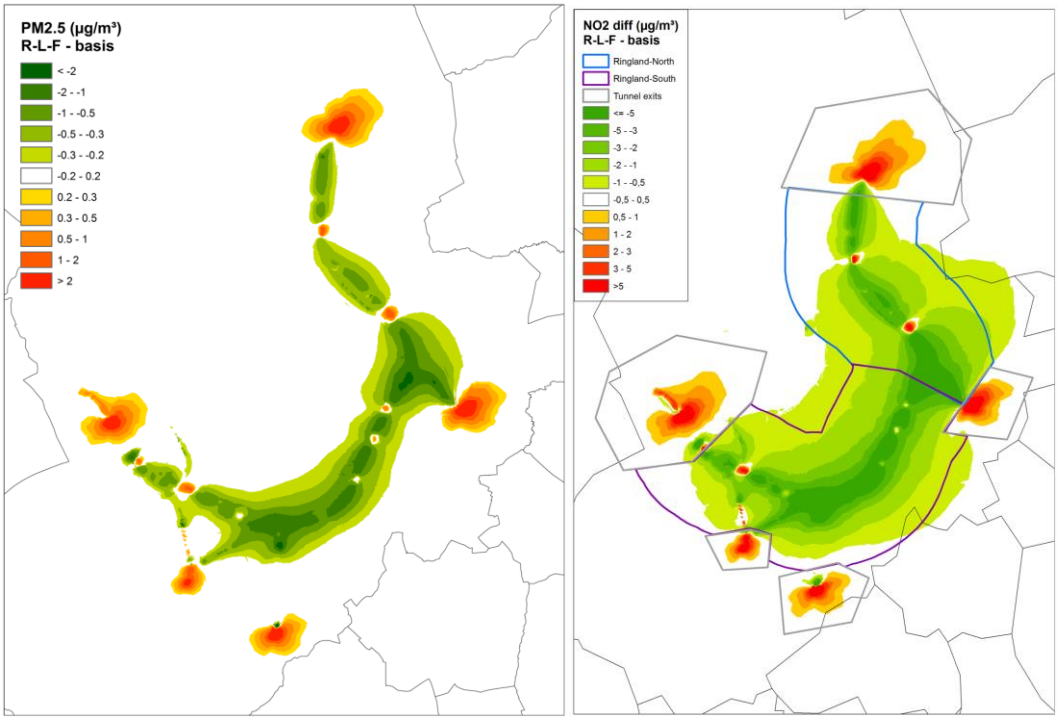

Figure 33: $PM_{2.5}$ and NO_2 differences of scenario RL-F (filtered tunnelled ring road) with the basic scenario (open air ring road). (Van Breusselen et al., 2016).

Other strategies to reduce traffic-related pollution is to act regulating traffic in city with specifically sequencing traffic lights such those planned in Leicester City. This sequencing system is thought to have less and smarter stages. This strategy aims to reduce journey times and improve bus services, which results in a faster traffic flow for the city, especially for the congested Glenhills Way junction.

For the pollutant reduction, it is furthermore possible to act on public transport and pollution awareness in general. The region of Haarlem-IJmond, is provided with a clean bus tender: a public transport with less emission of NO_x, particulate matter and soot. London is instead the city where the pilot project “Cleaner Air Champions” takes place. This measure recruits local residents in Hackney, Havering and Redbridge. These volunteers were trained and supported to raise awareness of local air quality issues within their communities and actions. This target is conducted through actions like anti-idling campaigns, information talks, led walks and rides.

As for others initiatives, these last presented measures are discussed in work groups. The proposals who succeed turn out to be primarily related to a system which encourages inhabitants to take interest and cooperate. At downside, the weakness stressed arise from the newness of initiatives: the sequencing lights could move traffic to other part of the city, the clean air bus tender has no noise pollution countermeasures and the “Cleaner Air Champion project” must deal with volunteers limited time and resources.

6.7 Vantaa (FI)

6.7.1 Air Quality

Vantaa belongs to the Helsinki Metropolitan Area, defined as the municipalities of Helsinki, Vantaa, Espoo and Kauniainen (Figure 34). The Helsinki Region Environmental Services Authority (HSY) monitors the air quality at 11 monitoring stations within the metropolitan area. Four of these sites have been chosen: Mannerheimintie (busy city centre of Helsinki), Mäkelänkatu (Street canyon), Kallio (residential area), Tikkurila (busy district centre of Vantaa) and Luukki (rural site). In addition, the Helsinki Urban Boundary-Layer Atmosphere Network (UrBAN) is a research network to study the physics of the urban micro-climate in Helsinki (Wood et al., 2013).

Figure 34: Map of the Helsinki Metropolitan Area with air quality measurement stations (European Environmental Agency, 2016).

The chosen stations will cover a large part of Helsinki region and different land use. In the following tables, annual mean concentrations and numbers of threshold exceedances are reported.

In the context of iSCAPE, Vantaa will access different green passive cooling system and find out different benefit's options both in current and future climate. The following tables will provide an overview of different environment in the Helsinki Metropolitan Area, by which the most pollutant areas are highlighted, and find what kind of intervention have to be considered with respect to the different distributions of pollutants.

Table 19 shows the annual mean concentrations of NO_2. Only the monitoring station called Mannerheimintie shows values close to the European limit, while the other data are lower than the European limit. Moreover, they are all decreasing trends, suggesting an intervention by local

authority with an improvement of the public health conditions. A high rate traffic-induced emissions probably account for the differences between the busy city centre of Helsinki, Mannerheimintie, and the smallest city of Vantaa and the residential area of Kallio. The rural site of Luukki is almost free from NO_2 pollution.

		Annual mean concentrations of NO_2 $(\mu g/m^3)$					
		2010	2011	2012	2013	2014	2015
Helsinki region	Tikkurila	30	28	25	27	25	21
	Mannerheimintie	41	39	37	37	36	32
	Kallio	23	20	20	20	20	18
	Luukki	8	7	7	5	6	4

Table 19: Annual mean concentrations of NO_2. Differences between urban traffic and background measurements are shown. The European limit for NO_2 annual mean concentrations is 40 µg/m^3. (Helsinki Region Environmental Services Authority).

Table 20 shows the annual mean concentration for ozone, calculated with 8-hours daily mean. No information can be obtained from a comparison with the European limit because it concerns the number of days in which the 8-hour mean concentration exceeds 120 µg/m^3. This number should not exceed 25 days, averaged over three years. The highest concentrations are measured in the rural site of Luukki, but the residential of Kallio is close. This is expected since emissions from rural wet soil, as well as consequence of agriculture and livestock, is an important component of the total ozone concentration in a wide region. As expected from the ozone formation cycle, O_3 maximum concentrations correspond to NO_2 minimum, and vice versa.

		Annual mean concentrations of O_3 $(\mu g/m^3)$					
		2010	2011	2012	2013	2014	2015
Helsinki region	Tikkurila	44	45	45	47	ND	ND
	Mannerheimintie	39	40	39	39	35	41
	Kallio	48	50	48	52	46	18
	Luukki	51	55	52	55	50	49

Table 20: Annual mean value of maximum daily 8-hour mean O_3 concentration. Differences between urban traffic and background measurements are shown. The European human health threshold for O_3 maximum daily 8-hour mean concentration is 120 µg/m^3 (not to be exceeded for more than 25 days averaged over three years). ND stands for no available data. (Helsinki Region Environmental Services Authority).

Table 21 shows the annual mean concentrations of PM_{10}. The mean concentrations obtained by all the monitoring stations Tikkurila and Kallio are more than a half lower than the European limit, while those measured by the monitoring station called Mannerheimintie are 35 % lower than the European limit. As said for NO_2, also PM_{10} concentrations are probably affected by traffic emissions, at least for the case of Mannerheimintie. However, the traffic emissions produce no difference between Vantaa and a residential site such as Kallio, despite NO_2 concentrations are

different. A possible explanation can come from the diverse rate of improvement on emissions reductions for gases and particulates, with an advantage for the second ones.

		Annual mean concentrations of PM_{10} $(\mu g/m^3)$					
		2010	2011	2012	2013	2014	2015
Helsinki region	Tikkurila	16	15	12	14	16	12
	Mannerheimintie	25	24	21	24	26	20
	Kallio	15	15	13	13	15	12

Table 21: Annual mean concentrations of PM_{10}. Differences between urban traffic and background measurements are shown. The European limit for PM_{10} annual mean concentrations is 40 μg/m^3. (Helsinki Region Environmental Services Authority).

Table 22 shows the number of days with PM_{10} concentrations exceeds 50 μg/m^3. It shows that this number is always lower than the European limit, close to zero for the values measured by the monitoring station Kallio, but it is starkly higher and variable in a trafficked environment such as Mannerheimintie.

		No of days with PM_{10} concentrations exceeds 50 $\mu g/m^3$					
		2010	2011	2012	2013	2014	2015
Helsinki region	Tikkurila	8	4	1	4	4	6
	Mannerheimintie	24	19	7	17	19	6
	Kallio	3	2	0	0	0	1

Table 22: Number of days with PM_{10} concentrations exceeds 50 μg/m^3 (value not to be exceeded more than 35 times per year). Different sites are shown. (Helsinki Region Environmental Services Authority).

Table 23 shows the annual mean concentrations of $PM_{2.5}$. The mean concentrations obtained by all the monitoring stations are lower than half of the European limit. There are not distinctions between different environments. Concentrations are also beneath the WHO guideline for human health (10 μg/m^3): this is both an indicator of healthy conditions, also in the busiest areas, a moderate human impact on the environment.

		Annual mean concentrations of $PM_{2.5}$ $(\mu g/m^3)$					
		2010	2011	2012	2013	2014	2015
Helsinki region	Tikkurila	9	8	7	7	8	6
	Mannerheimintie	11	10	8	9	10	7
	Kallio	9	8	7	7	8	5
	Luukki	8	7	7	6	7	5

Table 23: Annual mean concentrations of $PM_{2.5}$. Differences between urban traffic and background measurements are shown. The European limit for $PM_{2.5}$ annual mean concentrations is 25 μg/m^3. (Helsinki Region Environmental Services Authority).

Table 24 shows the number of days with $PM_{2.5}$ concentrations exceed 25 μg/m^3. Table 24 shows that this number is always lower than 5, for the years 2012-2015 and amply decreasing with respect to the previous two-years period, leading to more healthy conditions mainly for the Helsinki city centre inhabitants.

		No of days with $PM_{2.5}$ concentrations exceeds 25 $\mu g/m^3$					
		2010	2011	2012	2013	2014	2015
Helsinki region	Tikkurila	14	6	5	0	3	3
	Mannerheimintie	17	12	4	2	3	2
	Kallio	6	3	4	1	2	0
	Luukki	4	5	3	0	0	1

Table 24: Number of days with $PM_{2.5}$ concentrations exceeds 25 μg/m^3 (WHO threshold). Different sites are shown. (Helsinki Region Environmental Services Authority).

6.7.2 Long term trend in NO_2 emissions

Ozone ground-level concentration and vegetation exposure in Finland are here presented, both observed in the recent decade and estimated for the period 1900-2100. The estimation is achieved through a chemistry-transport model: the SRES (Special Report on Emissions Scenarios) scenarios of the Intergovernmental Panel on Climate Change and emission inventories (Laurila et al., 2004).

Figure 35 shows concentrations of NO_2 in Finland and in other country around Baltic sea, since NO_2 the precursor ozone is most sensible to (Simpson et al., 1997). This trend is not linked to an equivalent decrease of ozone concentration (figure not shown).

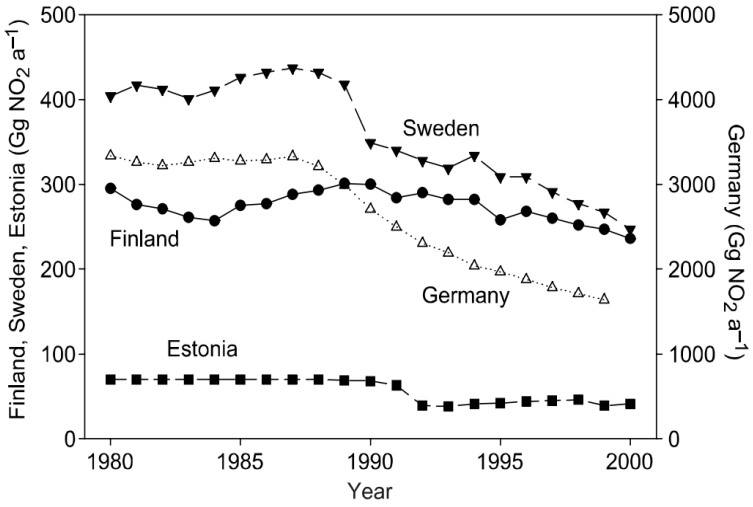

Figure 35: Annual NO_2 emissions in some countries around the Baltic Sea (Laurila et al., 2014).

6.8 A brief comparison

Having delineated the broad overview about air quality, research and policy foci of the iSCAPE cities, this section brings some information together to form a general picture. It is only a qualitative summary of the situation in the target cities, to understand general long term differences between them. Bottrop and Hasselt in general are only indicative for the city behaviour while the other cities have a more detailed structure, because there are much less available data (e.g. there is only the temporal evolution of pollutants, while the other cities have also spatial distribution). So, it is not intended as a comparison between two sites uncertainty, but just as a representation of spreading of their measures.

Bologna has the highest value of NO_2 annual mean concentration, almost 40 µg/m^3 (very close to the European limit). Values for the other cities fall in a range between 20 and 30 µg/m^3. A possible explanation for this big gap between Bologna and the other cities can be the geographic locations. Po Valley is a basin where pollutants flow into coming from different part of North Italy, and stagnate. Also, typical condition of thermal inversion contributes to the stagnation of pollutants at surface, suppressing the air recirculation. These suggestion is confirmed by the analysis of the other pollutants, where Bologna has always the higher concentrations. Traffic seems to be an important source of localised NO_2, so a big city like Bologna can be more affected by these kinds of emissions with respect to smaller centres like Hasselt or Guildford. On the other hand, comparable cities like Helsinki or Dublin can also be affected by the vicinity of the sea, which can mitigate the effect of pollutant stagnation thanks to breeze circulation.

Vantaa and Bologna have the highest values of O_3 concentrations, while Hasselt has the lowest. Vantaa is also the only city where O_3 and NO_2 concentrations are inversely proportional: trafficked roads have high concentrations of NO_2 and poor ones for O_3, while in rural areas the situation is overturned. These conditions suggest no other compounds interested in the ozone cycle, have sensible concentrations. In fact, considering only the possible photochemical reactions between O_3 and NO_2, an increase concentration for the first corresponds to a decrease for the second, and vice versa. In a real atmosphere, other compounds (e.g. VOCs) participate in the formation/destruction of ozone.

Bologna and Hasselt have the highest values of PM_{10} annual mean concentration. Trafficked environments play a key role for Bologna, enhancing the mean value for the city. Vantaa and

Dublin seems to have the strongest policies on trafficked-induced emissions and residential heating systems reductions, since their concentrations are the lowest.

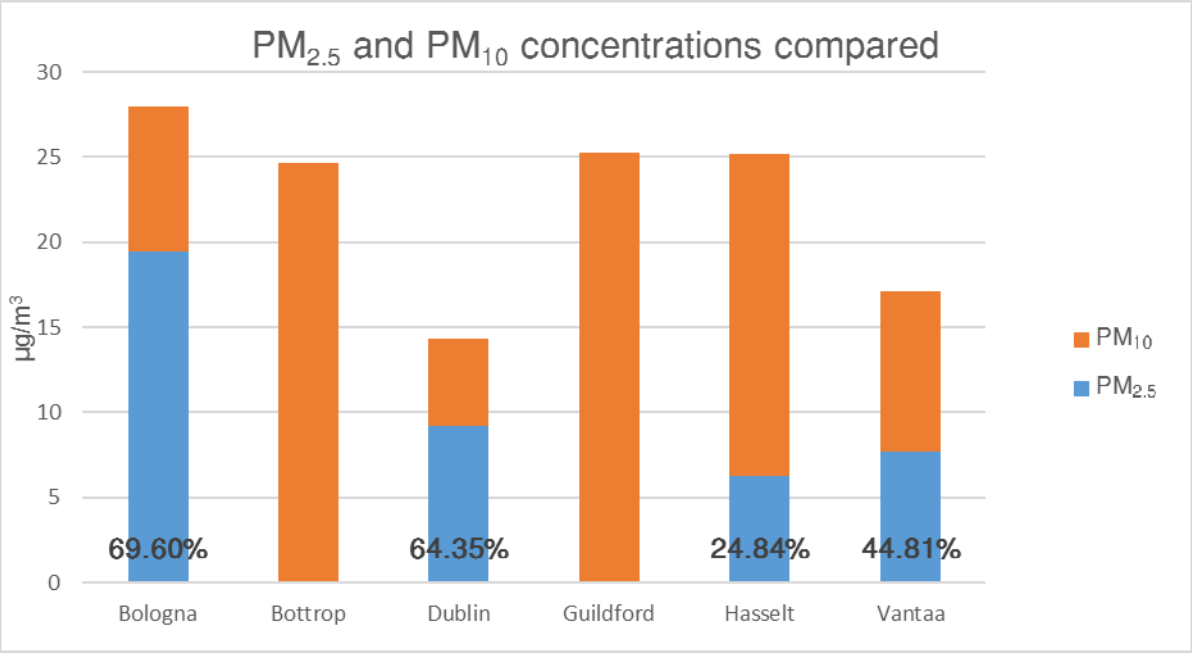

Figure 37: Comparison between annual mean concentrations of $PM_{2.5}$ and PM_{10} within and between target cities.

Bologna has the highest values of $PM_{2.5}$ annual mean concentration, twice the values of the ones shown by the other cities. Apart from Bologna, $PM_{2.5}$ concentrations remain beneath the WHO guideline for human health (10 µg/m^3 averaged over one year), which is a good indicator for the liveability of a city. Reduction of emission in Bologna has to become the priority, despite the obstacle represented by the number of ways by which $PM_{2.5}$ can be produced.

Figure 37 shows the comparison, for each city, between concentration of PM_{10} and $PM_{2.5}$. Where both measures are available, the percentage of the rate $PM_{2.5}/PM_{10}$ is also shown. Bologna and Dublin have the highest percentage of $PM_{2.5}/PM_{10}$ annual mean concentrations, while Hasselt and Vantaa have the lowest.

6.9 Outlook: green infrastructure as examples of mitigation and adaptation options

The information reported above serves as starting point for the future deployment of PCSs within iSCAPE. Central within iSCAPE is the role of green infrastructure as ways that to mitigate and/or to adapt to climate change to reduce urban air pollution. We recall that green infrastructure is being considered in the Living Labs of Vantaa, Guilford and Bologna. Literature is extensive but somehow fragmented. As classical example, we briefly discuss the role of green roofs. These are the most typical examples being used within the climate modelling community.

Green roofs are roofs that are partially or (almost) completely covered by vegetation as a result of planned action rather than as a result of negligence. Green roofs are an increasing feature of cities' urban planning tool set. Local adaptation plans around the world list green roofs as a tool

for both storm-water management, attenuation of urban heat-island effect and improving air quality, as is done in adaptation plans of e.g. Vancouver, Copenhagen, London, Melbourne, Singapore, Chicago and Barcelona (see Copenhagen, 2015, for a review and links to adaptation plans). Green roofs also decrease the energy consumption in buildings (e.g. Berardi et al. 2014). They are identified as a valuable strategy to make buildings more sustainable, and increase urban green in cities while avoiding the negative effects of lowering population densities.

Green roofs improve the air quality in cities by absorbing air pollutants. Tan and Sia (2005) found that levels of fine particles and sulphur dioxide decreased by 6 % and 37 % in the immediate air-space after a green roof was installed. Currie and Bass (2008) estimated that 109 ha of green roofs in Toronto could remove about 8 tons of air pollutants per year. In economic terms, the effect of removing fine particles is by far the most important aspect of pollution removal. In a cost-benefit analysis of green roofs (Nurmi et al. 2016) it was found that that at least 95 % of the air-quality benefits can be attributed to the removal of particulate matter, which is around 7 % of the installation cost of a green roof. Inclusion of other benefits, such as increased lifespan of the roof and storm-water management, usually results into positive net benefits, making green roofs a viable solution in urban areas from economic perspective.

7 Summary on air quality and climate change

The problem of air pollution in urban areas has a high degree of complexity; the challenges need to be addressed given that but high level of pollutant concentration impact on human health, and has direct bi-directional influence on climate change. Complexity is intrinsic in the urban environment; inhomogeneous features inside the city (e.g. street canyons, parks, beltways, etc.) are impacting upon local ventilation which in turn determines local pollutants distributions. Inhomogeneity also arises between different cities, mainly in terms of buildings and green areas distribution, geographical location, mean meteorological patterns. This inhomogeneity leads to different distributions and concentrations of pollutants, and so the best and most cost-effective policies to improve air quality can be diverse. For instance, Bologna is located in the Po Valley, where local meteorological and geographical conditions are less favourable to the dispersion of pollutants with respect to cities at sea side, which benefit from breezes influence. In broad sense, air quality is generally better in Northern Europe: the presence of widespread basins or the influence of sea breezes mitigate the stagnation effect which leads to higher pollutant concentration in surrounded basin and industrial areas.

At a local scale, pollutant concentrations have different impacts due to meteorological, geographical and structural features of the single city, but also as a result of local air quality policies. In general traffic-induced emissions (NO_2 and PM_{10}) have an influence on total concentration at street level, but not at urban scale. Residential heating systems also contribute again at street level, but its signal is weaker. Two pollutants, NO_2 and PM_{10} have a dependence on emissions at the street scale, while $PM_{2.5}$ is more homogeneous in the urban environment. Concerning the risks on human heath connected to exposure to high level of $PM_{2.5}$ has led to a decrease and an adjustment of concentrations at WHO suggested level for human health which is stricter than the European limit. Only Bologna, among the target cities requires to improve its efforts to mitigate the $PM_{2.5}$ concentrations. Ozone concentrations inside the urban environment seems to be influenced by the distribution of its precursors (NO_x and VOCs on top), but in general it is quite homogeneous at the city scale. In rural areas ozone concentrations sensibly grow, supported by favourable conditions. In the context of iSCAPE, single city analysis will be used as a reference baseline to undertake the different activities of each living lab, as suggests in the previous section.

The review on the influence of air pollution on climate change has highlighted three different climatological variables which interact the most with pollutants: surface temperature, precipitation and sea level pressure. Global and regional model simulations have indicated that the European region is projected to undergo a warming much larger than the global average. Temperature scenario is coupled with precipitation pattern projection and they facilitate an increase in pollutants such as ozone due to increased biogenic emissions and photochemical rates and reduced wet removal. Changes in meteorological variables can modify global sea level pressure patterns, with consequences on local circulations and distribution of air masses. In the end, climate change induced by enhanced pollutant emissions will in turn increase pollutant concentration. So, a positive feedback is established, leading to an intensification of climate changes in those regions highly affected by pollution.

All the described interactions take place at large scale; development at urban scale is yet to be investigated in the forthcoming future to verify or dismiss the large-scale trends. In the context of iSCAPE we have the possibility to study the climate impact at urban scale and its expected changes, with the aim of enhancing the liveability of our cities.

8 Appendix A: Air Quality Standards (European Commission, 2017)

Humans can be adversely affected by exposure to air pollutants in ambient air. In response, the European Union has developed an extensive body of legislation which establishes health based standards and objectives for several pollutants in air. These standards and objectives are summarised in the table below. These apply over differing periods of time because the observed health impacts associated with the various pollutants occur over different exposure times.

Pollutant	Concentration	Averaging Period	Legal nature	Exceeding per year
Fine particles ($PM_{2.5}$)	25 µg/m^3***	1 year	Target value entered into force 1.1.2010 Limit value enters into force 1.1.2015	n/a
Sulphur dioxide (SO_2)	350 µg/m^3	1 hour	Limit value entered into force 1.1.2005	24
	125 µg/m^3	24 hours	Limit value entered into force 1.1.2005	3
Nitrogen dioxide (NO_2)	200 µg/m^3	1 hour	Limit value entered into force 1.1.2010	18
	40 µg/m^3	1 year	Limit value entered into force 1.1.2010*	n/a
PM_{10}	50 µg/m^3	24 hours	Limit value entered into force 1.1.2005**	35
	40 µg/m^3	1 year	Limit value entered into force 1.1.2005**	n/a
Lead (Pb)	0.5 µg/m^3	1 year	Limit value entered into force 1.1.2005 (or 1.1.2010 in the immediate vicinity of specific, notified industrial sources; and a 1.0 µg/m3 limit value applied from 1.1.2005 to 31.12.2009)	n/a
Carbon monoxide (CO)	10 mg/m^3	Maximum daily 8-hour mean	Limit value entered into force 1.1.2005	n/a
Benzene	5 µg/m^3	1 year	Limit value entered into force 1.1.2010**	n/a
Ozone	120 µg/m^3	Maximum daily 8-hour mean	Target value entered into force 1.1.2010	25 days averaged over 3 years
Arsenic (As)	6 ng/m^3	1 year	Target value enters into force 31.12.2012	n/a
Cadmium (Cd)	5 ng/m^3	1 year	Target value enters into force 31.12.2012	n/a
Nickel (Ni)	20 ng/m^3	1 year	Target value enters into force 31.12.2012	n/a

Polycyclic Aromatic Hydrocarbons	1 ng/m^3 (expressed as concentration of Benzo(a)pyrene)	1 year	Target value enters into force 31.12.2012	n/a

*Under the new Directive the member State can apply for an extension of up to five years (i.e. maximum up to 2015) in a specific zone. Request is subject to assessment by the Commission. In such cases within the time extension period the limit value applies at the level of the limit value + maximum margin of tolerance (48 µg/m^3 for annual NO_2 limit value).

**Under the new Directive the Member State could apply for an extension until three years after the date of entry into force of the new Directive (i.e. May 2011) in a specific zone. Request was subject to assessment by the Commission. In such cases within the time extension period the limit value applies at the level of the limit value + maximum margin of tolerance (35 days at 75 µg/m^3 for daily PM_{10} limit value, 48 µg/m^3 for annual PM_{10} limit value).

***Standard introduced by the new Directive.

9 References / Bibliography

Aalto, J., P. Pirinen, and K. Jylhä (2016), New gridded daily climatology of Finland: Permutation-based uncertainty estimates and temporal trends in climate, *J. Geophys. Res. Atmos.*, 121, 3807-3823. doi:10.1002/2015JD024651

Ahmad K, M. Khare and K.K. Chaudhry, (2005) Wind tunnel simulation studies on dispersion at urban street canyons and intersections - a review, *Journal of Wind Engineering and Industrial Aerodynamics* 93:697–717. doi: 10.1016/j.jweia.2005.04.002

Air Quality Monitoring and Noise Control Unit Annual Report 2010, *Dublin City Council*.

Air Quality Monitoring and Noise Control Unit Annual Report 2011, *Dublin City Council*.

Air Quality Monitoring and Noise Control Unit Annual Report 2012, *Dublin City Council*.

Air Quality Monitoring and Noise Control Unit Annual Report 2013, *Dublin City Council*.

Air Quality Monitoring and Noise Control Unit Annual Report 2014, *Dublin City Council*.

Air Quality Monitoring and Noise Control Unit Annual Report 2015, *Dublin City Council*.

Alexander L. (2010), Extreme heat rooted in dry soils, *Nat. Geosci*, 4, 12-13

Antolini, G., Auteri, L., Pavan, V., Tomei, F., Tomozeiu, R. and Marletto, V. (2016), A daily high-resolution gridded climatic data set for Emilia-Romagna, Italy, during 1961–2010. *Int. J. Climatol*., 36: 1970–1986. doi:10.1002/joc.4473

ARPA Emilia-Romagna, (2016) la Qualità dell'ambiente in Emilia-Romagna: annuario dei dati 2015

ARPA Emilia-Romagna, (2016) Rete regionale di monitoraggio e valutazione della qualità dell'aria provincia di Bologna: report dei dati 2015

Balsamo, G., Viterbo, P., Beljaars, A., van den Hurk, B., Hirschi, M., Betts, A. K., and Scipal, K. (2009): A Revised Hydrology for the ECMWF Model: Verification from Field Site to Terrestrial Water Storage and Impact in the Integrated Forecast System, *J. Hydrometeor.*, 10, 623–643

Barriopedro D., E.M. Fischer, J. Luterbacher, R.M. Trigo, R. García-Herrera (2011), The hot Summer of 2010: redrawing the temperature record map of Europe, *Science*, 332(6026), 220-224

Belcher S. E., J. N. Hacker and D. S. Powell, (2009) Constructing design weather data for future climates. *Building Serv Eng Res Technol*, 26, 49-61

Beniston M. (2015) Ratios of record high to record low temperatures in Europe exhibit sharp increases since 2000 despite a slowdown in the rise of mean temperatures. *Climatic Change*, 129:225–237

Beniston M., D.B. Stephenson, O.B. Christensen, C.A.T. Ferro, C. Frei, S. Goyette, K. Halsnaes, T. Holt, K. Jylhä, B. Koffi, J. Palutikof, R. Schöll, T. Semmler, K. Woth (2007), Future extreme events in Europe climate: an exploration of regional climate model projections, *Springer Science*, Climatic Change, 81:71-95, doi: 10.1007/s10584-006-9226-z

Berardi U., GhaffarianHoseini A., GhaffarianHoseini A. (2014), State-of-the-art analysis of the environmental benefits of green roofs, *Applied Energy*, vol. 115, pp. 411-428

Berndes G., B. Abt, A. Asikainen, A. Cowie, V. Dale, G. Egnell, M. Lindner, L. Marelli, D. Paré, K. Pingoud and S. Yeh (2016) Forest biomass, carbon neutrality and climate change mitigation. *From Science to Policy*, 3. http://www.efi.int/files/attachments/publications/efi_fstp_3_2016.pdf

Best, M. J., Grimmond, C., and Villani, M. (2006): Evaluation of the Urban Tile in MOSES using Surface Energy Balance Observations, *Bound. Lay. Meteorol.*, 118, 503–525

Best, M. J., Pryor, M., Clark, D. B., Rooney, G. G., Essery, R. L. H., Ménard, C. B., Ewards, J. M., Hendry, M. A., Porson, A., Gedney, N., Mercado, L. M., Sitch, S., Blyth, E., Boucher, O., Cox, P. M., Grimmond, C. S. B., and Harding, R. J. (2011): The Joint UK Land Environment Simulator (JULES), model description – Part 1: Energy and water fluxes, *Geosci. Model Dev.*, 4, 677–699, doi: 10.5194/gmd-4-677-2011

Blocken B., Y. Tominaga and T. Stathopoulos, (2013) CFD simulation of micro-scale pollutant dispersion in the built environment, *Building and Environment*, 64:225-230, doi:10.1016/j.buildenv.2013.01.001

Brady J. and M. O'Mahony, (2011) Travel to work in Dublin. The potential impacts of electric vehicles on climate change and urban air quality, *Transportation Research Part D: Transport and Environment*, 16(2), 188-193

Brasseur G.P. and coauthors, (1998) Past and future changes in global tropospheric ozone: impact and radiative forcing, *Geophys. Res. Lett.* 25 3807–3810

Britter R.E. and S.R. Hanna, (2003) Flow and dispersion in urban areas, *Annual Review of Fluid Mechanics*, 35:469-496, doi: 10.1146/annurev.fluid.35.101101.161147

Brunetti, M., M. Maugeri, F. Monti, and T. Nanni (2004), Changes in daily precipitation frequency and distribution in Italy over the last 120 years, *J. Geophys. Res.*, 109, D05102, doi:10.1029/2003JD004296

Brunetti, M., Maugeri, M., Monti, F. and Nanni, T. (2006), Temperature and precipitation variability in Italy in the last two centuries from homogenised instrumental time series. *Int. J. Climatol.*, 26: 345–381. doi:10.1002/joc.1251

Bueno, B., Pigeon, G., Norford, L. K., Zibouche, K., and Marchadier, C., (2012): Development and evaluation of a building energy model integrated in the TEB scheme, *Geosci. Model Dev.*, 5, 433-448, doi:10.5194/gmd-5-433-2012

Chan A. L. S. (2011), Developing future hourly weather files for studying the impact of climate change on building energy performance in Hong Kong. *Energy and Building*, 43, 2860–2868

Chiesa I., (2013) Studio delle relazioni tra concentrazione di ozono e temperatura dell'aria per l'elaborazione di scenari futuri. Tesi di Laurea Magistrale in Fisica, Università di Bologna, AA 2012/2013

Christensen, J. H., T. R. Carter, and F. Giorgi (2002), PRUDENCE employs new methods to assess European climate change, *Eos Trans. AGU*, 83(13), 147–147, doi:10.1029/2002EO000094

Christensen, J. and Christensen, O. (2007): A summary of the PRUDENCE model projections of changes in European climate by the end of this century, *Climatic Change*, 81, 7–30, doi:10.1007/s10584-006-9210-7

Chrysanthou, A., G. van der Schrier, E. J. M. van den Besselaar, A. M. G. Klein Tank, and T. Brandsma (2014), The effects of urbanization on the rise of the European temperature since 1960, *Geophys. Res. Lett.*, 41, 7716–7722, doi:10.1002/2014GL061154

City of Surrey, Surrey Climate Change Strategy, 2009

Clark, D. B., Mercado, L. M., Sitch, S., Jones, C. D., Gedney, N., Best, M. J., Pryor, M., Rooney, G. G., Essery, R. L. H., Blyth, E., Boucher, O., Harding, R. J., Huntingford, C., and Cox, P. M. (2011): The Joint UK Land Environment Simulator (JULES), model description – Part 2: Carbon fluxes and vegetation dynamics, *Geosci. Model Dev.*, 4, 701–722, doi:10.5194/gmd-4-701-2011

Copenhagen, 2015. http://en.klimatilpasning.dk/media/704006/1017_sJ43Q6DDyY.pdf

Crawley et al. 2008) D. B. Crawley D. B., J. Hand, M. Kummert and B. T. Griffith, (2008) Contrasting the capabilities of building energy performance simulation programs. *Building and Environment*, 43, 661-673

Currie, Beth A., Bass, Brad. (2008), Estimate of air pollution mitigation with green plants and green roofs using the UFORE model, *Urban Ecosystems*, Vol. 11., pp. 409-422

de Munck C., G. Pigeon, V. Masson, F. Meunier, P. Bousquet, B. Trmac, M. Merchat, P. Poeuf and C. Marchadier (2012), How much can air conditioning increase air temperatures for a city like Paris, France, *Int. J. Climatol*. 33, 210–227

de Munck, C. S., Lemonsu, A., Bouzouidja, R., Masson, V., and Claverie, R., (2013): The

GREENROOF module (v7.3) for modelling green roof hydrological and energetic performances within TEB, *Geosci. Model Dev.*, 6, 1941-1960, doi:10.5194/gmd-6-1941-2013

De Ridder K. and coauthors (2008), Simulating the impact of urban sprawl on air quality and population exposure in the German Ruhr area. Part I: Reproducing the base state, *Atmospheric environment*, *42*(30), 7059-7069

De Ridder K. and coauthors (2008), Simulating the impact of urban sprawl on air quality and population exposure in the German Ruhr area. Part II: Development and evaluation of an urban growth scenario, *Atmospheric environment*, *42*(30), 7070-7077

Della Marta P.M., M.R. Haylock, J. Luterbacher, H. Wanner (2007a), Doubled length of western European summer heat waves since 1880, *J. Geophys. Res. Atmos.*, 112(D15)

Dempsey N., 2008 Government Announces Plans for the Electrification of Irish Motoring, *Department of Transport*, Dublin

Deque M. and co-authors, (2005) Global high-resolution vs. regional climate model climate change scenarios over Europe: quantifying confidence level from PRUDENCE results, *Clim. Dyn*. 25 653–670

Derwent R.G., W.J. Collins, C.E. Johnson, D.S. Stevenson, (2001) Transient behaviour of tropospheric ozone precursors in a global 3D CTM and their indirect greenhouse effects, *Clim. Change*, 49, 463–487

Diffenbaugh N.S., J.S. Pal, F. Giorgi, X. Gao (2007), Heat stress intensification in the Mediterranean climate change hotspot, *Geophys. Res. Lett.*, 34(11)

Domonkos, P. and Coll, J. (2016), Homogenisation of temperature and precipitation time series with ACMANT3: method description and efficiency tests. *Int. J. Climatol.* doi:10.1002/joc.4822

Dupont, S. and Mestayer, P. G., (2006), Parameterization of the Urban Energy Budget with the Submesoscale Soil Model, *J. Appl. Meteor. Climatol.*, 45, 1744–1765.Domonkos and Coll, 2016

Eames M., T. Kershaw and D. Coley, (2011), The creation of wind speed and direction data for the use in probabilistic future weather files, *Building Serv. Eng. Res. Technol*., 32, 143-158

Ek, M. B., Mitchell, K. E., Lin, Y., Rogers, E., Grunmann, P., Koren, V., Gayno, G. and Tarpley, J. D. 2003: Implementation of Noah land surface model advances in the National Centers for Environ-mental Prediction operational mesoscale Eta model, *J. Geophys. Res.*, 108, 8851, doi: 10.1029/2002JD003296

EN ISO 15927-4:2005, Hygrothermal performance of buildings – calculation and presentation of climatic data. Part 4: data for assessing the annual energy for heating and cooling, (2005)

Environmental & Engineering Strategic Policy Committee, (2008-2012) Climate Change Strategy for Dublin City

Environmental Protection Agency, 2009, Ireland's Greenhouse Gas Emissions in 2008, *Environmental Protection Agency*, Wexford

Environmental Protection Agency Maps, http://gis.epa.ie/Envision

Ericson B., D. Hanrahan and V. Kong, (2008) The World's worst pollution problem: the top ten toxic twenty, Project Report Blacksmith Institute, New York, Available at: http://www.worstpolluted.org

EU ToPDAd project, http://www.topdad.eu/

European Commission, (2017) Air Quality Standards, http://ec.europa.eu/environment/air/quality/standards.htm

European Environmental Agency, 2016, http://www.eea.europa.eu/themes/air/air-quality/map/airbase/air-quality-statistics-at-reporting-stations

Eyring, V., Bony, S., Meehl, G. A., Senior, C. A., Stevens, B., Stouffer, R. J., and Taylor, K. E. (2016), Overview of the Coupled Model Intercomparison Project Phase 6 (CMIP6) experimental design and organization, *Geosci. Model Dev.*, 9, 1937-1958, doi:10.5194/gmd-9-1937-2016

Fischer E.M. and Schär C. (2010), Consistent geographical patterns of changes in high-impact European heatwaves, *Nat. Geosci*, 3 (6), 398-403

Flanders Environmental Agency (2014) Air Quality in the Flemish Region. http://en.vmm.be/publications/air-quality-in-flanders-2014

Forkel R. and R. Knocke, (2006) Regional climate change and its impact on photooxidant concentrations in southern Germany: simulations with a coupled regional climate–chemistry model, *J. Geophys. Res*. 111 (12) D12302

Gallagher J., R. Baldauf, C.H. Fuller, P. Kumar, L.W. Gill and A. McNabola, (2015) Passive methods for improving air quality in the built environment: a review of porous and solid barriers, *Atmospheric Environment*, 120:61-70, doi: 10.1016/j.atmosenv.2015.08.075

Gharbia, S.S., Gill, L., Johnston, P. (2016), Multi-GCM ensembles performance for climate projection on a GIS platform, *Model. Earth Syst. Environ*. 2: 102. doi:10.1007/s40808-016-0154-2

Giorgi F., (2006) Regional climate modelling. Status and perspectives, *J. Phys*. IV 139 101–118

Giorgi F. and co-authors, (2001) Emerging patterns of simulated regional climatic changes for the 21st century due to anthropogenic forcing, *Geophys. Res. Lett.* 28 3317–3320

Giorgi, F. and Gutowski, W.J. (2016), Coordinated Experiments for Projections of Regional Climate Change, *Current Climate Change Reports*, 2, 4, 202

Giorgi F. and Lionello P., (2008). Climate change projections for the Mediterranean region, *Global and Planetary Change* 63, 90–104.

Giorgi F. and F. Meleux (2007), Modelling the regional effects of climate change on air quality, *C.R. Geoscience*, 339 (2007), 721-733

Giorgi F. and X. Bi, (2005) Regional changes in surface climate interannual variability for the 21st century from ensembles of global model simulations, *Geophys. Res. Lett.* 32 L13701

Giorgi F. and X. Bi, (2005) Updated regional precipitation and temperature changes for the 21st century from ensembles of recent AOGCM simulations, *Geophys. Res. Lett.* 32 L21715

Giorgi F., X. Bi, J. Pal, (2004) Mean, interannual variability and trends in a regional climate change experiment over Europe. I: climate change scenarios (2071–2100), *Clim. Dyn*. 23 839–858

Guijt J. and M. Dijkema, (2015) The implementation and valuation of health relevant air quality policy measures in North-western Europe, *Joaquin – Joint Air Quality Initiative*

Guildford Borough Council, 2016, Air Quality Annual Status Report (ASR), Environmental Act 1995, *Local Air Quality Management*

Grimmond, C. S. B., Blackett, M., Best, M. J., Barlow, J., Baik, J.-J., Belcher, S. E., Bohnenstengel, S. I., Calmet, I., Chen, F., Dandou, A., Fortuniak, K., Gouvea, M. L., Hamdi, R., Hendry, M., Kawai, T., Kawamoto, Y., Kondo, H., Krayenhoff, E. S., Lee, S.-H., Loridan, T., Martilli, A., Masson, V., Miao, S., Oleson, K., Pigeon, G., Porson, A., Ryu, Y.-H., Salamanca, F., Shashua-Bar, L., Steeneveld, G.-J., Tombrou, M., Voogt, J., Young, D., and Zhang, N., (2010), The International Urban Energy Balance Models Comparison Project: First Results from Phase 1, *J. Appl. Meteorol. Climatol.*, 49, 1268–1292

Grimmond, C. S. B., Blackett, M., Best, M. J., Baik, J.-J., Belcher, S. E., Beringer, J., Bohnenstengel, S. I., Calmet, I., Chen, F., Coutts, A., Dandou, A., Fortuniak, K., Gouvea, M. L., Hamdi, R., Hendry, M., Kanda, M., Kawai, T., Kawamoto, Y., Kondo, H., Krayenhoff, E. S., Lee, S.-H., Loridan, T., Martilli, A., Masson, V., Miao, S., Oleson, K., Ooka, R., Pigeon, G., Porson, A., Ryu, Y.-H., Salamanca, F., Steeneveld, G., Tombrou, M., Voogt, J. A., Young, D. T., and Zhang, N., (2011), Initial results from Phase 2 of the international urban energy balance model comparison, *Int. J. Climatol.*, 31, 244–272

Haylock, M., N. Hofstra, A. Klein Tank, E. Klok, P. Jones, and M. New (2008), A European daily high- resolution gridded data set of surface temperature and precipitation for 1950–2006, *Journal of Geophysical Research: Atmospheres* (1984–2012), 113(D20)

Heal M.R., P. Kumar and R.M. Harrison, (2012) Particles, air quality, policy, health. *Chemical Society Reviews*, 41:6606-6630, doi: 10.1039/c2cs35076a

Hellsten A., K. Ketelsen, F. Barmpas, G. Tsegas, N. Moussiopoulos and S. Raasch, (2016) Nested multi-scale system in the PALM large-eddy simulation model, *22nd Symposium on Boundary Layers and Turbulence*, 20 Jun. 2016 https://ams.confex.com/ams/32AgF22BLT3BG/webprogram/Paper295810.html

Helsinki Region Environmental Services Authority, https://www.hsy.fi/en/experts/regional-data/Pages/default.aspx

Helsinki Region Environmental Services Authority, https://www.hsy.fi/fi/asiantuntijalle/avoindata/Sivut/default.aspx

Hilbert C. and C. Palmer, (2014) Urban development and air pollution: evidence from a global panel of cities, *Grantham Research Institute on Climate Change and the Environment*, Working Paper No. 175, http://www.lse.ac.uk/GranthamInstitute/wp-content/uploads/2014/12/Working-Paper-175- Hilber-Palmer-2014.pdf

Horton D.E., S. Harshvardhan, N.S Diffenbaugh (2012) Response of air stagnation frequency to anthropogenically enhanced radiative forcing. *Environmental Research Letters*, 7, 044034

HSY - Helsingin seudun ympäristöpalvelut -kuntayhtymä. Monitoring stations in the Helsinki Metropolitan Area. https://www.hsy.fi/en/residents/theairyoubreathe/monitoring-stations-helsinki-metropolitan-area/Pages/default.aspx

IIASA (International Institute for Applied Systems Analysis), (2012a), SSP Database, version 0.93. [URL: https://secure.iiasa.ac.at/web-apps/ene/SspDb]. Retrieved 7/2013

IIASA (International Institute for Applied Systems Analysis), (2012b), Supplementary note for the SSP data sets. [URL: https://secure.iiasa.ac.at/web-apps/ene/SspDb/static/download/ssp_suplementary%20text.pdf]. Retrieved 7/2013

IIASA (International Institute for Applied Systems Analysis), 2012c, GEA Scenario database, Version 2.0.2 [URL: http://www.iiasa.ac.at/web-apps/ene/geadb/dsd?Action=htmlpage&page=welcome] Retrieved 7/2013

IPCC (2001) Climate Change 2001: The Scientific Basis, Contribution of Working Group I to the Third Assessment Report of the Intergovernmental Panel on Climate Change, Appendix II - SRES Tables. Cambridge University Press

IPCC, 2010, *IPCC Workshop on Socio-Economic scenarios*, Workshop Report, Victor's

Residenz Hotel, Berlin, Germany 1-3 November 2010. [URL: http://www.ipcc.ch/pdf/supporting-material/IPCC_WoSES_Report_final_web.pdf], retrieved 6/2013

IPCC (2013) Climate Change 2013: The Physical Science Basis. Cambridge University Press https://www.ipcc.ch/report/ar5/wg1/

Jacob D., Petersen, J., Eggert, B. et al. Reg Environ Change (2014) 14: 563. doi:10.1007/s10113-013-0499-2

Jentsch M. F., A. S. Bahaj and P. A. B. James (2008), Climate change future proofing of buildings—Generation and assessment of building simulation weather files, *Energy and Buildings*, 40, 2148–2168

Johnson C.E., D.S. Stevenson, W.J. Collins, R.G. Derwent, (1999) Relative role of climate and emissions changes on future tropospheric oxidant concentrations, *J. Geophys. Res.* 104 18631–18645

Johnson C.E., D.S. Stevenson, W.J. Collins, R.G. Derwent, (2001) Role of climate feedback on methane and ozone studied with a coupled ocean-atmosphere-chemistry model, *Geophys. Res. Lett.* 28 1723–1726

Jones PG, Thornton PK. (2013), Generating downscaled weather data from a suite of climate models for agricultural modelling applications. *Agricultural Systems* 114: 1-5. DOI: https://dx.doi.org/10.1016/j.agsy.2012.08.002

Jylhä K, Kalamees T, Tietäväinen H, Ruosteenoja K, Jokisalo J, Hyvönen R, Ilomets S, Saku S, Hutila A, (2011), Rakennusten energialaskennan testivuosi TRY2012 ja arviot ilmastonmuutoksen vaikutuksista. (Test reference year 2012 for building energy demand and impacts of climate change), *Finnish Meteorological Institute*, Reports, 2011:6, 110 p

Jylhä K., Laapas, M., Ruosteenoja, K., Arvola, L., Drebs, A., Kersalo, J., Saku, S., Gregow, H., Hannula, H.-R. & Pirinen, P., (2014), Climate variability and trends in the Valkea-Kotinen region, southern Finland: comparisons between the past, current and projected climates. *Boreal Env. Res.*, 19 (suppl. A): 4–30

Jylhä K., J. Jokisalo, K. Ruosteenoja, K. Pilli-Sihvola, T. Kalamees, T. Seitola, H. Mäkelä, R. Hyvönen, M. Laapas and A. Drebs, (2015a), Energy demand for the heating and cooling of residential houses in Finland in a changing climate. *Energy and Buildings*, 99, 104-106, doi: 10.1016/j.enbuild.2015.04.001

Jylhä K., K. Ruosteenoja, J. Jokisalo, K. Pilli-Sihvola, T. Kalamees, H. Mäkelä, R. Hyvönen, and A. Drebs, (2015b), Hourly test reference weather data in the changing climate of Finland for building energy simulations. *Data in Brief*, 4, 162-169. doi: 10.1016/j.dib.2015.04.026

Järvi L, Grimmond CSB, Christen A. (2011), The surface urban energy and water balance scheme (SUEWS): Evaluation in Los Angeles and Vancouver. *J. Hydrol.* 411: 219–237, doi: 10.1016/j.jhydrol.2011.10.001.Jones and Thornton, 2013)

Kalamees T., Jylhä K., Tietäväinen H., Jokisalo J., Ilomets S., Hyvönen R., Saku S., (2012), Development of weighting factors for climate variables for selecting the energy reference year according to the EN ISO 15927-4 standard. *Energy and Buildings*, 47, 53-60. doi: 10.1016/j.enbuild.2011.11.031

Kenyon J. and Hegerl G.C. (2008), Influence of modes of climate variability on global temperature extremes, *J. Clim*, 21 (15), 3872-3889

Klein Tank, A. M. G., and Coauthors, (2002), Daily dataset of 20th-century surface air temperature and precipitation series for the European Climate Assessment. Int. J. Climatol., 22, 1441–1453, doi:10.1002/joc.773

KLIMAKS TechReport, (2012), Mitarbeiter der Stadt Stuttgart. Klimaanpassungskonzept Stuttgart KLIMAKS, Stadt Stuttagrt, 2012

Knutti, R. (2008), Should we believe model predictions of future climate change? *Phil. Trans. R. Soc. A* 2008 366 4647-4664; DOI: 10.1098/rsta.2008.0169

Kondo, H., Genchi, Y., Kikegawa, Y., Ohashi, Y., Yoshikado, H., and Komiyama, H. (2005), Development of a Multi-Layer Urban Canopy Model for the Analysis of Energy Consumption in a Big City: Structure of the Urban Canopy Model and its Basic Performance, *Bound. Lay. Meteorol.*, 116, 395–421

Kotlarski, S., Keuler, K., Christensen, O. B., Colette, A., Déqué, M., Gobiet, A., Goergen, K., Jacob, D., Lüthi, D., van Meijgaard, E., Nikulin, G., Schär, C., Teichmann, C., Vautard, R., Warrach-Sagi, K., and Wulfmeyer, V. (2014), Regional climate modeling on European scales: a joint standard evaluation of the EURO-CORDEX RCM ensemble, *Geosci. Model Dev.*, 7, 1297-1333, doi:10.5194/gmd-7-1297-2014

Krinner, G., Viovy, N., de Noblet-Ducoudré, N., Ogée, J., Polcher, J., Friedlingstein, P., Ciais, P., Sitch, S., and Prentice, I. C., 2005: A dynamic global vegetation model for studies of the coupled atmosphere-biosphere system, *Glob. Biogeochem. Cycles*, 19, GB1015, doi: 10.1029/2003GB002199

Kumar P., M. Ketzel, S. Vardoulakis, L. Pirjola and R. Britter, (2011) Dynamics and dispersion modelling of nanoparticles from road traffic in the urban atmospheric environment – a review. *Journal of Aerosol Science*, 42:580-603. Doi: 10.1016/j.jaerosci.2011.06.001

Kumar P., M. Khare, R.M. Harrison, W.J. Bloss, A.C. Lewis H. Coe and L. Morawska, (2015) New directions: Air pollution challenges for developing megacities like Delhi, *Atmospheric Environment*, 122:657-661, doi: 10.1016/j.atmosenv.2015.10.032

Kumar, S. V., Peters-Lidard, C. D., Tian, Y., Houser, P. R., Geiger, J., Olden, S., Lighty, L., Eastman, J. L., Doty, B., Dirmeyer, P., Adams, J., Mitchell, K., Wood, E. F., and Sheffield, J. (2006), Land Information System – An interoperable framework for high resolution land surface modeling, *Environ. Modell. Softw.*, 21, 1402–1415

Kurzfassung der Jahreskenngrößen, 2015, kontinuierlich gemessener Immissionskonzentrationen in NRW, *Landesamt für Natur, Umwelt and Verbraucherschutz Nordhein-Westffalen*

Langner J., R. Bergström, V. Foltescu, (2005) Impact of climate change on surface ozone and deposition of sulphur and nitrogen in Europe, *Atmos. Environ*. 39 1129–1141

LANUV-Fachbericht 73, Bericht über die Luftqualität im Jahre 2015, *Landesamt für Natur, Umwelt and Verbraucherschutz Nordhein-Westffalen*, Recklinghausen 2016

Lateb M., R.N. Meroney, M. Yataghene, H. Fellouah, F. Saleh and M.C. Boufadel, (2016) On the use of numerical modelling for near-field pollutant dispersion in urban environments. A review, *Environmental Pollution*, 208:271-283. Doi: 10.1016/j.envpol.2015.07.039

Laurila T., J.P. Tuovinen, V. Tarvainen, and D. Simpson, (2004) Trends and scenarios of ground-level ozone concentrations in Finland, *Boreal Environmental Research*, 9 167-184

Lawrence, D., Oleson, K. W., Flanner, M. G., Thorton, P. E., Swenson, S. C., Lawrence, P. J., Zeng, X., Yang, Z.-L., Levis, S., Skaguchi, K., Bonan, G. B., and Slater, A. G. (2011), Parameterization Improvements and Functional and Structural Advances in Version 4 of the Community Land Model, *J. Adv. Model. Earth Syst.*, 3,27 pp

Lemaire, V. E. P., Colette, A., and Menut, L. (2016), Using statistical models to explore ensemble uncertainty in climate impact studies: the example of air pollution in Europe, *Atmos. Chem. Phys.*, 16, 2559-2574, doi:10.5194/acp-16-2559-2016

Lemonsu, A., Grimmond, C. S. B., and Masson, V., (2004), Modeling the surface energy balance of the core of an old Mediterranean city: Marseille, *J. Appl. Meteorol.*, 43, 312–327

Le Quéré, C., Andrew, R. M., Canadell, J. G., Sitch, S., Korsbakken, J. I., Peters, G. P., Manning, A. C., Boden, T. A., Tans, P. P., Houghton, R. A., Keeling, R. F., Alin, S., Andrews, O. D., Anthoni, P., Barbero, L., Bopp, L., Chevallier, F., Chini, L. P., Ciais, P., Currie, K., Delire, C., Doney, S. C., Friedlingstein, P., Gkritzalis, T., Harris, I., Hauck, J., Haverd, V., Hoppema, M., Klein Goldewijk, K., Jain, A. K., Kato, E., Körtzinger, A., Landschützer, P., Lefèvre, N., Lenton, A., Lienert, S., Lombardozzi, D., Melton, J. R., Metzl, N., Millero, F., Monteiro, P. M. S., Munro, D. R., Nabel, J. E. M. S., Nakaoka, S., O'Brien, K., Olsen, A., Omar, A. M., Ono, T., Pierrot, D., Poulter, B., Rödenbeck, C., Salisbury, J., Schuster, U., Schwinger, J., Séférian, R., Skjelvan, I., Stocker, B. D., Sutton, A. J., Takahashi, T., Tian, H., Tilbrook, B., van der Laan-Luijkx, I. T., van der Werf, G. R., Viovy, N., Walker, A. P., Wiltshire, A. J., and Zaehle, S. (2016), Global Carbon Budget 2016, Earth Syst. Sci. Data, 8, 605-649, doi:10.5194/essd-8-605-2016, http://www.earth-syst-sci-data.net/8/605/2016/

Letzel, M., (2007), High resolution large-eddy simulation of turbulent flow around buildings. PhD thesis, Leibniz Universität Hannover. Available online: http://www.muk.uni-hannover.de/institut/dissertationen.htm

Maraun, D., et al. (2010), Precipitation downscaling under climate change: Recent developments to bridge the gap between dynamical models and the end user, *Rev. Geophys.*, 48, RG3003, doi:10.1029/2009RG000314

Manara V., M. Brunetti, A. Celozzi, M. Maugeri, A. Sanchez-Lorenzo, and M. Wild (2016), Detection of dimming/brightening in Italy from homogenized all-sky and clear-sky surface solar radiation records and underlying causes (1959–2013) Atmos. Chem. Phys., 16, 11145-11161, doi:10.5194/acp-16-11145-2016

Maraun, D., et al. (2010), Precipitation downscaling under climate change: Recent developments to bridge the gap between dynamical models and the end user, Rev. Geophys., 48, RG3003, doi:10.1029/2009RG000314

Maraun, D., M. Widmann, J. M. Gutiérrez, S. Kotlarski, R. E. Chandler, E. Hertig, J. Wibig, R. Huth, and R. A. I. Wilcke (2015), VALUE: A framework to validate downscaling approaches for climate change studies, *Earth's Future*, 3,1–14, doi:10.1002/2014EF000259

Martilli, A. (2002), Numerical Study of Urban Impact on Boundary Layer Structure: Sensitivity to Wind Speed, Urban Morphology, and Rural Soil Moisture, *J. Appl. Meteorol.*, 41, 1247–1266

Masson V., (2000), A physically-based scheme for the urban energy budget in atmospheric models. *Boundary-Layer Meteorol.* 94: 357–397, doi: 10.1023/a:1002463829265

Masson, V. (2006), Urban surface modeling and the meso-scale impact of cities, *Theor. Appl. Climatol*, 84, 35–45

Masson, V., Le Moigne, P., Martin, E., Faroux, S., Alias, A., Alkama, R., Belamari, S., Barbu, A., Boone, A., Bouyssel, F., Brousseau, P., Brun, E., Calvet, J.-C., Carrer, D., Decharme, B., Delire, C., Donier, S., Essaouini, K., Gibelin, A.-L., Giordani, H., Habets, F., Jidane, M., Kerdraon, G., Kourzeneva, E., Lafaysse, M., Lafont, S., Lebeaupin Brossier, C., Lemonsu, A., Mahfouf, J.-F., Marguinaud, P., Mokhtari, M., Morin, S., Pigeon, G., Salgado, R., Seity, Y., Taillefer, F., Tanguy, G., Tulet, P., Vincendon, B., Vionnet, V., and Voldoire, A., (2013), The SURFEXv7.2 land and ocean surface platform for coupled or offline simulation of earth surface variables and fluxes, *Geosci. Model Dev.*, 6, 929-960, doi:10.5194/gmd-6-929-2013

Matthews T., D. Mullan, R.L. Wilby, C. Broderick, C. Murphy (2016), Past and future climate change in the context of memorable seasonal extremes, *Climate Risk Management*, 11, 37-52, http://dx.doi.org/10.1016/j.crm.2016.01.004

Maugeri M, Brunetti M, Monti F, Nanni T. (2003), The Italian Air Force sea-level pressure data set (1951–2000). Il Nuovo Cimento 26C: 453–467

Maugeri, M., Brunetti, M., Monti, F. and Nanni, T. (2004), Sea-level pressure variability in the Po Plain (1765–2000) from homogenized daily secular records. Int. J. Climatol., 24: 437–455. doi:10.1002/joc.991

Meehl, G., C. Covey, K. Taylor, T. Delworth, R. Stouffer, M. Latif, B. McAvaney, and J. Mitchell, (2007), THE WCRP CMIP3 Multimodel Dataset: A New Era in Climate Change Research. *Bull. Amer. Meteor. Soc*., 88, 1383–1394, doi: 10.1175/BAMS-88-9-1383

Mikkonen, S., M. Laine, H. Mäkelä, H. Gregow, H, Tuomenvirta, M. Lahtinen and A. Laaksonen (2015), Trends in the average temperature in Finland, 1847–2013. Stochastic Environmental Research and Risk Assessment, 29(6), 1521-1529

Mills, G.; Cleugh, H.; Emmanuel, R.; Endlicher, W.; Erell, E.; McGranahan, G.; Ng, E.; Nickson, A.; Rosenthal, J. & Steemer, K. (2010), Climate Information for Improved Planning and Management of Mega Cities (Needs Perspective) World Climate Conference - 3, *Elsevier Science Bv*, 1, 228-246

Monks P.S. and co-authors, (2009) Atmospheric composition change – global and regional air quality, *Atmospheric Environmental*, 43, 5268-5350

Morgillo A. et al. (2016) May Weather Types and Wind Patterns Enhance Our Understanding of the Relationship Between the Local Air Pollution and the Synoptic Circulation? Steyn D., Chaumerliac N. (eds) *Air Pollution Modelling and its Application XXIV*. Springer Proceedings in Complexity. Springer, Cham

Moss, R.H., Edmonds, J.A., Hibbard, K.A., Manning, M.R., Rose, S.K., van Vuuren, D.P., Carter, T.R., Emore, S., Kainuma, M., Kram, T., Meehl, G.A., Mitchell, J.F.B., Nakicenovic, N., Riahl, K., Smith, S.J., Stouffer, R.J., Thomson, A.M., Weyant, J.P. & Wilbanks, T.J., (2010), The next generation of scenarios for climate change research and assessment, *Nature*, Vol. 463, Iss. 7282, pp. 747-756

Noone, S., Murphy, C., Coll, J., Matthews, T., Mullan, D., Wilby, R. L. and Walsh, S. (2016), Homogenization and analysis of an expanded long-term monthly rainfall network for the Island of Ireland (1850–2010). *Int. J. Climatol.*, 36: 2837–2853. doi:10.1002/joc.4522

Nurmi V. Votsis, A. Perrels, A. Lehvävirta S. (2016), Green Roof Cost Benefit Analysis: Special Emphasis on Scenic Benefits. *Journal of Benefit-Cost Analysis*, vol. 7, pp 488-522

O'Dwyer Michael, (2015), Air Quality in Ireland 2015: key indicators of Ambient Air Quality, National Ambient Air Quality Program, *Environmental Protection Agency*

O'Neill, B.C., Kriegler, E., Riahi, K., Ebi, K.L., Hallegatte, S., Carter, T.R., Mathur, R., van Vuuren, D.P., (2014), A new scenario framework for climate change research: the concept

of shared socioeconomic pathways. *Clim. Change* 122, 387–400. doi:10.1007/s10584-013-0905-2

Ouedraogo, B. I., G. J. Levermore and J. B. Parkinson, (2012) Future energy demand for public buildings in the context of climate change for Burkina Faso, *Building and Environment*, 49, 270-282

Pal J.S., F. Giorgi, X. Bi, (2004) Consistency of recent European summer precipitation trends and extremes with future regional climate projections, *Geophys. Res. Lett*. 31 L13202

Parrish D.D. and W.R. Stockwell, (2015) Urbanization and Air Pollution: Then and Now, *EOS Earth & Space Science News*, https://eos.org/features/urbanization-air-pollution-now

Perkins Sarah E. (2015), A review on the scientific understanding of heatwaves - Their measurement, driving mechanisms, and changes at the global scale, *Atmospheric Research*, 164-165 (2015) 242-267

Petersen, R. (1997), A wind tunnel evaluation of methods for estimating surface roughness length at industrial facilities, *Atmos. Environ*., 31, 45–57

Porson, A., Harman, I., Bohnenstengel, S., and Belcher, S. (2009), How Many Facets are Needed to Represent the Surface Energy Balance of an Urban Area? *Bound. -Lay. Meteorol.*, 132, 107–128

Räisänen, J. and O. Räty (2013), Projections of daily mean temperature variability in the future: cross-validation tests with ENSEMBLES regional climate simulations, *Clim. Dyn*., 41(5-6), 1553-1568

Robinson P.J. (2001), On the definition of a heat wave, *J. Appl. Meteorol.*, 40:762-775

Rummukainen, M. (2010), State-of-the-art with regional climate models. WIREs Clim Change, 1: 82–96. doi:10.1002/wcc.8

Rummukainen, M. (2016), Added value in regional climate modeling. WIREs Clim Change, 7: 145–159. doi:10.1002/wcc.378

Ruosteenoja K., Jylhä K., Kämäräinen M., (2016), Climate projections for Finland under the RCP forcing scenarios. *Geophysica*, 51, 17-50

Räisänen, J. and O. Räty (2013), Projections of daily mean temperature variability in the future: cross-validation tests with ENSEMBLES regional climate simulations, Clim. Dyn., 41(5-6), 1553-1568

Sailor, D. J. (2011), A review of methods for estimating anthropogenic heat and moisture emissions in the urban environment, *Int. J. Climatol*., 31, 189–199

Russo, S., A. Dosio, R. G. Graversen, J. Sillmann, H. Carrao, M. B. Dunbar, A. Singleton, P.

Montagna, P. Barbola, and J. V. Vogt (2014), Magnitude of extreme heat waves in present climate and their projection in a warming world, *J. Geophys. Res. Atmos.*, *119*, 12,500–12,512, doi:10.1002/2014JD022098.

Schär C., and coauthors, (2004) The role of increasing temperature variability in European summer heat waves, *Nature* 427 332–336

Simolo, C., M. Brunetti, M. Maugeri, T. Nanni, and A. Speranza (2010), Understanding climate change–induced variations in daily temperature distributions over Italy, J. Geophys. Res., 115, D22110, doi:10.1029/2010JD014088

Seneviratne S.I., D. Lüthi, M. Litschi, C. Schär (2006), Land-atmosphere coupling and climate change in Europe, *Nature*, 443 (7108), 205-209

Statistisches Jahrbuch 2014 der Stadt Bottrop, *Amt für Informationsverarbeitung, Sachgebiet Statistik und Wahlen*

Stefanon M., F. D'Andrea, P. Drobinski (2012), Heatwave classification over Europe and the Mediterranean region, *Environ. Res. Lett.*, 7(2012) 014023, doi: 10.1088/1748-9326/7/1/014023

Szopa S., D. Hauglustaine, R. Vautard, L. Menut, (2006) Evolution of the tropospheric composition in 2030: impact on European air quality, *Geophys. Res. Lett*. 33 L14805

Tan, Puay. Sia, Angelina. (2005), A pilot green roof research project in Singapore, *In Proceedings of Third Annual Greening Rooftops for Sustainable Communities Conference*, Awards and Trade Show, Washington, DC, May 4-6, 2005

Taylor KE, Stouffer RJ, Meehl GA (2012), An overview of CMIP5 and the experiment design. *Bull Am Meteorol Soc* 93:485–498

Tham, T. Muneer, G. J. Levermore and D. Chow, (2011), An examination of UKCIP02 and UKCP09 solar radiation data sets for the UK climate related to their use in building design, *Building Serv. Eng. Res. Technol*., 32, 207–228

Tietäväinen, H., H. Tuomenvirta, and A. Venäläinen (2010), Annual and seasonal mean temperatures in Finland during the last 160 years based on gridded temperature data, *Int. J. Climatol.*, 30(15), 2247-2256. doi:10.1002/joc.2046

Tietäväinen H, Johansson M., Saku S., Gregow H., Jylhä K., (2012), Extreme Weather, Sea Level Rise and Nuclear Power Plants in the Present and Future Climate in Finland. In: 11th International Probabilistic Safety Assessment and Management Conference and the Annual European Safety and Reliability Conference 2012 (PSAM11 ESREL 2012). Curran Associates, Inc. pp. 5487-5496

Tomozeiu R., C. Cacciamani, V. Pavan, A. Morgillo, A. Busuioc (2007) Climate change

scenarios for surface temperature in Emilia-Romagna (Italy) obtained using statistical downscaling models. *Theoretical and Applied Climatology*, 90, p. 25-47

Tomozeiu R., F. Tomei, G. Villani, V. Marletto, L. Botarelli (2010) Acquisizione, calibrazione e downscaling di scenari climatici futuri a livello locale http://agroscenari.entecra.it/public/upload/documenti/incontri/incontro_Oristano/ARPA_1a.pdf

Tomozeiu R., Agrillo, G., Cacciamani, C., Pavan V. (2014), Statistically downscaled climate change projections of surface temperature over Northern Italy for the periods 2021–2050 and 2070–2099. Nat Hazards, 72: 143. doi:10.1007/s11069-013-0552-y

Tuomenvirta, H., Alexandersson, H., Drebs, A., Frich, P., Nordli, P. O. (2010), Trends in Nordic and Arctic temperature extremes and ranges. *J. Climate*, 13, 977-990

Tuomenvirta, H. (2001), Homogeneity adjustments of temperature and precipitation series-Finnish and Nordic data. *Int. J. Climatol.*, 21: 495–506. doi:10.1002/joc.616

UN-Habitat, (2016) Urbanization and Development: Emerging Futures. World Cities Report 2016, *United Nations Human Settlements Programme (UN-Habitat)*, Nairobi, Kenya, http://wcr.unhabitat.org/main-report

Valmassoi A., M. Zampieri, P. Malguzzi, S. Di Sabatino (2016), Impact of irrigation on atmospheric parameters: a methodological approach through numerical modelling applied to the Po Valley, in: F. Ventura, L. Pieri (Eds.), New adversity and new services for agroecosystems, Bologna, 2016, pp 80-84, doi: 10.6092/unibo/amsacta/5164

Van Breusselen D., W. Arrazola de Oñate, B. Maiheu, S. Vranckx, W. Lefebvre, S. Janssen, T.S. Nawrot, B. Nemery, D. Avonts, (2016) Health Impact Assessment of a Predicted Air Quality Change by Moving Traffic from an Urban Ring Road into a Tunnel. The case of Antwerp, Belgium. *PLoS ONE* 11(5): e0154052. doi:10.1371/journal. pone.0154052

van der Linden, P. and Mitchell, J.F.B., Eds. (2009) ENSEMBLES: Climate Change and Its Impacts: Summary of Research and Results from the ENSEMBLES Project. Met Office Hadley Centre, Exeter, 160

Van Vuuren, D.P., Riahi, K., Moss, R., Edmonds, J., Thomson, A., Nakicenovic, N., Kram. T., Berkhout, F., Swart, R., Janetos, A., Rose, S.K and Arnell, N., (2012a), A proposal for a new scenario framework to support research and assessment in different climate research communities, *Global Environmental Change*, Vol. 22., Iss. 1., pp. 21-35

Van Vuuren, D.P., Kok, M.T.J., Girod, B., Lucas, P.L. and de Vries, B., (2012b), Scenarios in Global Environmental Assessments: Key characteristics and lessons for future use, *Global Environmental Change*, Vol. 22., Iss. 4., pp. 884-895

Verseghy, D. L., (1991) CLASS: A Canadian land surface scheme for GCMS. I. Soil model, *Int. J. Climatol*, 11, 111–133

Villani G., F. Tomei, R. Tomozeiu, V. Marletto (2011) Climatic scenarios and their impacts on irrigated agriculture in Emilia-Romagna, Italy. *Italian Journal of Agrometeorology* - 1/2011

Wang, X. Wang, D. Chen and Z. Ren (2010), Assessment of climate change impact on residential building heating and cooling energy requirement in Australia, *Building and Environment*, 45, 1663–1682

Wieringa, J. (1993), Representative roughness parameters for homogeneous terrain, *Bound. Lay. Meteorol.*, 63, 323–363

Wood, C. R. and co-authors (2013), An overview of the urban boundary layer atmosphere network in Helsinki. *Bulletin of the American Meteorological Society*, *94*(11), 1675-1690